Density Model for Sperm Whale (*Physeter macrocephalus*) for the U.S. Gulf of Mexico: Supplementary Report

Duke University Marine Geospatial Ecology Lab*

Model Version 4.2 - 2015-05-14

Citation

When referencing our methodology or results generally, please cite our open-access article:

Roberts JJ, Best BD, Mannocci L, Fujioka E, Halpin PN, Palka DL, Garrison LP, Mullin KD, Cole TVN, Khan CB, McLellan WM, Pabst DA, Lockhart GG (2016) Habitat-based cetacean density models for the U.S. Atlantic and Gulf of Mexico. Scientific Reports 6: 22615. doi: 10.1038/srep22615

To reference this specific model or Supplementary Report, please cite:

Roberts JJ, Best BD, Mannocci L, Fujioka E, Halpin PN, Palka DL, Garrison LP, Mullin KD, Cole TVN, Khan CB, McLellan WM, Pabst DA, Lockhart GG (2015) Density Model for Sperm Whale (*Physeter macrocephalus*) for the U.S. Gulf of Mexico Version 4.2, 2015-05-14, and Supplementary Report. Marine Geospatial Ecology Lab, Duke University, Durham, North Carolina.

Copyright and License

Revision History

Version	Date	Description of changes
1	2014-08-06	Initial version.
2	2014-10-16	Adjusted detection functions to be consistent with East Coast model. Updated distance to eddy predictors using Chelton et al.'s 2014 database. Removed wind speed predictor; it was not ecologically justified. Fixed missing pixels in several climatological predictors, which led to not all segments being utilized. Added documentation.
3	2014-11-22	Adjusted Without Belly Observer detection function to be consistent with change to East Coast model. Removed CumVGPM180 predictor. Updated documentation.
4	2015-01-09	Added three missing sightings and refitted models.
4.1	2015-02-02	Updated the documentation. No changes to the model.
4.2	2015-05-14	Updated calculation of CVs. Switched density rasters to logarithmic breaks. No changes to the model.

*For questions, or to offer feedback about this model or report, please contact Jason Roberts (jason.roberts@duke.edu)

Survey Data

Survey	Period	Length (1000 km)	Hours	Sightings
SEFSC GOMEX92-96 Aerial Surveys	1992-1996	27	152	0
SEFSC Gulf of Mexico Shipboard Surveys, 2003-2009	2003-2009	19	1156	137
SEFSC GulfCet I Aerial Surveys	1992-1994	50	257	28
SEFSC GulfCet II Aerial Surveys	1996-1998	22	124	9
SEFSC GulfSCAT 2007 Aerial Surveys	2007-2007	18	95	0
SEFSC Oceanic CetShip Surveys	1992-2001	49	3102	175
SEFSC Shelf CetShip Surveys	1994-2001	10	707	11
Total		195	5593	360

Table 2: Survey effort and sightings used in this model. Effort is tallied as the cumulative length of on-effort transects and hours the survey team was on effort. Sightings are the number of on-effort encounters of the modeled species for which a perpendicular sighting distance (PSD) was available. Off effort sightings and those without PSDs were omitted from the analysis.

Period	Length (1000 km)	Hours	Sightings
1992-2009	195	5592	360
1998-2009	62	2679	222
% Lost	68	52	38

Table 3: Survey effort and on-effort sightings having perpendicular sighting distances. % Lost shows the percentage of effort or sightings lost by restricting the analysis to surveys performed in 1998 and later, the era in which remotely-sensed chlorophyll and derived productivity estimates are available. See Figure 1 for more information.

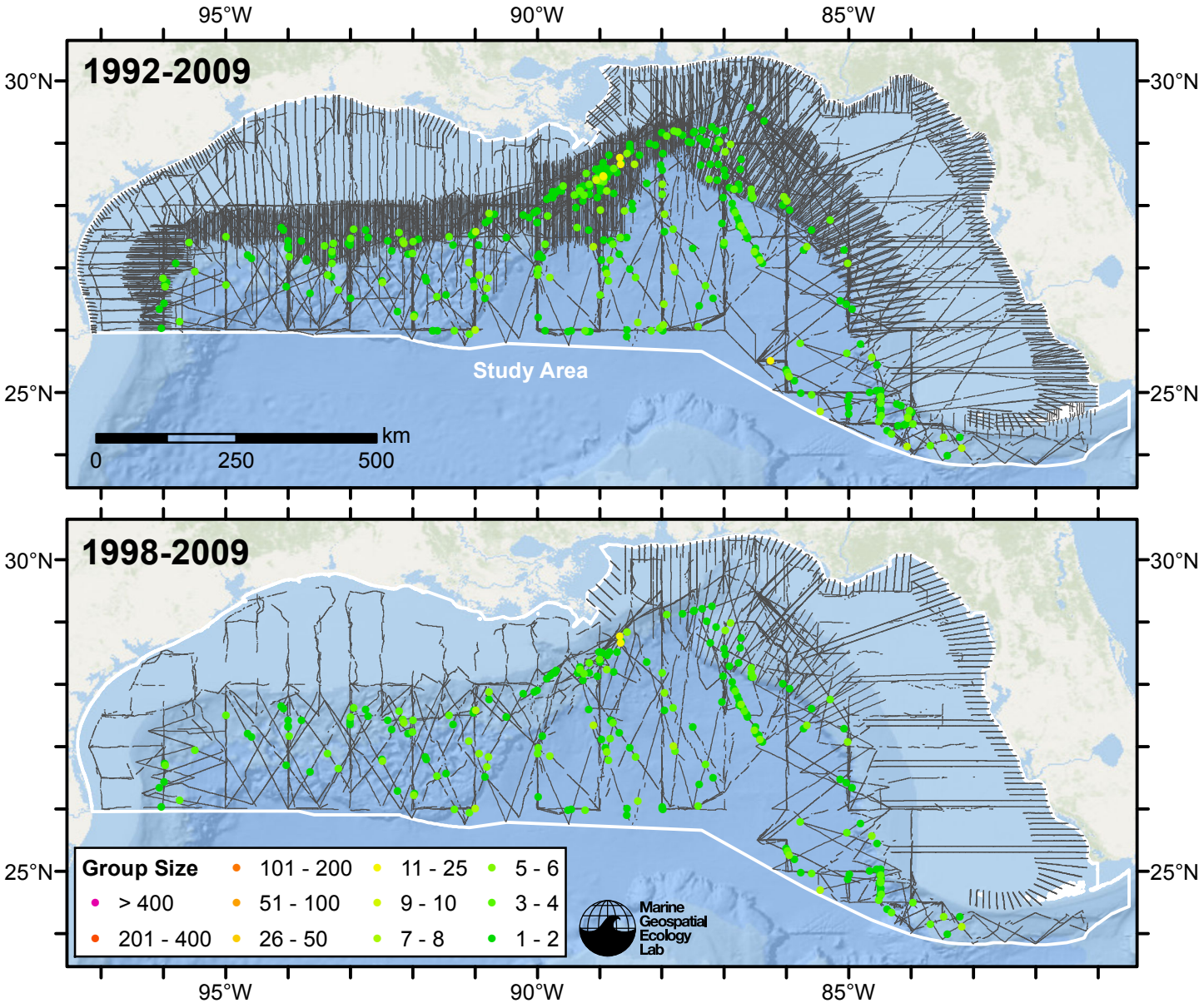

Figure 1: Sperm whale sightings and survey tracklines. The top map shows all surveys. The bottom map shows surveys performed in 1998 or later. the era in which remotely-sensed chlorophyll and derived productivity estimates are available. Models fitted to contemporaneous (day-of-sighting) estimates of those predictors only utilize these surveys. These maps illustrate the survey data lost in order to utilize those predictors. Models fitted to climatogical estimates of those predictors do not suffer this data loss.

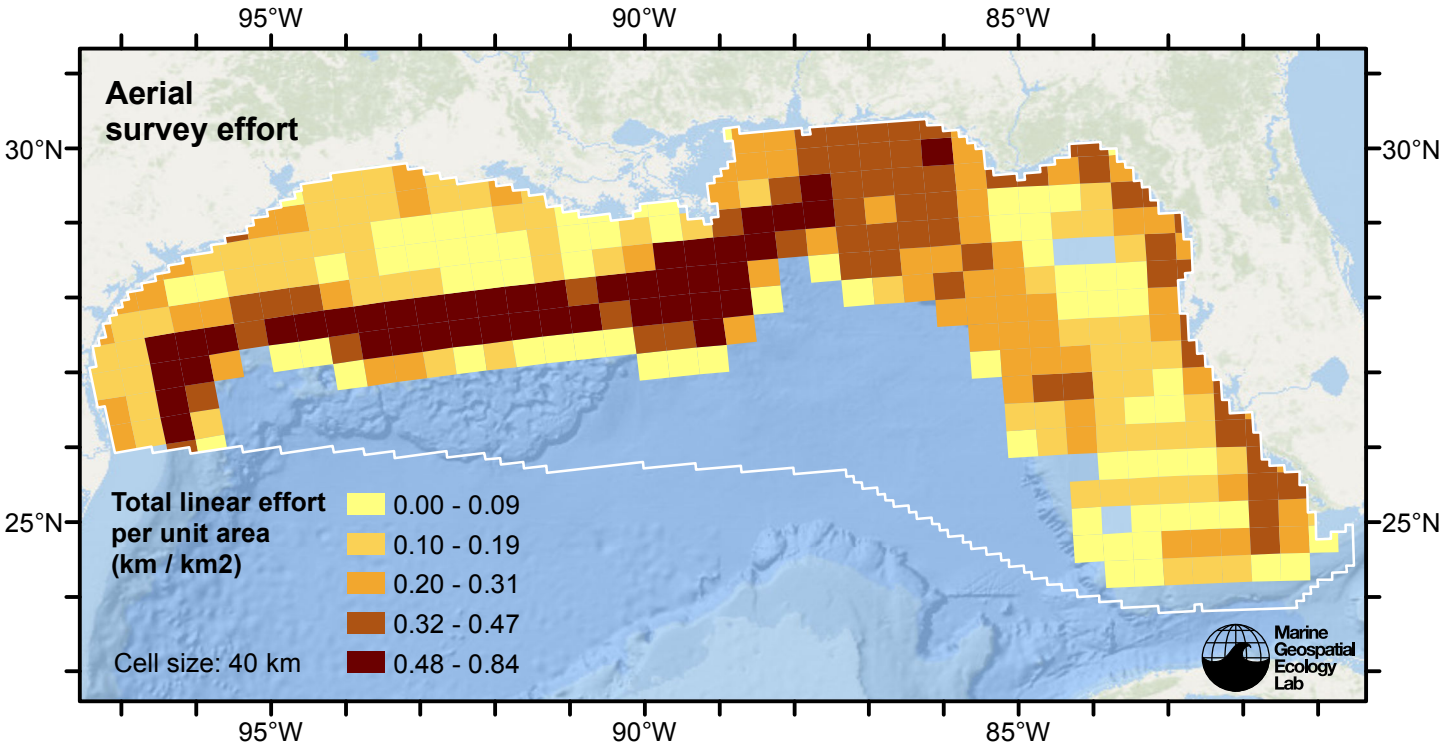

Figure 2: Aerial linear survey effort per unit area.

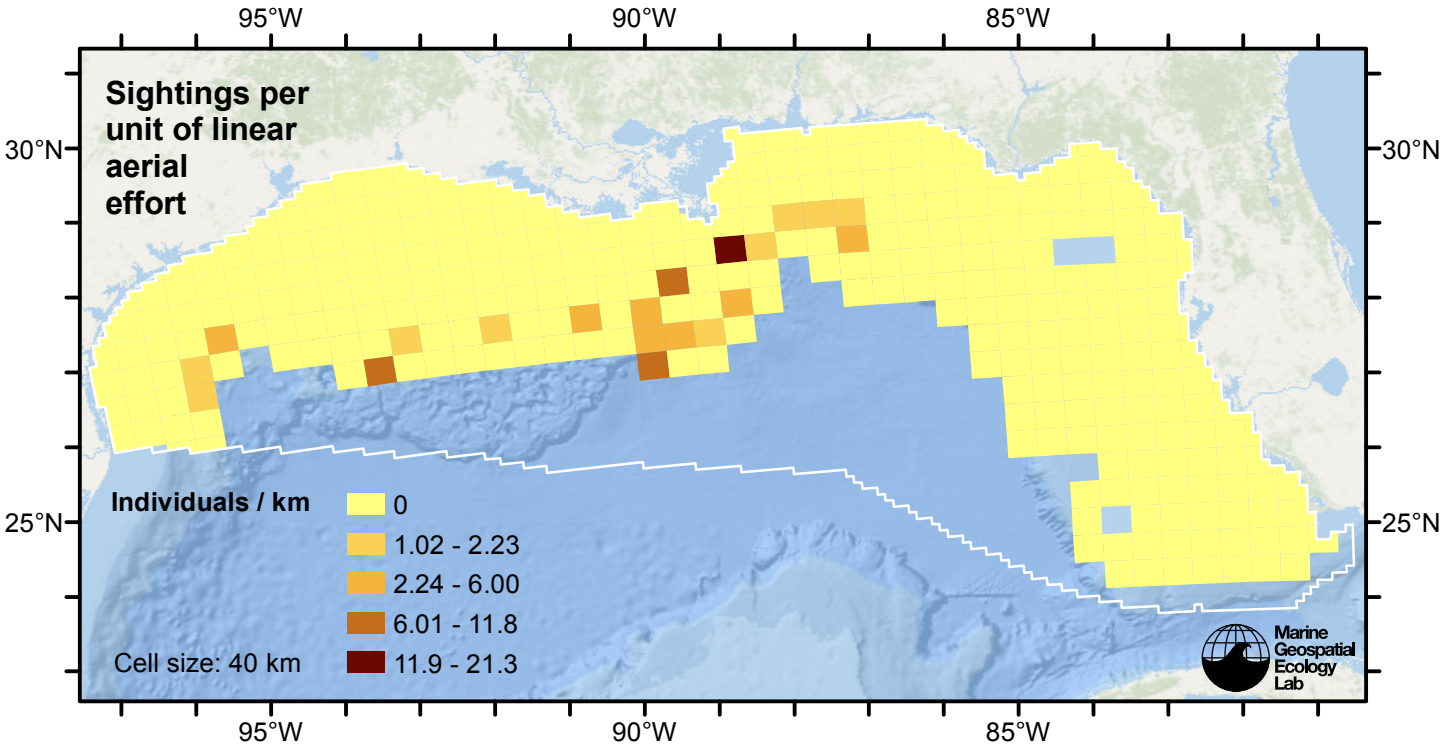

Figure 3: Sperm whale sightings per unit aerial linear survey effort.

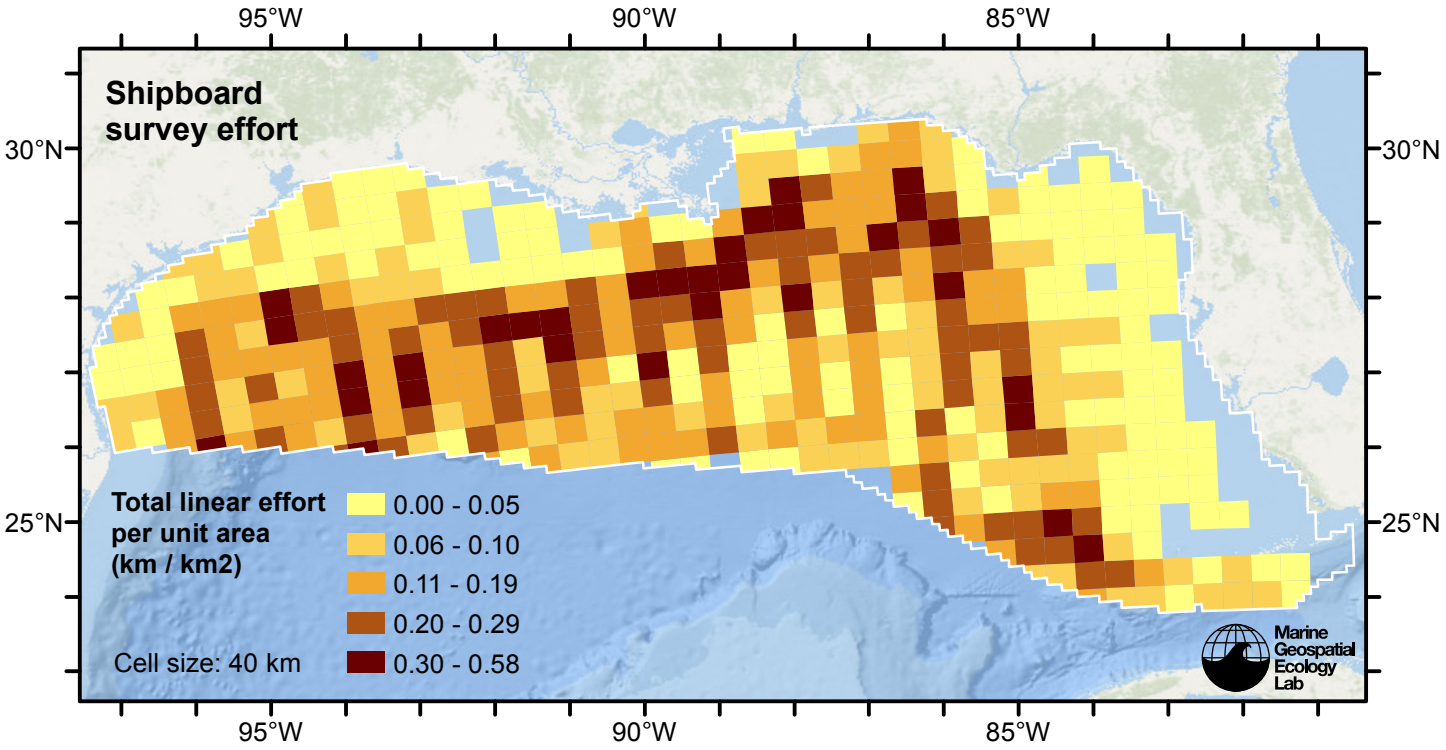

Figure 4: Shipboard linear survey effort per unit area.

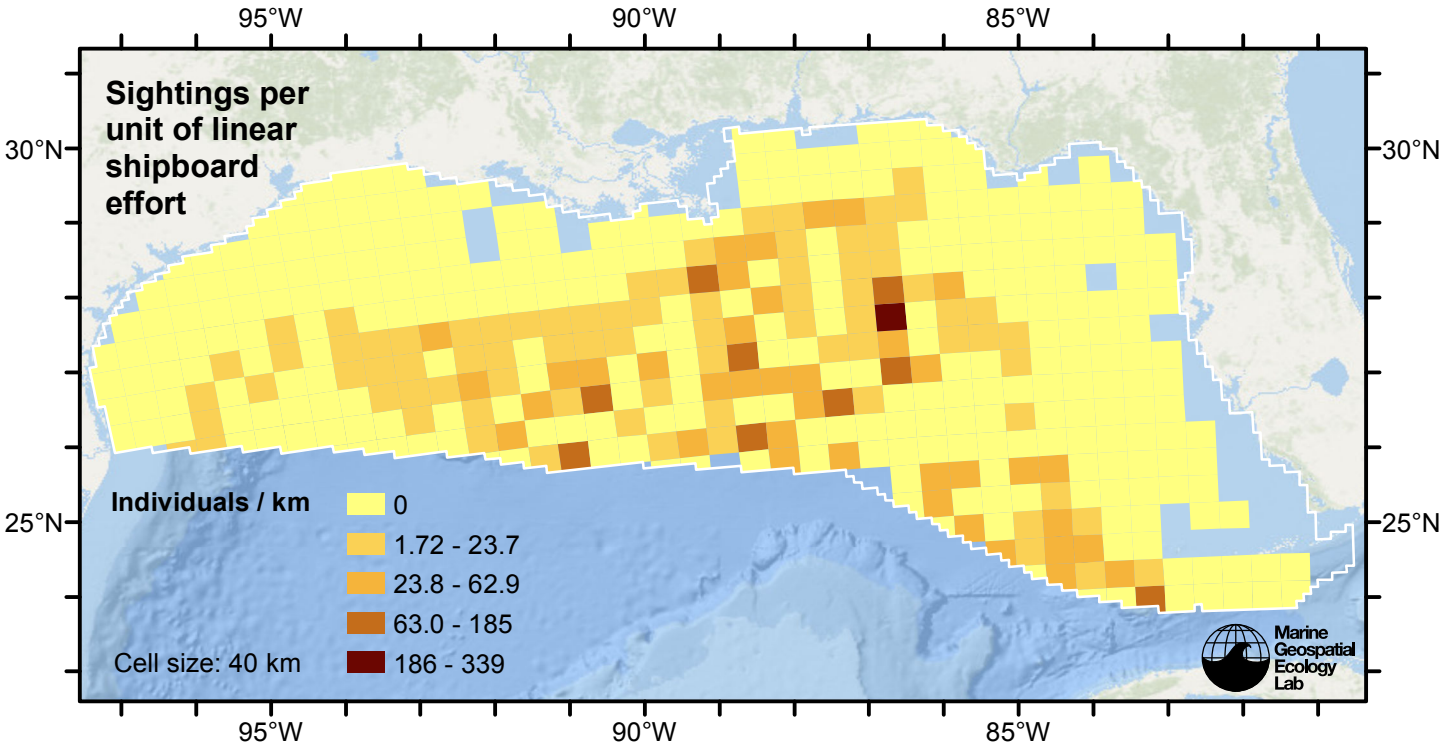

Figure 5: Sperm whale sightings per unit shipboard linear survey effort.

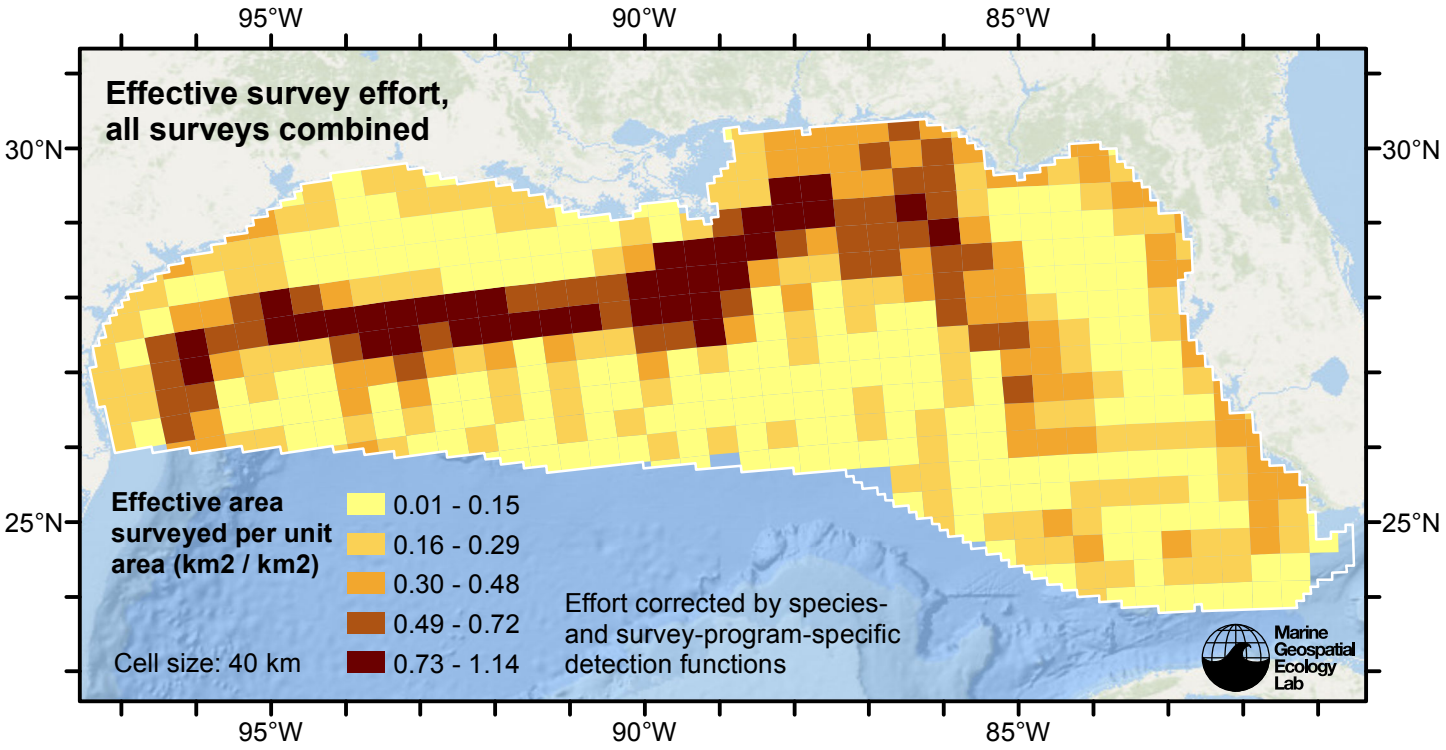

Figure 6: Effective survey effort per unit area, for all surveys combined. Here, effort is corrected by the species- and survey-program-specific detection functions used in fitting the density models.

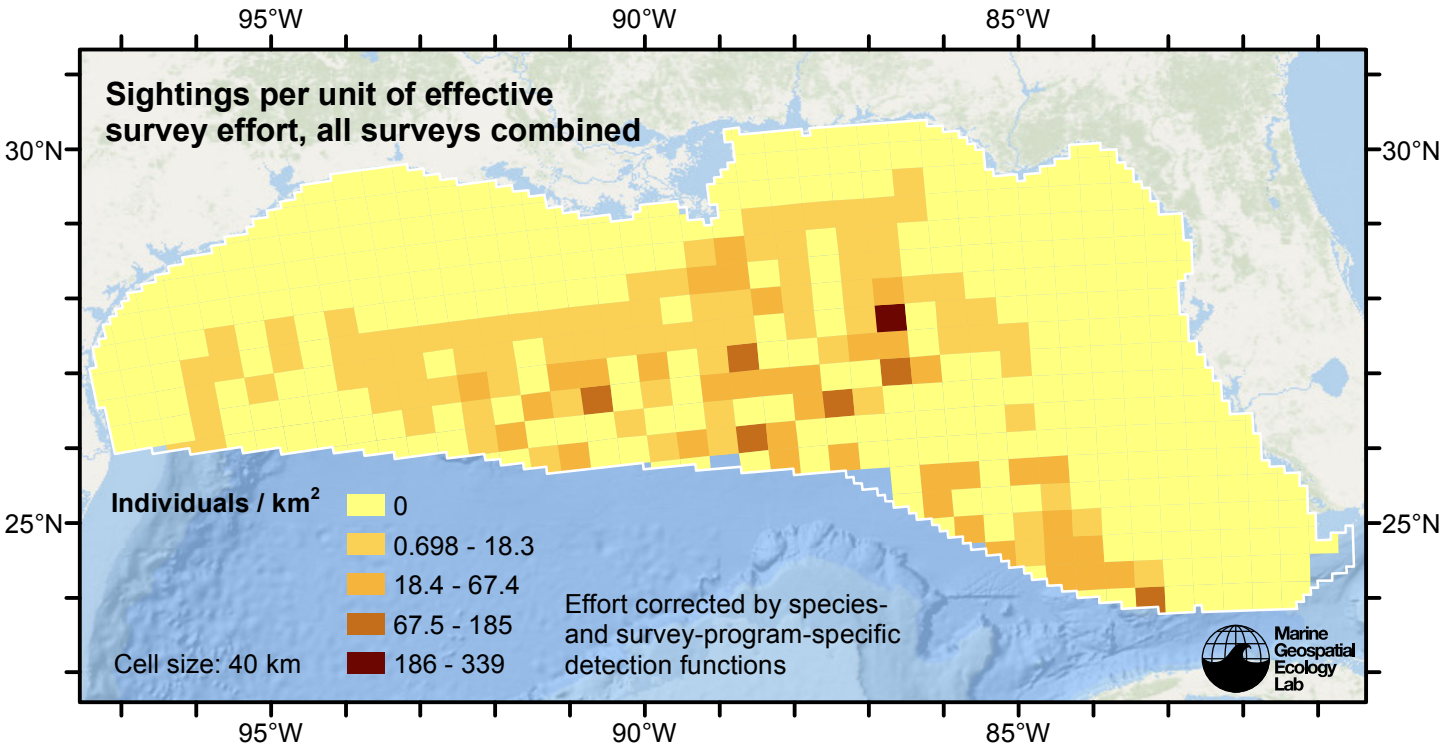

Figure 7: Sperm whale sightings per unit of effective survey effort, for all surveys combined. Here, effort is corrected by the species- and survey-program-specific detection functions used in fitting the density models.

Detection Functions

The detection hierarchy figures below show how sightings from multiple surveys were pooled to try to achieve Buckland et. al's (2001) recommendation that at least 60-80 sightings be used to fit a detection function. Leaf nodes, on the right, usually represent individual surveys, while the hierarchy to the left shows how they have been grouped according to how similar we believed the surveys were to each other in their detection performance.

At each node, the red or green number indicates the total number of sightings below that node in the hierarchy, and is colored green if 70 or more sightings were available, and red otherwise. If a grouping node has zero sightings–i.e. all of the surveys within it had zero sightings–it may be collapsed and shown as a leaf to save space.

Each histogram in the figure indicates a node where a detection function was fitted. The actual detection functions do not appear in this figure; they are presented in subsequent sections. The histogram shows the frequency of sightings by perpendicular sighting distance for all surveys contained by that node. Each survey (leaf node) recieves the detection function that is closest to it up the hierarchy. Thus, for common species, sufficient sightings may be available to fit detection functions deep in the hierarchy, with each function applying to only a few surveys, thereby allowing variability in detection performance between surveys to be addressed relatively finely. For rare species, so few sightings may be available that we have to pool many surveys together to try to meet Buckland's recommendation, and fit only a few coarse detection functions high in the hierarchy.

A blue Proxy Species tag indicates that so few sightings were available that, rather than ascend higher in the hierarchy to a point that we would pool grossly-incompatible surveys together, (e.g. shipboard surveys that used big-eye binoculars with those that used only naked eyes) we pooled sightings of similar species together instead. The list of species pooled is given in following sections.

Shipboard Surveys

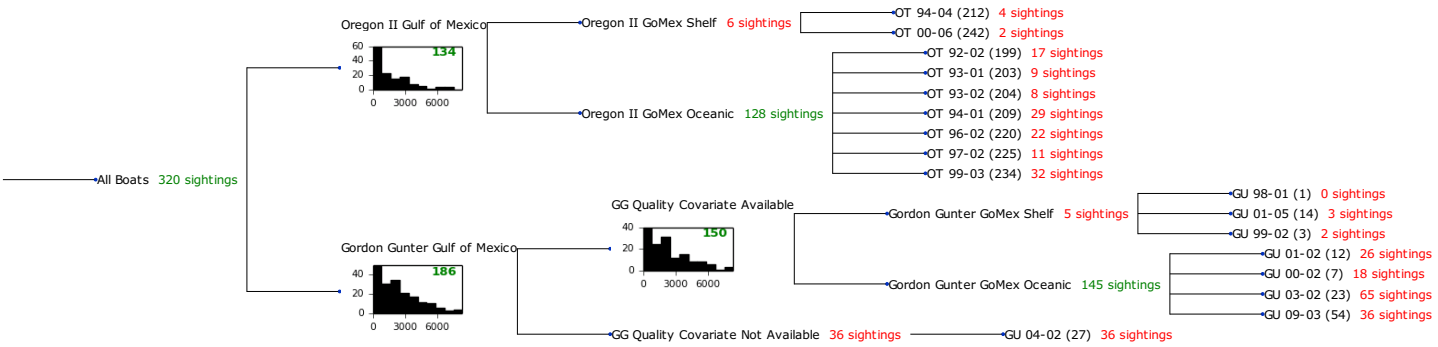

Figure 8: Detection hierarchy for shipboard surveys

Oregon II Gulf of Mexico

The sightings were right truncated at 7000m.

Covariate	Description
beaufort	Beaufort sea state.
quality	Survey-specific index of the quality of observation conditions, utilizing relevant factors other than Beaufort sea state (see methods).
size	Estimated size (number of individuals) of the sighted group.

Table 4: Covariates tested in candidate "multi-covariate distance sampling" (MCDS) detection functions.

Key	Adjustment	Order	Covariates	Succeeded	Δ AIC	Mean ESHW (m)
hr			quality, size	Yes	0.00	2083
hr			quality	Yes	0.49	2007
hn			quality, size	Yes	5.53	2864
hn			beaufort, quality, size	Yes	5.97	2835
hn			beaufort, quality	Yes	6.61	2808
hr	poly	4		Yes	6.64	1627
hn			quality	Yes	6.69	2835
hr				Yes	6.81	1696
hr			size	Yes	6.83	1809
hr	poly	2		Yes	8.81	1696
hn			beaufort	Yes	18.51	2790
hn				Yes	19.60	2794
hn			beaufort, size	Yes	19.98	2786
hn			size	Yes	20.72	2791
hn	cos	3		Yes	21.57	2792
hn	cos	2		Yes	21.58	2793
hn	cos	1		Yes	21.60	2794
hn	herm	4		Yes	21.60	2794
hr			beaufort	No		
hr			beaufort, quality	No		
hr			beaufort, size	No		
hr			beaufort, quality, size	No		

Table 5: Candidate detection functions for Oregon II Gulf of Mexico. The first one listed was selected for the density model.

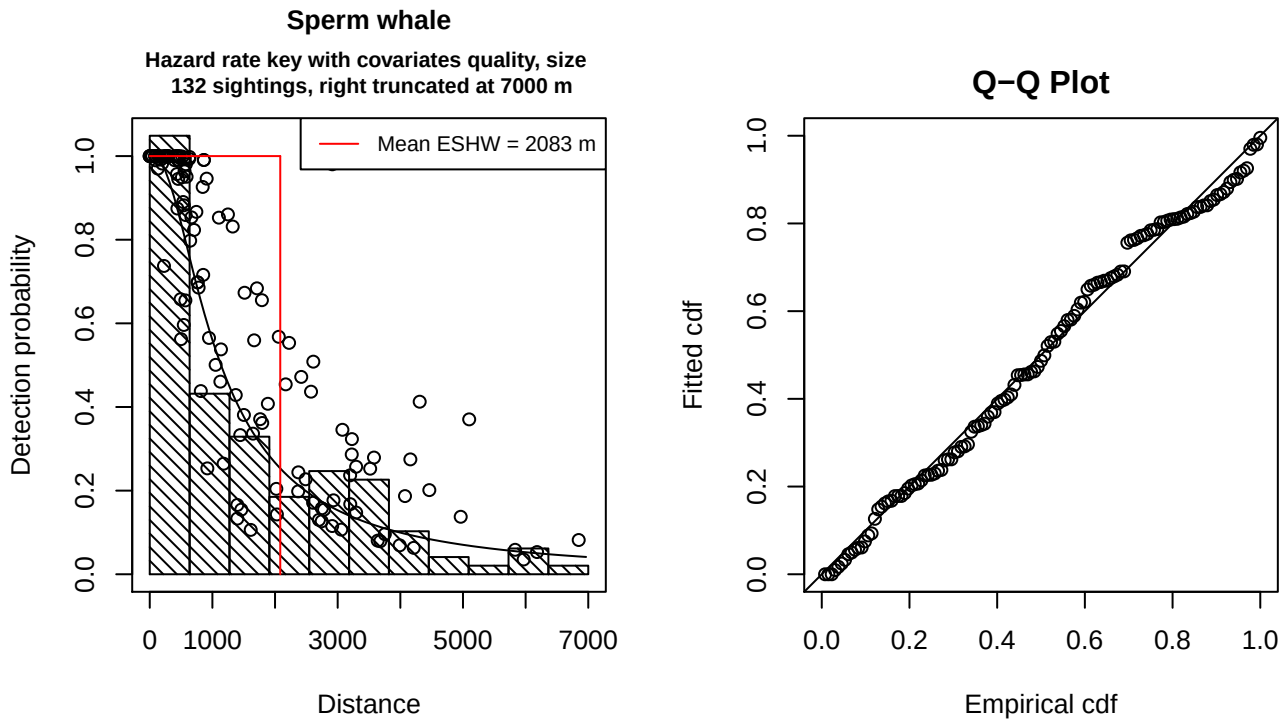

Figure 9: Detection function for Oregon II Gulf of Mexico that was selected for the density model

Statistical output for this detection function:

```
Summary for ds object
Number of observations :  132
Distance range         :  0  -  7000
AIC                    :  2206.877

Detection function:
 Hazard-rate key function

Detection function parameters
Scale Coefficients:
             estimate         se
(Intercept)  7.2488888 0.33367096
quality     -0.3860532 0.12127773
size         0.1392861 0.07772271

Shape parameters:
            estimate        se
(Intercept) 0.532807 0.1715144

                       Estimate          SE        CV
Average p              0.2467392  0.03846843 0.1559073
N in covered region 534.9779303 93.27509888 0.1743532
```

Additional diagnostic plots:

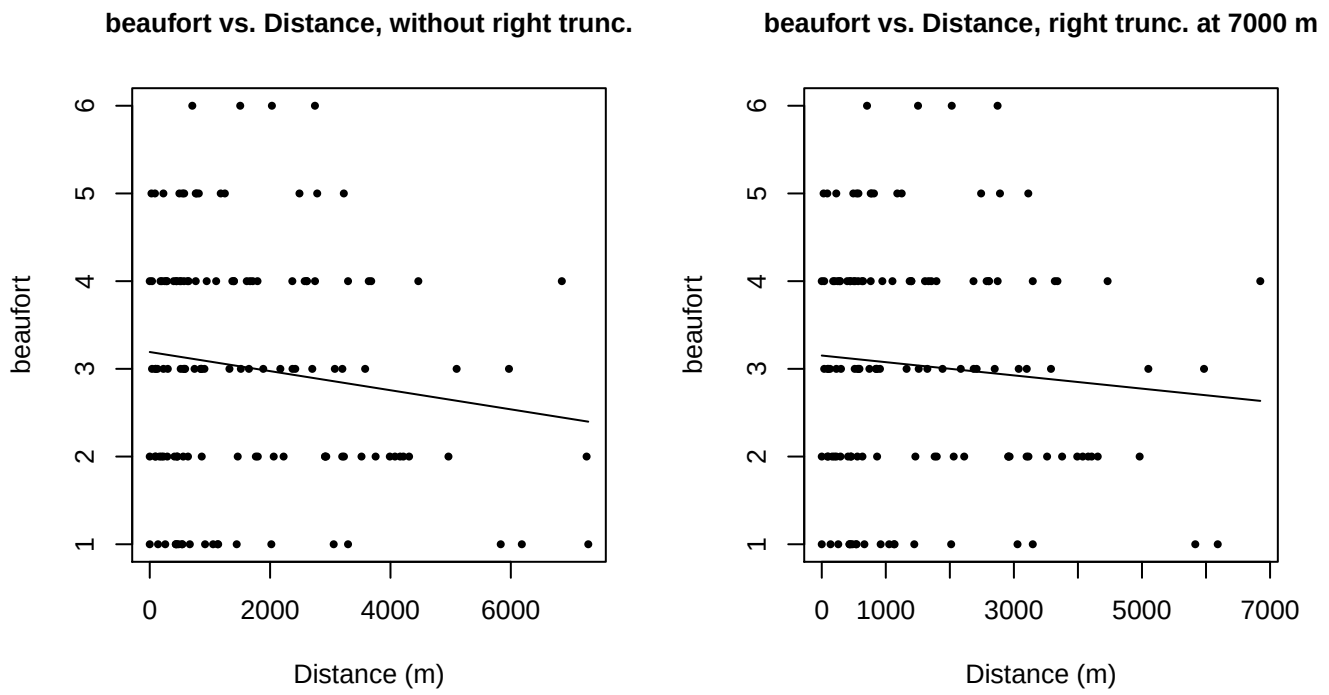

Figure 10: Scatterplots showing the relationship between Beaufort sea state and perpendicular sighting distance, for all sightings (left) and only those not right truncated (right). The line is a simple linear regression.

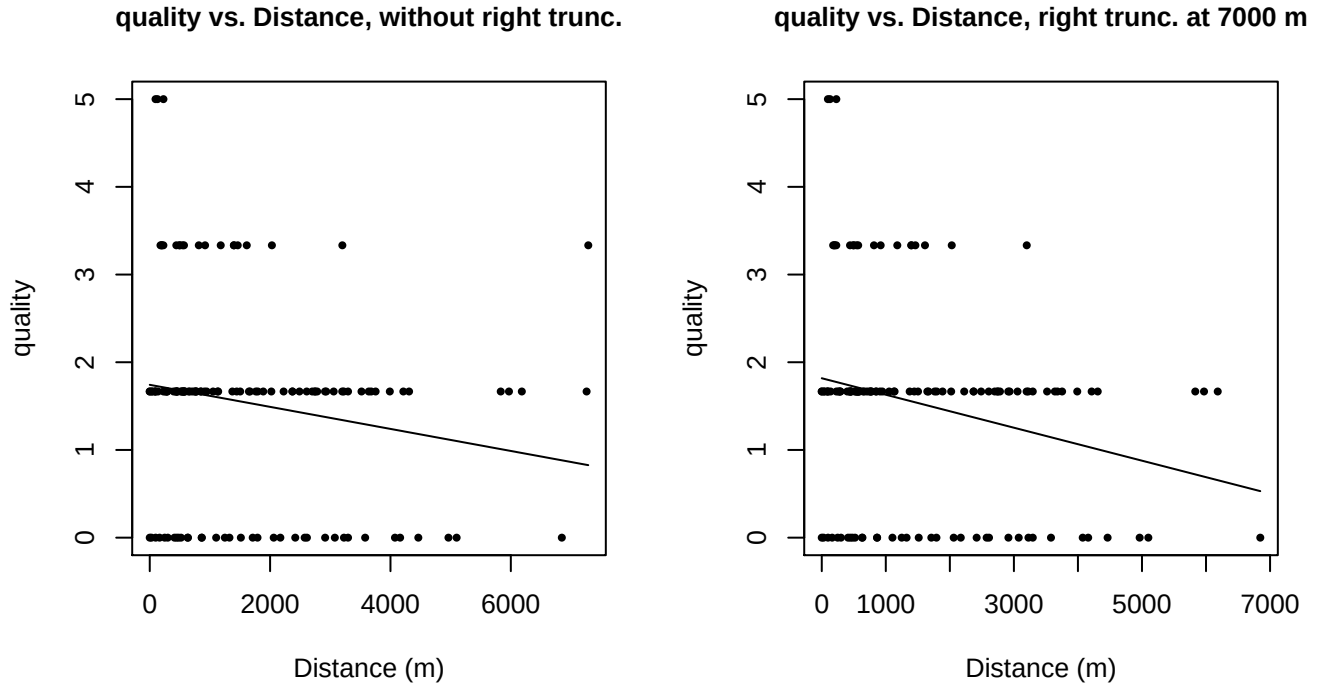

Figure 11: Scatterplots showing the relationship between the survey-specific index of the quality of observation conditions and perpendicular sighting distance, for all sightings (left) and only those not right truncated (right). Low values of the quality index correspond to better observation conditions. The line is a simple linear regression.

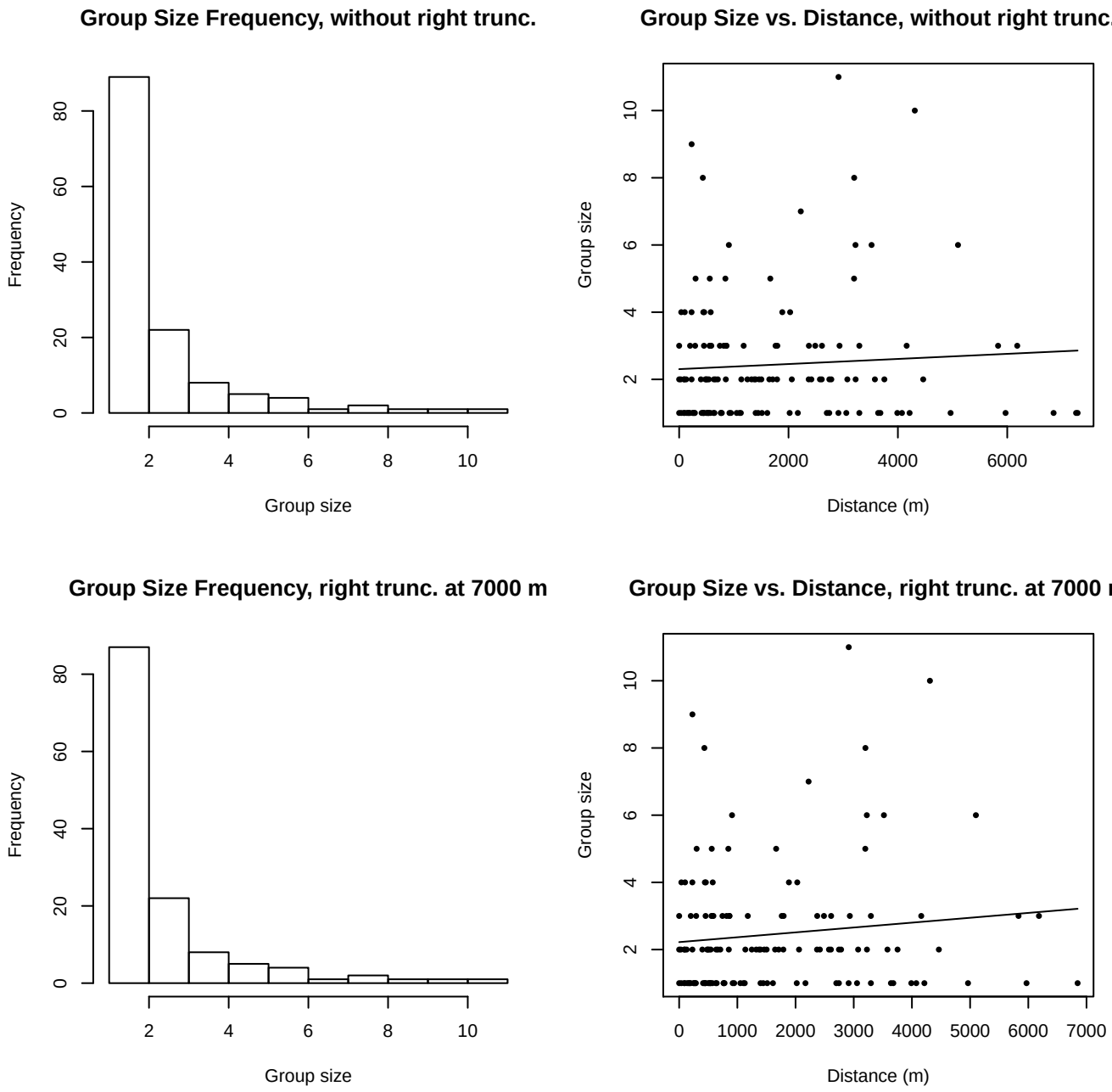

Figure 12: Histograms showing group size frequency and scatterplots showing the relationship between group size and perpendicular sighting distance, for all sightings (top row) and only those not right truncated (bottom row). In the scatterplot, the line is a simple linear regression.

Gordon Gunter Gulf of Mexico

The sightings were right truncated at 8000m.

Covariate	Description
beaufort	Beaufort sea state.
size	Estimated size (number of individuals) of the sighted group.

Table 6: Covariates tested in candidate "multi-covariate distance sampling" (MCDS) detection functions.

Key	Adjustment	Order	Covariates	Succeeded	Δ AIC	Mean ESHW (m)
hn			beaufort	Yes	0.00	3806
hn				Yes	1.00	3791
hn			beaufort, size	Yes	1.41	3811
hn			size	Yes	2.60	3792
hn	cos	3		Yes	3.00	3791
hn	cos	2		Yes	3.00	3791
hn	cos	1		Yes	3.00	3791
hn	herm	4		Yes	3.00	3791
hr	poly	2		Yes	3.37	3203
hr			beaufort	Yes	4.09	3813
hr	poly	4		Yes	4.12	3222
hr			beaufort, size	Yes	5.05	3772
hr				Yes	5.85	3846
hr			size	Yes	6.94	3759

Table 7: Candidate detection functions for Gordon Gunter Gulf of Mexico. The first one listed was selected for the density model.

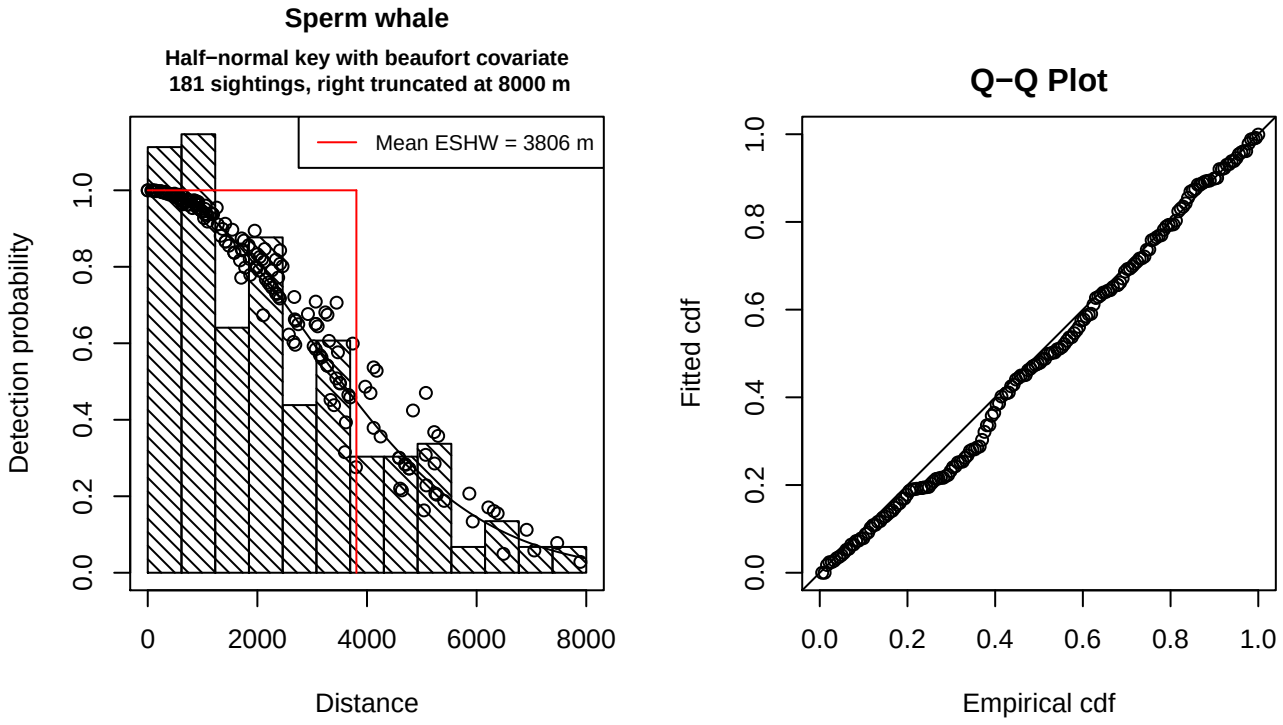

Figure 13: Detection function for Gordon Gunter Gulf of Mexico that was selected for the density model

Statistical output for this detection function:

```
Summary for ds object
Number of observations :  181
Distance range         :  0  -  8000
AIC                    :  3152.754

Detection function:
 Half-normal key function

Detection function parameters
Scale Coefficients:
             estimate         se
(Intercept)  8.3262140 0.20375291
beaufort    -0.1113671 0.06722417

                       Estimate          SE         CV
Average p             0.4695499  0.02583324 0.05501703
N in covered region 385.4755452 29.83876617 0.07740768
```

Additional diagnostic plots:

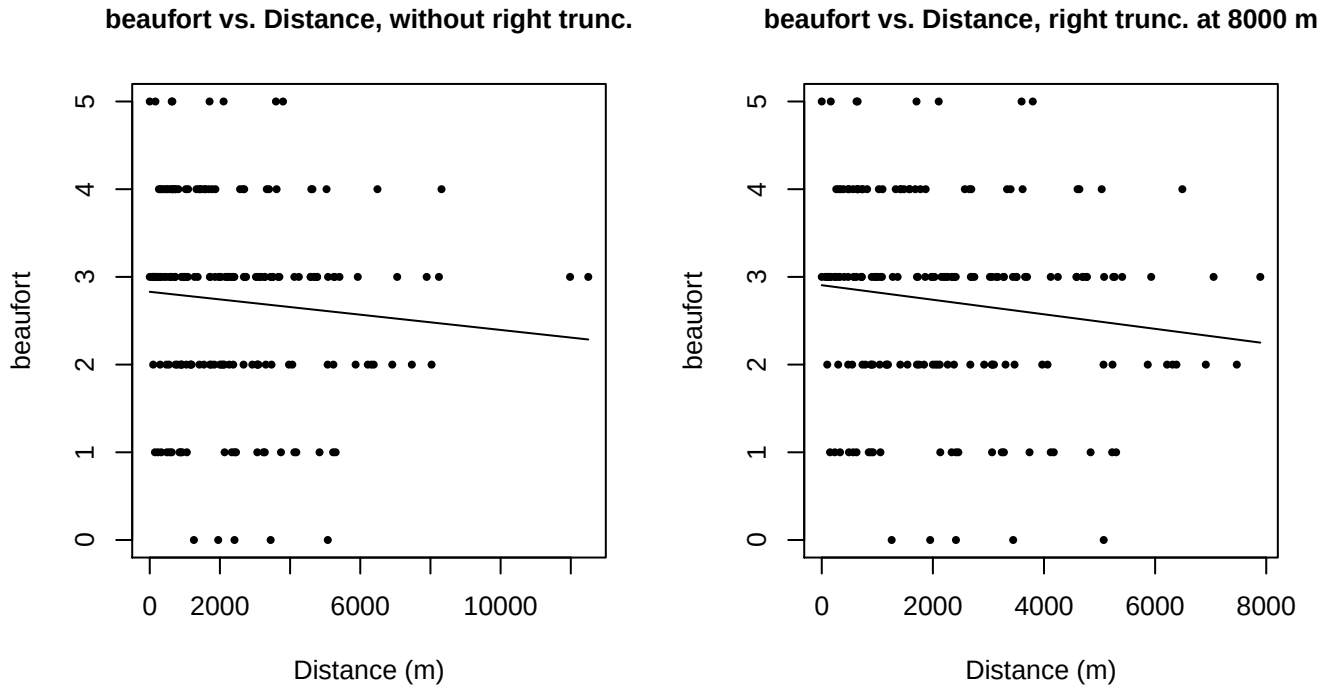

Figure 14: Scatterplots showing the relationship between Beaufort sea state and perpendicular sighting distance, for all sightings (left) and only those not right truncated (right). The line is a simple linear regression.

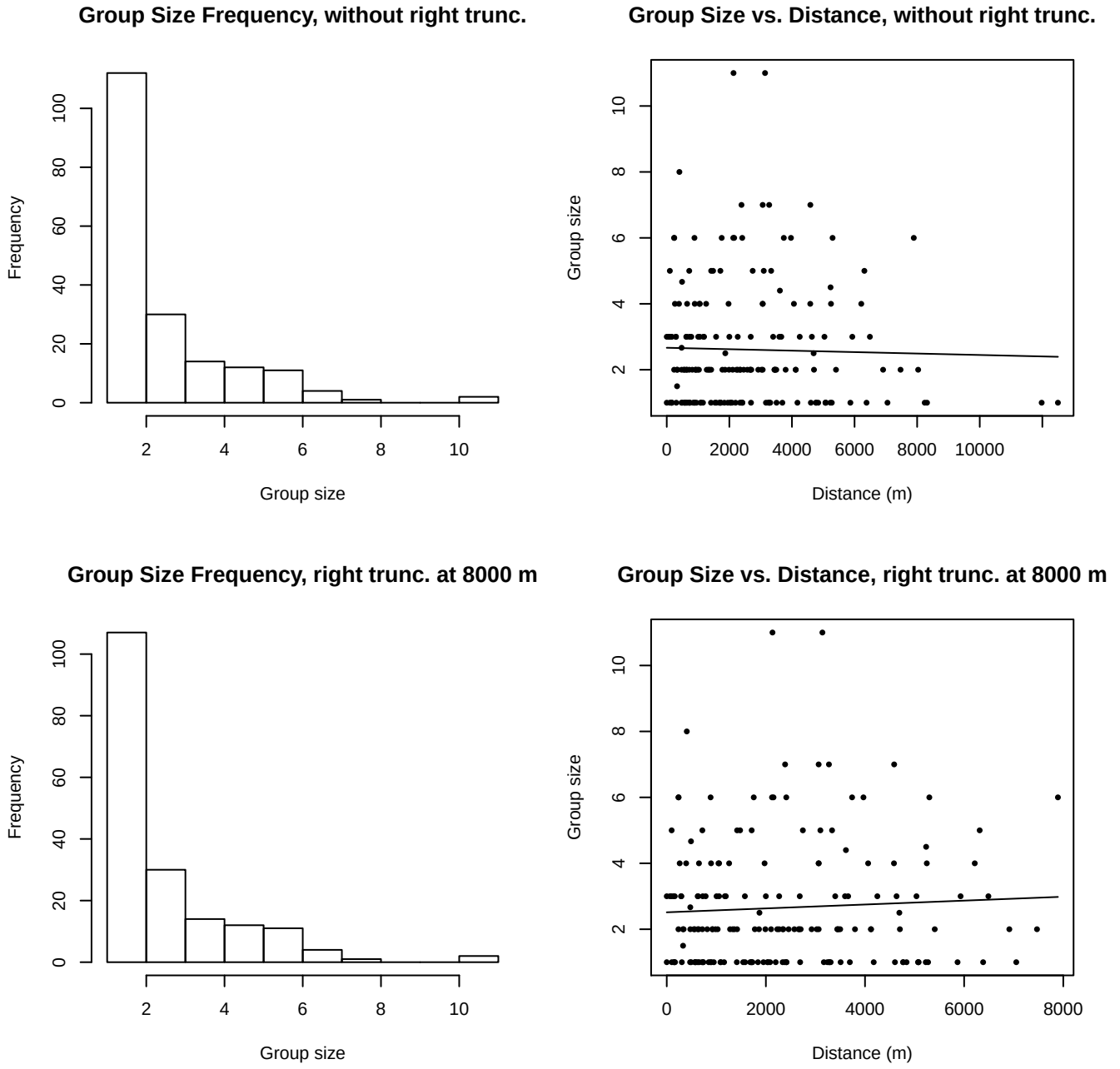

Figure 15: Histograms showing group size frequency and scatterplots showing the relationship between group size and perpendicular sighting distance, for all sightings (top row) and only those not right truncated (bottom row). In the scatterplot, the line is a simple linear regression.

GG Quality Covariate Available

The sightings were right truncated at 8000m.

Covariate	Description
beaufort	Beaufort sea state.
quality	Survey-specific index of the quality of observation conditions, utilizing relevant factors other than Beaufort sea state (see methods).
size	Estimated size (number of individuals) of the sighted group.

Table 8: Covariates tested in candidate "multi-covariate distance sampling" (MCDS) detection functions.

Key	Adjustment	Order	Covariates	Succeeded	Δ AIC	Mean ESHW (m)
hn			quality	Yes	0.00	3614
hn			beaufort, quality	Yes	1.76	3612
hn			quality, size	Yes	1.99	3614
hn			beaufort, quality, size	Yes	3.75	3612
hr			quality	Yes	7.06	4315
hr			beaufort, quality	Yes	8.39	4246
hr			quality, size	Yes	8.74	4184
hn				Yes	9.02	3610
hn			beaufort	Yes	9.15	3614
hr	poly	2		Yes	9.83	3090
hr			beaufort, quality, size	Yes	9.91	4076
hr	poly	4		Yes	10.37	3116
hn			size	Yes	10.84	3610
hn			beaufort, size	Yes	10.96	3616
hn	cos	3		Yes	11.00	3608
hn	cos	2		Yes	11.02	3610
hn	cos	1		Yes	11.02	3610
hn	herm	4		Yes	11.02	3610
hr			beaufort	Yes	13.18	3688
hr			beaufort, size	Yes	13.74	3648
hr				Yes	14.93	3673
hr			size	Yes	15.60	3500

Table 9: Candidate detection functions for GG Quality Covariate Available. The first one listed was selected for the density model.

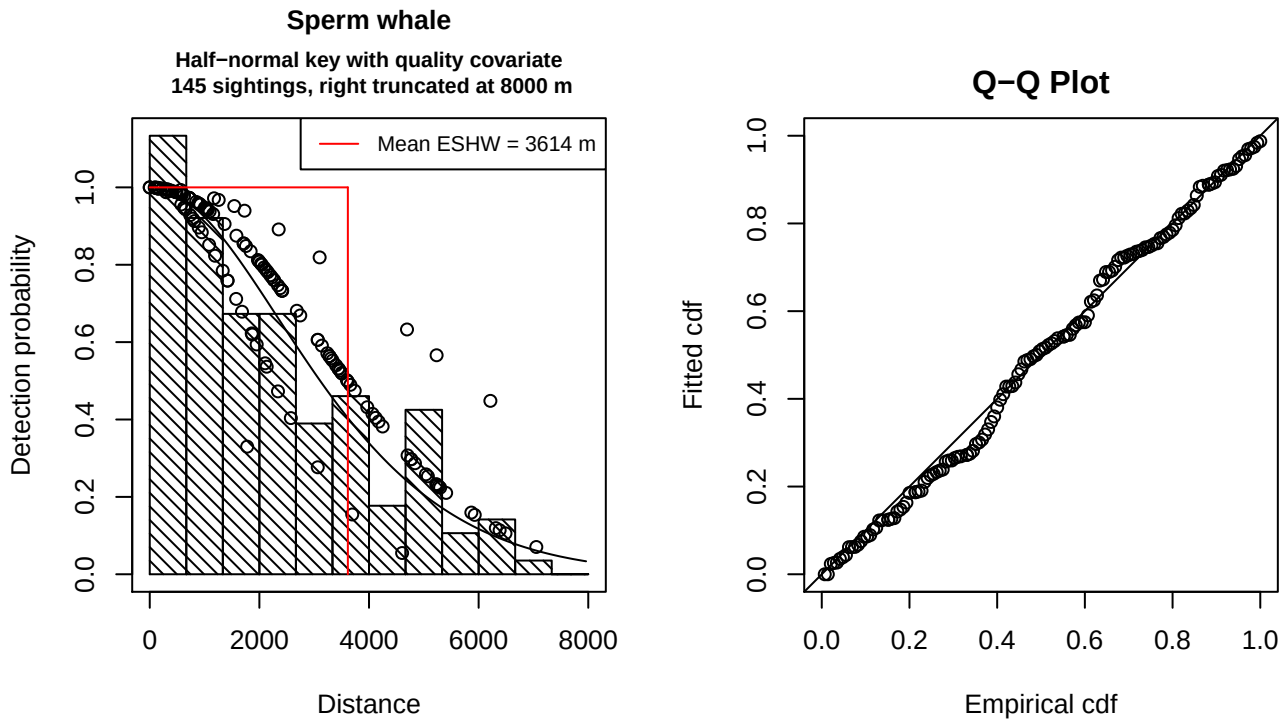

Figure 16: Detection function for GG Quality Covariate Available that was selected for the density model

Statistical output for this detection function:

```
Summary for ds object
Number of observations :  145
Distance range         :  0  -  8000
AIC                    :  2506.408

Detection function:
 Half-normal key function

Detection function parameters
Scale Coefficients:
             estimate         se
(Intercept)  8.4981362 0.19796972
quality     -0.2827478 0.09024415

                      Estimate          SE         CV
Average p             0.4279984  0.02992985 0.06992981
N in covered region 338.7863375 32.13847439 0.09486355
```

Additional diagnostic plots:

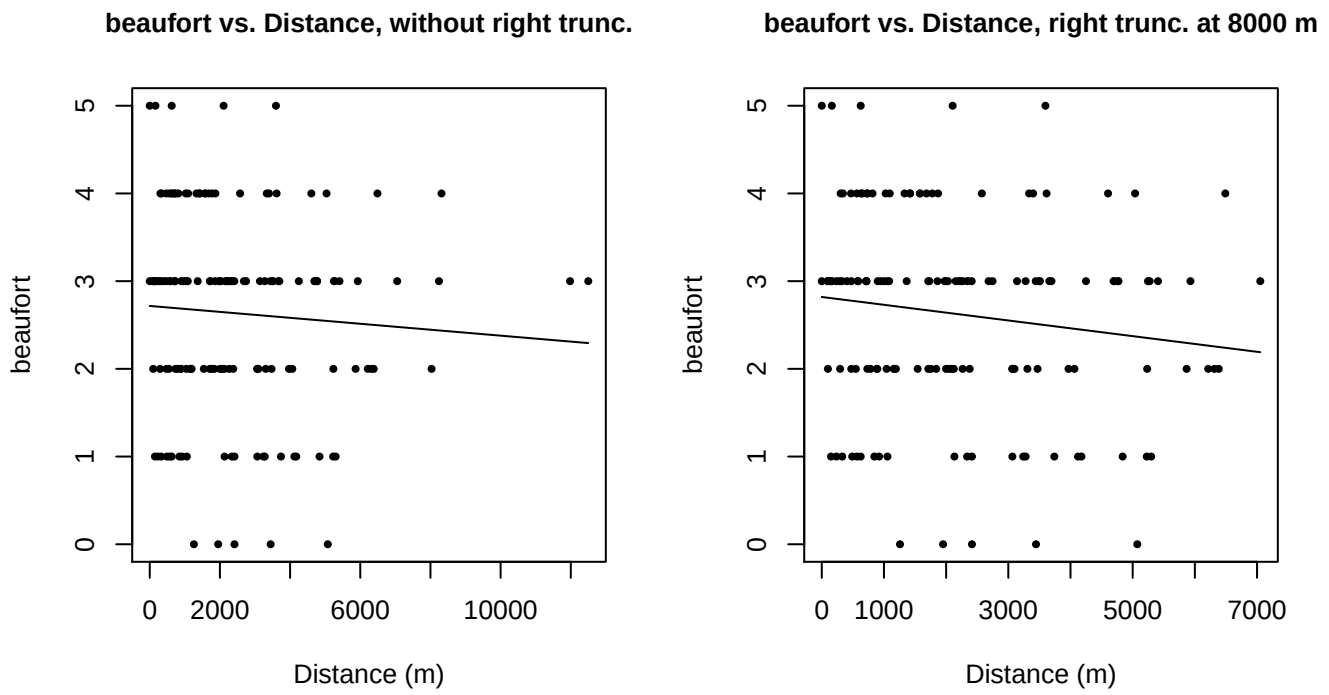

Figure 17: Scatterplots showing the relationship between Beaufort sea state and perpendicular sighting distance, for all sightings (left) and only those not right truncated (right). The line is a simple linear regression.

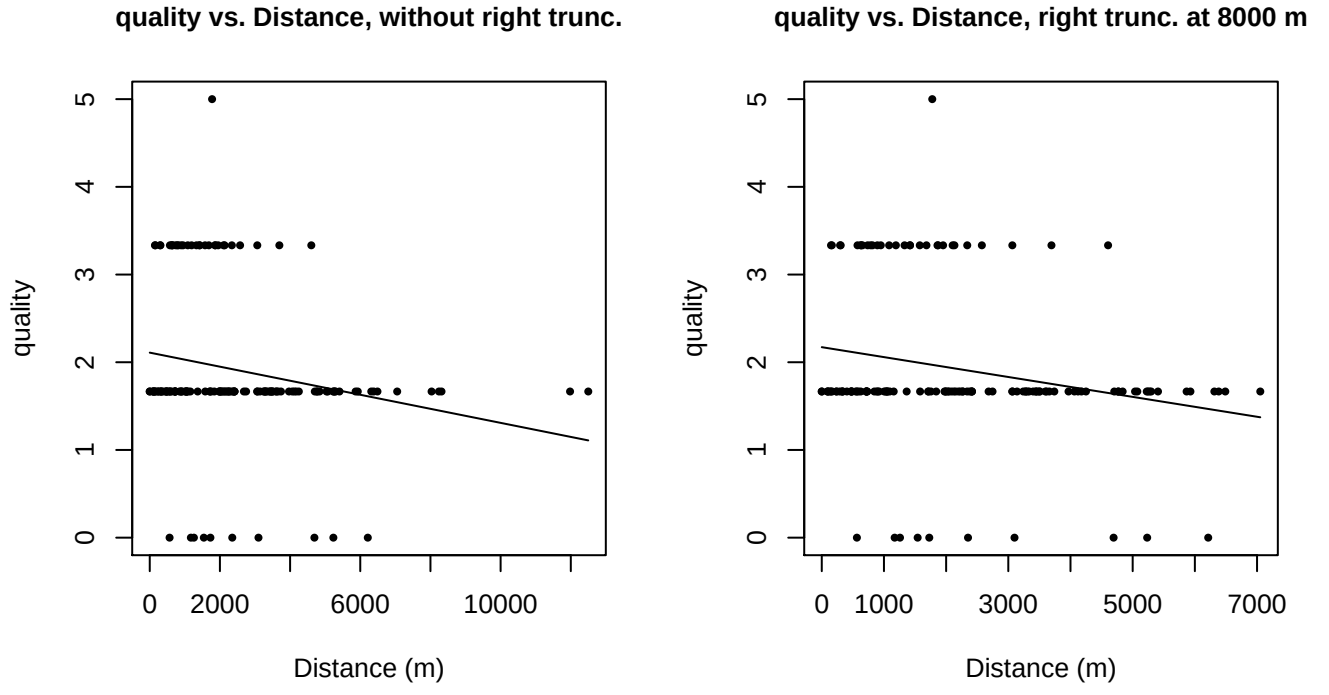

Figure 18: Scatterplots showing the relationship between the survey-specific index of the quality of observation conditions and perpendicular sighting distance, for all sightings (left) and only those not right truncated (right). Low values of the quality index correspond to better observation conditions. The line is a simple linear regression.

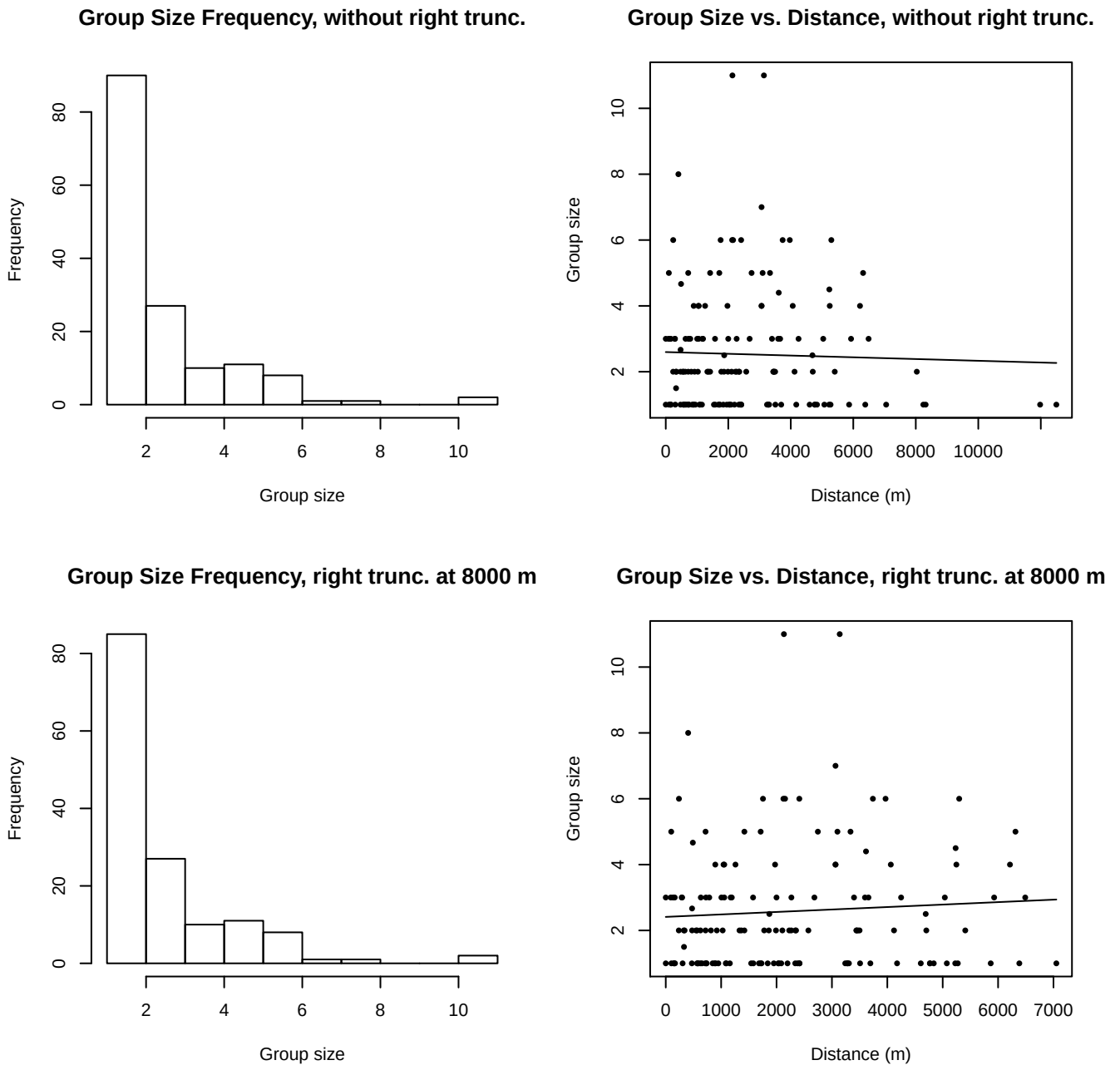

Figure 19: Histograms showing group size frequency and scatterplots showing the relationship between group size and perpendicular sighting distance, for all sightings (top row) and only those not right truncated (bottom row). In the scatterplot, the line is a simple linear regression.

Aerial Surveys

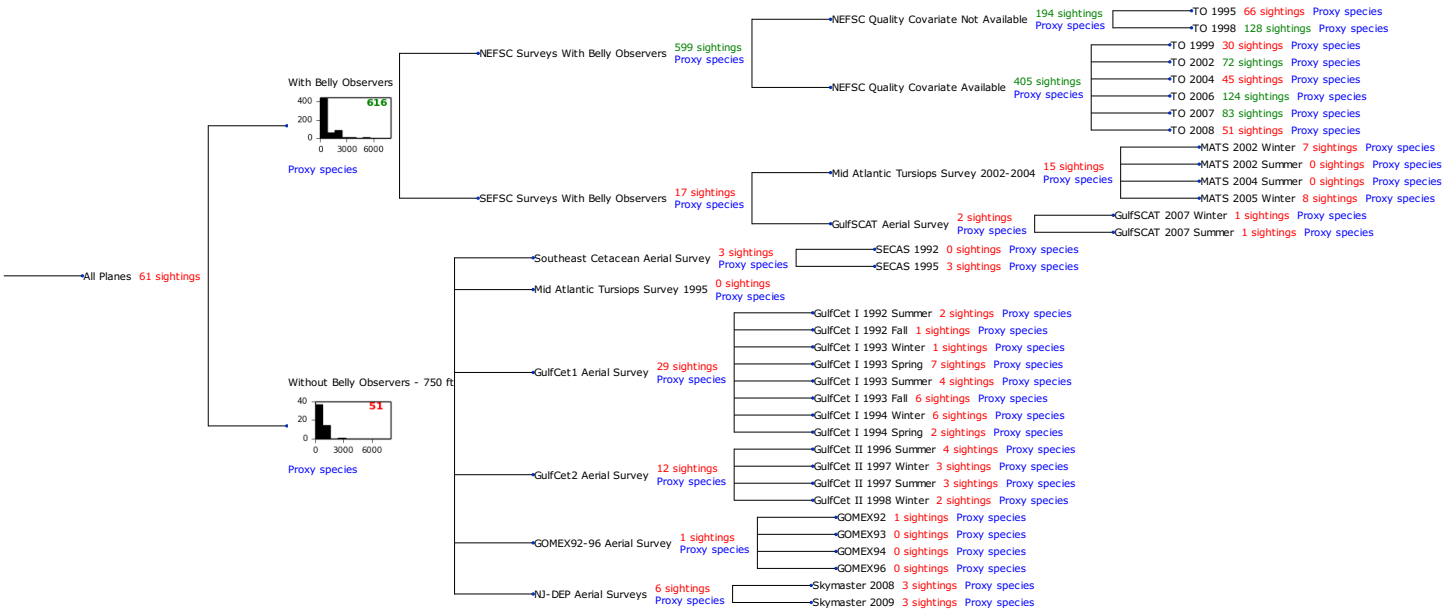

Figure 20: Detection hierarchy for aerial surveys

With Belly Observers

Because this taxon was sighted too infrequently to fit a detection function to its sightings alone, we fit a detection function to the pooled sightings of several other species that we believed would exhibit similar detectability. These "proxy species" are listed below.

Reported By Observer	Common Name	n
Balaenoptera	Balaenopterid sp.	2
Balaenoptera acutorostrata	Minke whale	97
Balaenoptera borealis	Sei whale	14
Balaenoptera borealis/edeni	Sei or Bryde's whale	0
Balaenoptera borealis/physalus	Fin or Sei whale	0
Balaenoptera edeni	Bryde's whale	2
Balaenoptera musculus	Blue whale	1
Balaenoptera physalus	Fin whale	235
Eubalaena glacialis	North Atlantic right whale	43
Eubalaena glacialis/Megaptera novaeangliae	Right or humpback whale	0
Megaptera novaeangliae	Humpback whale	198
Physeter macrocephalus	Sperm whale	24
Total		616

Table 10: Proxy species used to fit detection functions for With Belly Observers. The number of sightings, n, is before truncation.

The sightings were right truncated at 2000m.

Covariate	Description
beaufort	Beaufort sea state.
size	Estimated size (number of individuals) of the sighted group.

Table 11: Covariates tested in candidate "multi-covariate distance sampling" (MCDS) detection functions.

Key	Adjustment	Order	Covariates	Succeeded	Δ AIC	Mean ESHW (m)
hn	cos	2		Yes	0.00	593
hr	poly	4		Yes	2.46	609
hr			size	Yes	6.54	633
hr				Yes	8.64	629
hr	poly	2		Yes	10.64	629
hn	cos	3		Yes	11.17	586
hn			size	Yes	21.95	700
hn				Yes	22.65	698
hn	herm	4		Yes	24.22	697
hr			beaufort	No		
hn			beaufort	No		
hr			beaufort, size	No		
hn			beaufort, size	No		

Table 12: Candidate detection functions for With Belly Observers. The first one listed was selected for the density model.

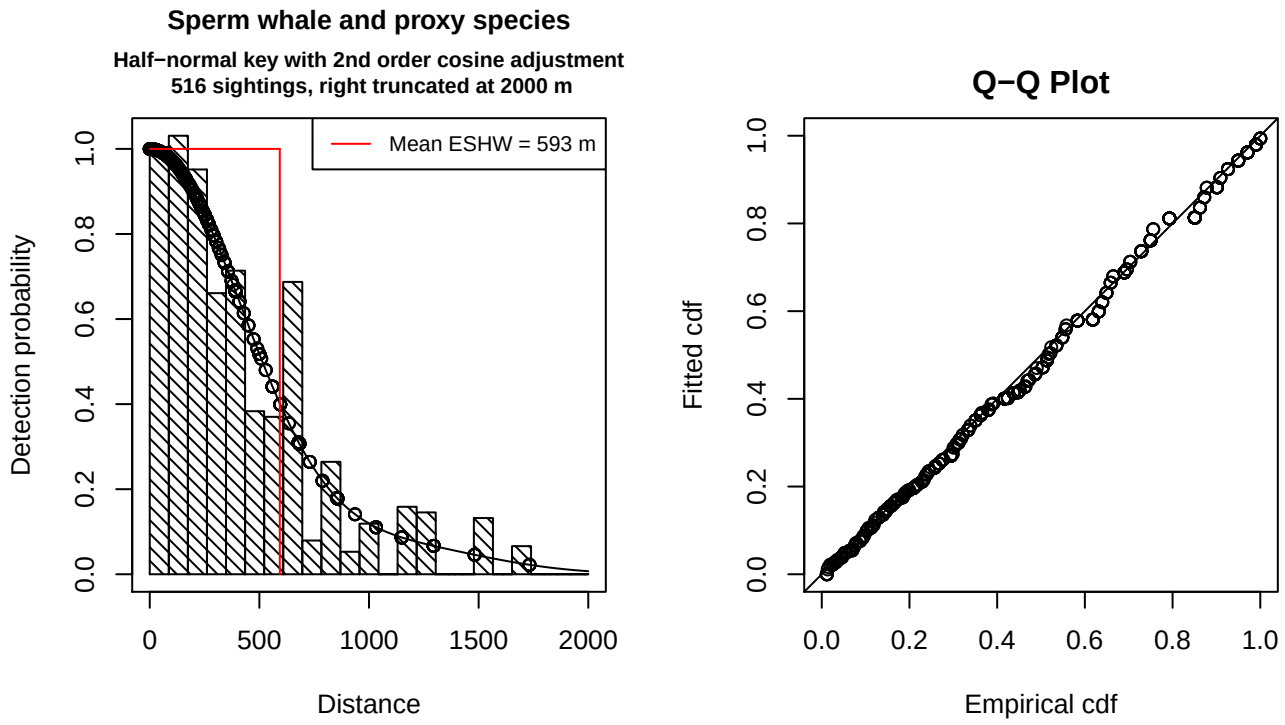

Figure 21: Detection function for With Belly Observers that was selected for the density model

Statistical output for this detection function:

```
Summary for ds object
Number of observations :  516
Distance range         :  0  -  2000
AIC                    :  7251.083

Detection function:
 Half-normal key function with cosine adjustment term of order 2

Detection function parameters
Scale Coefficients:
            estimate         se
(Intercept) 6.456112 0.04236696

Adjustment term parameter(s):
             estimate         se
cos, order 2  0.41854 0.07899307


Monotonicity constraints were enforced.
                        Estimate          SE         CV
Average p              0.2965255  0.01114114 0.03757228
N in covered region 1740.1541496 91.66829334 0.05267826

Monotonicity constraints were enforced.
```

Additional diagnostic plots:

Figure 22: Scatterplots showing the relationship between Beaufort sea state and perpendicular sighting distance, for all sightings (left) and only those not right truncated (right). The line is a simple linear regression.

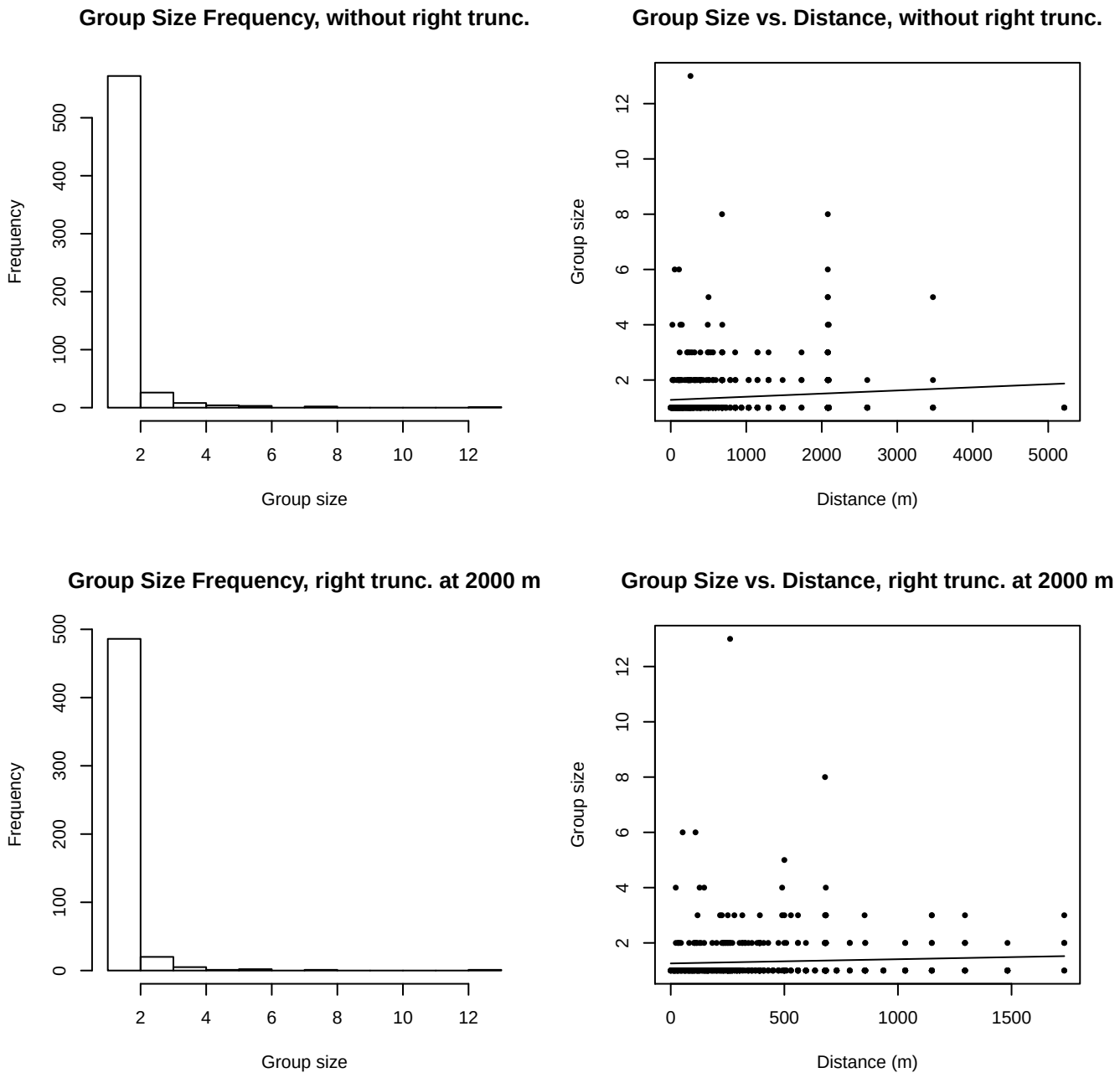

Figure 23: Histograms showing group size frequency and scatterplots showing the relationship between group size and perpendicular sighting distance, for all sightings (top row) and only those not right truncated (bottom row). In the scatterplot, the line is a simple linear regression.

Without Belly Observers - 750 ft

Because this taxon was sighted too infrequently to fit a detection function to its sightings alone, we fit a detection function to the pooled sightings of several other species that we believed would exhibit similar detectability. These "proxy species" are listed below.

Reported By Observer	Common Name	n
Balaenoptera	Balaenopterid sp.	1
Balaenoptera acutorostrata	Minke whale	0

Balaenoptera borealis	Sei whale	0
Balaenoptera borealis/edeni	Sei or Bryde's whale	2
Balaenoptera borealis/physalus	Fin or Sei whale	0
Balaenoptera edeni	Bryde's whale	3
Balaenoptera musculus	Blue whale	0
Balaenoptera physalus	Fin whale	2
Eubalaena glacialis	North Atlantic right whale	0
Eubalaena glacialis/Megaptera novaeangliae	Right or humpback whale	0
Megaptera novaeangliae	Humpback whale	6
Physeter macrocephalus	Sperm whale	37
Total		51

Table 13: Proxy species used to fit detection functions for Without Belly Observers - 750 ft. The number of sightings, n, is before truncation.

The sightings were right truncated at 600m. Due to a reduced frequency of sightings close to the trackline that plausibly resulted from the behavior of the observers and/or the configuration of the survey platform, the sightings were left truncted as well. Sightings closer than 40 m to the trackline were omitted from the analysis, and it was assumed that the the area closer to the trackline than this was not surveyed. This distance was estimated by inspecting histograms of perpendicular sighting distances. The vertical sighting angles were heaped at 10 degree increments, so the candidate detection functions were fitted using linear bins scaled accordingly.

Key	Adjustment	Order	Covariates	Succeeded	Δ AIC	Mean ESHW (m)
hn	cos	2		Yes	0.00	216
hr				Yes	0.59	251
hn	cos	3		Yes	2.31	255
hn	herm	4		Yes	2.46	316
hr	poly	2		Yes	2.59	251
hr	poly	4		Yes	2.68	244
hn				No		

Table 14: Candidate detection functions for Without Belly Observers - 750 ft. The first one listed was selected for the density model.

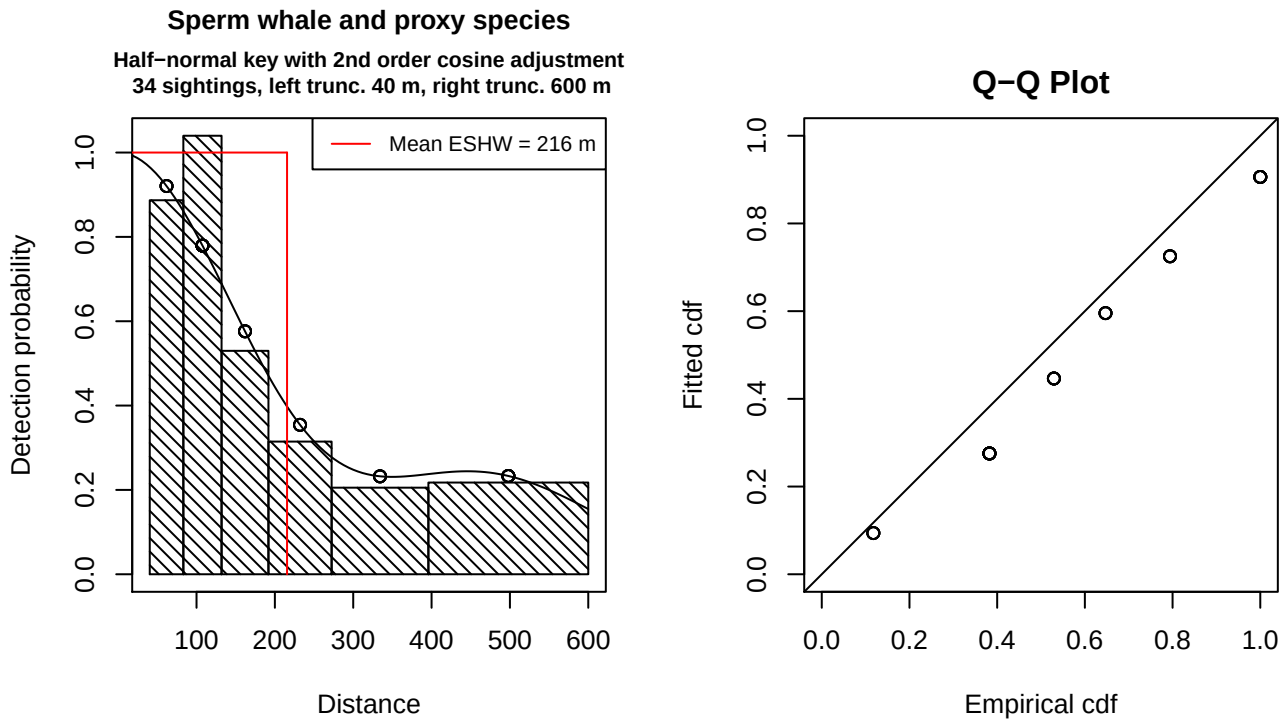

Figure 24: Detection function for Without Belly Observers - 750 ft that was selected for the density model

Statistical output for this detection function:

```
Summary for ds object
Number of observations :  34
Distance range         :  40.30835  -  600
AIC                    :  124.984

Detection function:
 Half-normal key function with cosine adjustment term of order 2

Detection function parameters
Scale Coefficients:
            estimate        se
(Intercept) 5.738324 0.1838281

Adjustment term parameter(s):
              estimate       se
cos, order 2 0.4333817 0.242253


Monotonicity constraints were enforced.
                     Estimate         SE        CV
Average p            0.3592781  0.0870934 0.2424122
N in covered region 94.6341992 26.3634680 0.2785829

Monotonicity constraints were enforced.
```

Additional diagnostic plots:

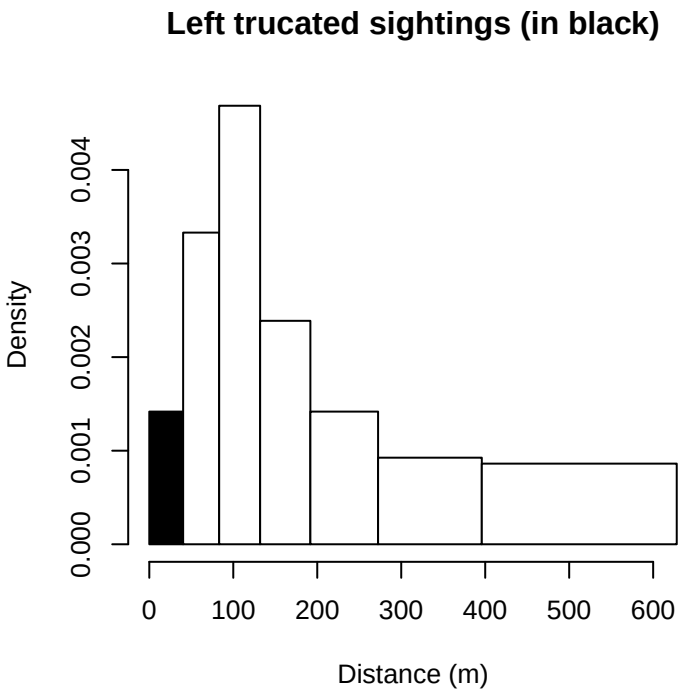

Figure 25: Density of sightings by perpendicular distance for Without Belly Observers - 750 ft. Black bars on the left show sightings that were left truncated.

g(0) Estimates

Platform	Surveys	Group Size	*g(0)*	Biases Addressed	Source
Shipboard	All	Any	0.53	Both	Barlow and Sexton (1996)
Aerial	All	Any	0.154	Availability	Watwood et al. (2006)

Table 15: Estimates of *g(0)* used in this density model.

No survey-specific g(0) estimates were available for our shipboard surveys. Instead, we relied on results from Barlow and Sexton's (1996) simulation model, using dive data reported by Watwood et al. (2006). Using DTAGs, Watwood et al. tracked sperm whales in three regions and reported an average dive cycle consisting of a 45 min dive followed by a 9 min surface interval, with sperm whales in the Gulf of Mexico averaging 45.5 min and 8.1 min, yielding a total dive cycle of 53.6 min. Using these data, we consulted Barlow and Sexton (1996), who modeled g(0) for sperm whales observed from shipboard surveys that utilized 25x binoculars. Their estimates accounted for both availability and perception bias. For a 60 min dive cycle, Barlow and Sexton estimated g(0)=0.53. Note that this differs from other publications such as Whitehead (2002) that assumed a 30 min dive cycle, yielding g(0)=0.87. Barlow and Sexton described the 30 minute cycle as typical for mixed groups with calves and the 60 minute cycle as typical for solitary large males. But Watwood et al. reported that their 53.6 min dive cycle was obtained from groups composed predominantly of females and immature whales, and advised that their results were most relevant for those age/sex classes.

No estimate of g(0) was available in the literature for sperm whales sighted on aerial surveys. Sperm whales are long-diving animals (Barlow and Sexton, 1996), thus availability bias is likely to be substantial. Utilizing equation (3) of Carretta et al. (2000) (which follows Barlow et al. 1988), we computed the availability bias component of g(0) from the mean surface and dive intervals (8.1 min and 45.5 min) for sperm whales in the Gulf of Mexico reported by Watwood et al. (2006). We did not obtain an estimate of perception bias, but perception bias for whales is expected to be negligible (Carretta et al. 2000).

Density Models

Sperm whales are distributed throughout the off-shelf waters of the Gulf of Mexico, including within the exclusive economic zones of the United States, Mexico, and Cuba. Studies of sperm whale morphology, genetics, vocalizations, and movements of individuals indicate that the Gulf of Mexico population is distinct from the North Atlantic population (Waring et al. 2013). Satellite tracks of 52 whales showed no discernible seasonal migrations, with some Gulf-wide movements occurring primarily along the northern slope of the Gulf (Jochens et al. 2008).

Sperm whales can occur anywhere in the Gulf of Mexico off the continental shelf, but are often associated with the continental slope and canyons, particularly those near the Mississippi River (Jochens et al. 2008). Although the prey species of Gulf sperm whales is unknown, a series of studies advanced the hypothesis that eddies transport nutrient-rich water from the shelf or upwell it from depth, driving primary productivity along the continental slope and supporting assemblages of possible prey (Biggs et al. 2005, Jochens et al. 2008). As elsewhere, sperm whales foraging in the Gulf of Mexico undertake long, deep dives (Watwood et al. 2006, Jochens et al. 2008).

Given this year-round presence with no discernible seasonal migrations, we modeled sperm whale abundance with a single, year-round model that incorporated all available survey data. There were no sightings on the continental shelf by any survey; we assumed sperm whales were always absent here and fitted a model only to the off-shelf survey segments. We used the 100m isobath as the shelf break, to ensure that the model included some segments that were shallower than the shallowest sperm whale sightings. Although the bulk of the survey effort was in non- winter months, we allowed the models to predict through all months of the year. The results should be viewed with caution (see Discussion section below).

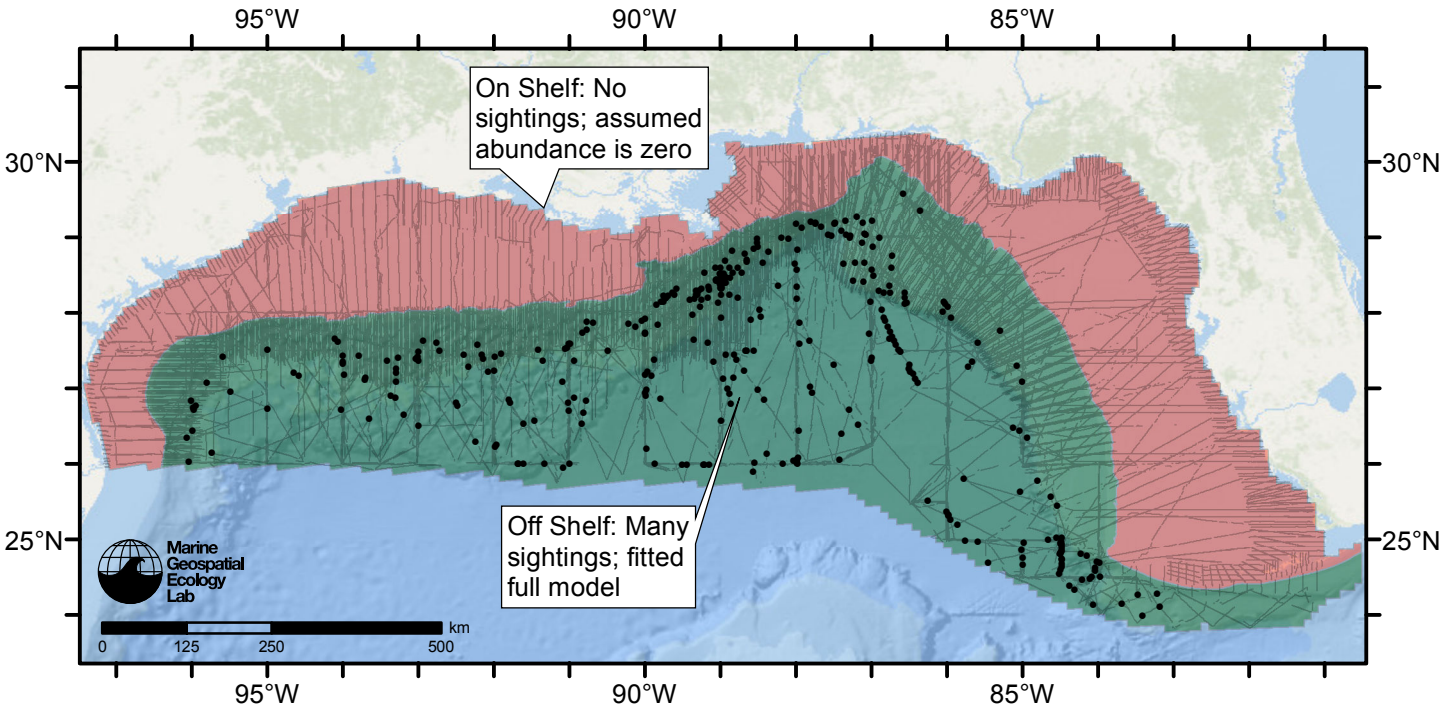

Figure 26: Sperm whale density model schematic. All on-effort sightings are shown, including those that were truncated when detection functions were fitted.

Climatological Model

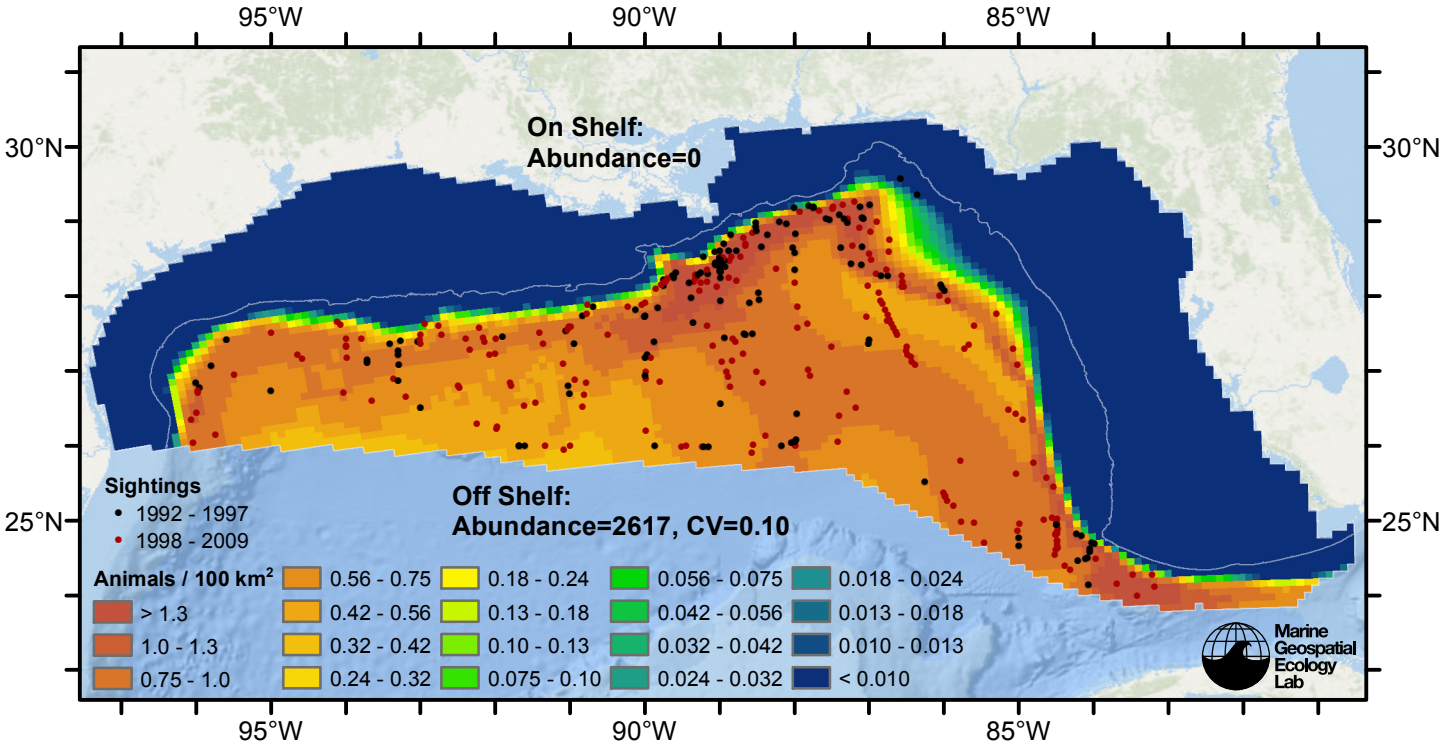

Figure 27: Sperm whale density predicted by the climatological model that explained the most deviance. Pixels are 10x10 km. The legend gives the estimated individuals per pixel; breaks are logarithmic. Abundance for each region was computed by summing the density cells occuring in that region.

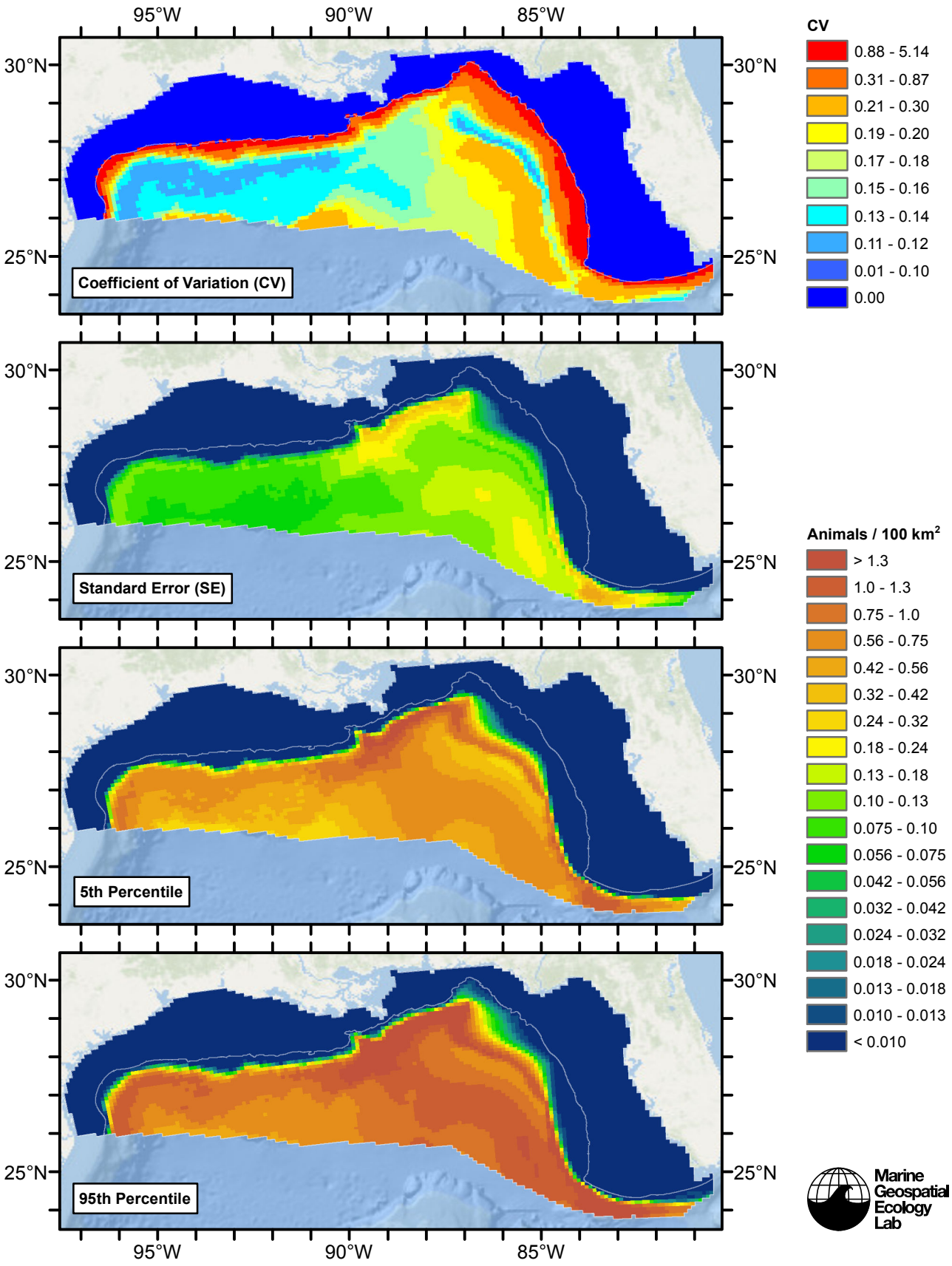

Figure 28: Estimated uncertainty for the climatological model that explained the most deviance. These estimates only incorporate the statistical uncertainty estimated for the spatial model (by the R mgcv package). They do not incorporate uncertainty in the detection functions, g(0) estimates, predictor variables, and so on.

Off Shelf

Statistical output

```
Rscript.exe: This is mgcv 1.8-3. For overview type 'help("mgcv-package")'.


Family: Tweedie(p=1.312)
Link function: log

Formula:
abundance ~ offset(log(area_km2)) + s(log10(Depth), bs = "ts",
    k = 5) + s(log10(pmax(ClimEKE, 0.001)), bs = "ts", k = 5) +
    s(ClimChl1, bs = "ts", k = 5)

Parametric coefficients:
            Estimate Std. Error t value Pr(>|t|)
(Intercept)  -6.4820     0.2406  -26.94   <2e-16 ***
---
Signif. codes:  0 '***' 0.001 '**' 0.01 '*' 0.05 '.' 0.1 ' ' 1

Approximate significance of smooth terms:
                                edf Ref.df      F  p-value
s(log10(Depth))                3.368      4 18.185  < 2e-16 ***
s(log10(pmax(ClimEKE, 0.001))) 1.999      4  4.406 3.72e-05 ***
s(ClimChl1)                    2.396      4 11.456 1.07e-11 ***
---
Signif. codes:  0 '***' 0.001 '**' 0.01 '*' 0.05 '.' 0.1 ' ' 1

R-sq.(adj) =  0.0121   Deviance explained = 16.7%
-REML = 2468.4  Scale est. = 30.276    n = 14455

All predictors were significant. This is the final model.
Creating term plots.
Diagnostic output from gam.check():

Method: REML   Optimizer: outer newton
full convergence after 10 iterations.
Gradient range [-0.0001889608,0.0001301519]
(score 2468.363 & scale 30.2759).
Hessian positive definite, eigenvalue range [0.547907,1153.429].
Model rank =  13 / 13

Basis dimension (k) checking results. Low p-value (k-index<1) may
indicate that k is too low, especially if edf is close to k'.

                                  k'   edf k-index p-value
s(log10(Depth))                4.000 3.368   0.787    0.00
s(log10(pmax(ClimEKE, 0.001))) 4.000 1.999   0.807    0.03
s(ClimChl1)                    4.000 2.396   0.806    0.04

Predictors retained during the model selection procedure: Depth, ClimEKE, ClimChl1

Predictors dropped during the model selection procedure: Slope, DistToCanyon, ClimSST,
ClimDistToFront1, ClimDistToAEddy, ClimDistToCEddy
```

Model term plots

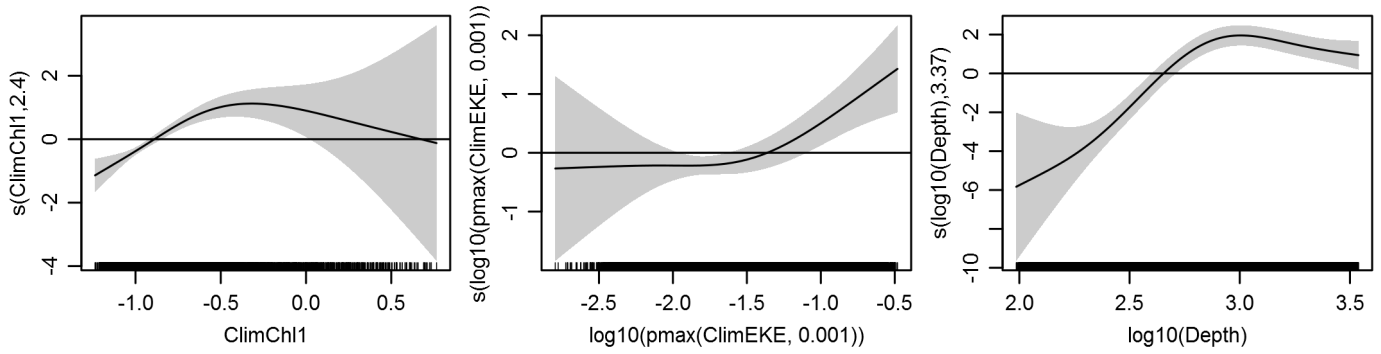

Diagnostic plots

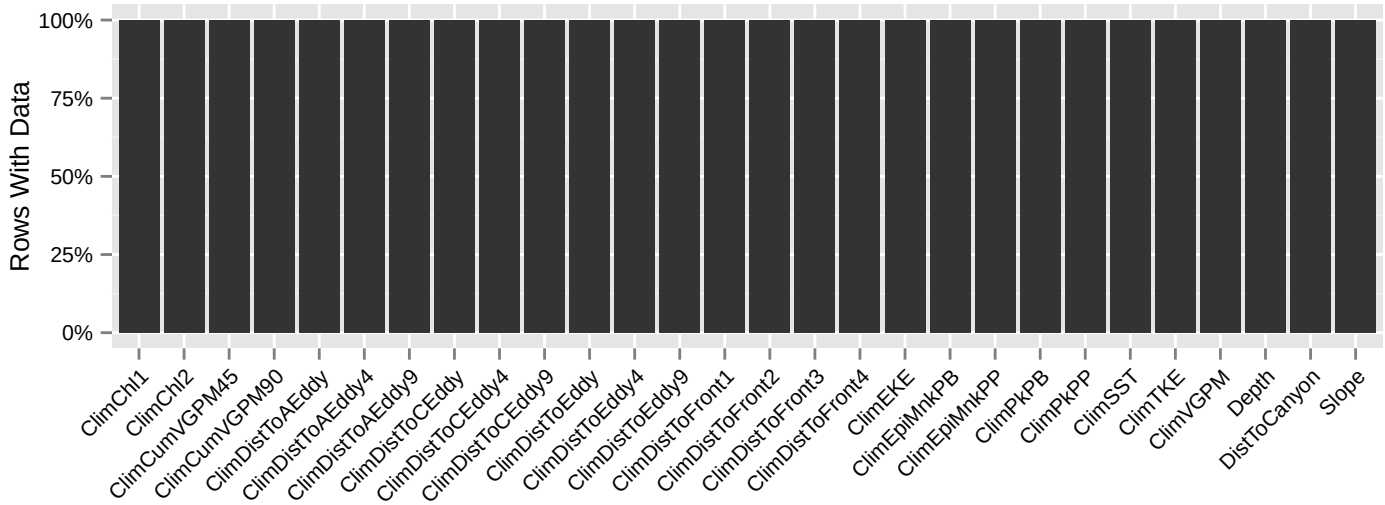

Figure 29: Segments with predictor values for the Sperm whale Climatological model, Off Shelf. This plot is used to assess how many segments would be lost by including a given predictor in a model.

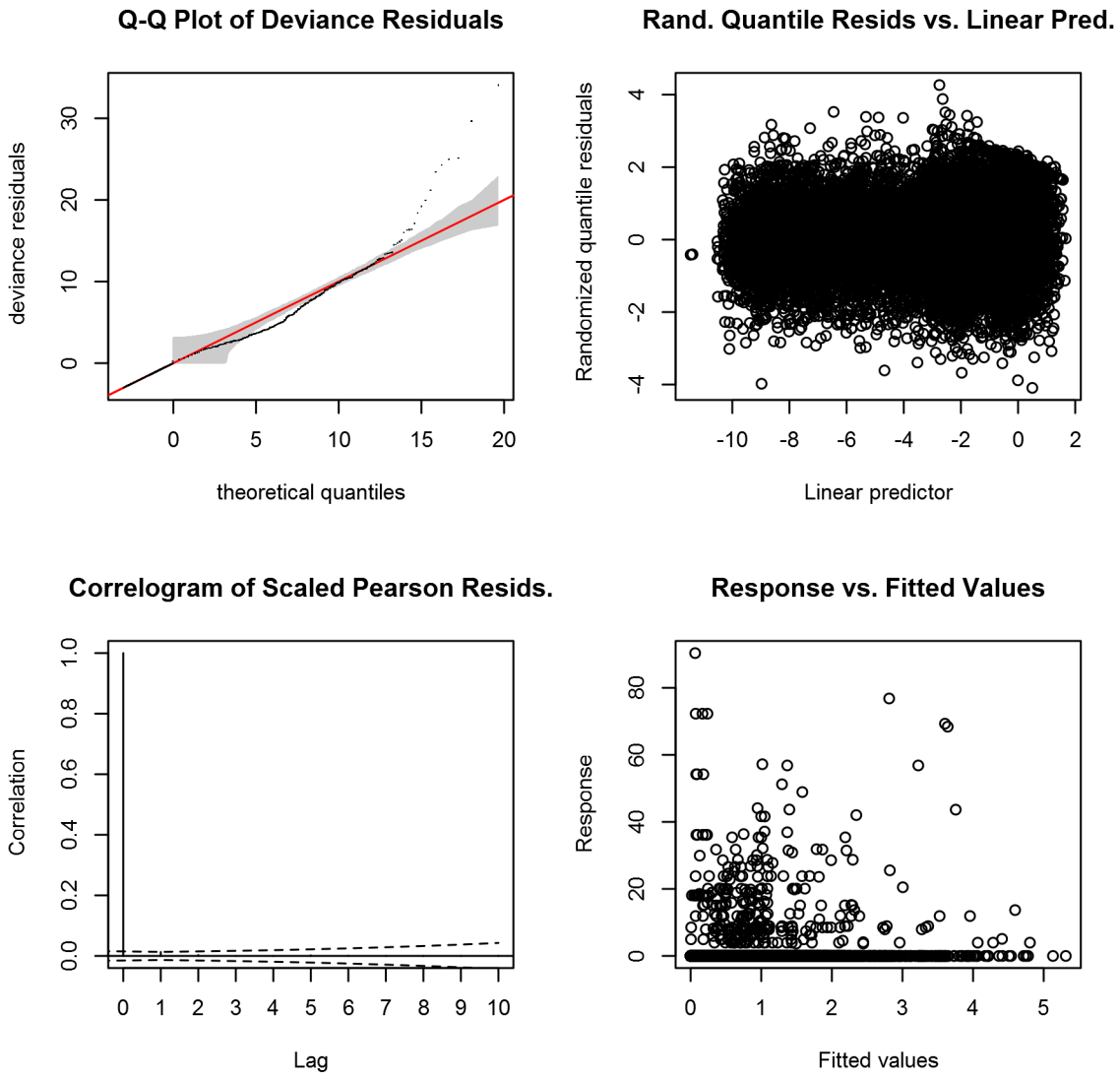

Figure 30: Statistical diagnostic plots for the Sperm whale Climatological model, Off Shelf.

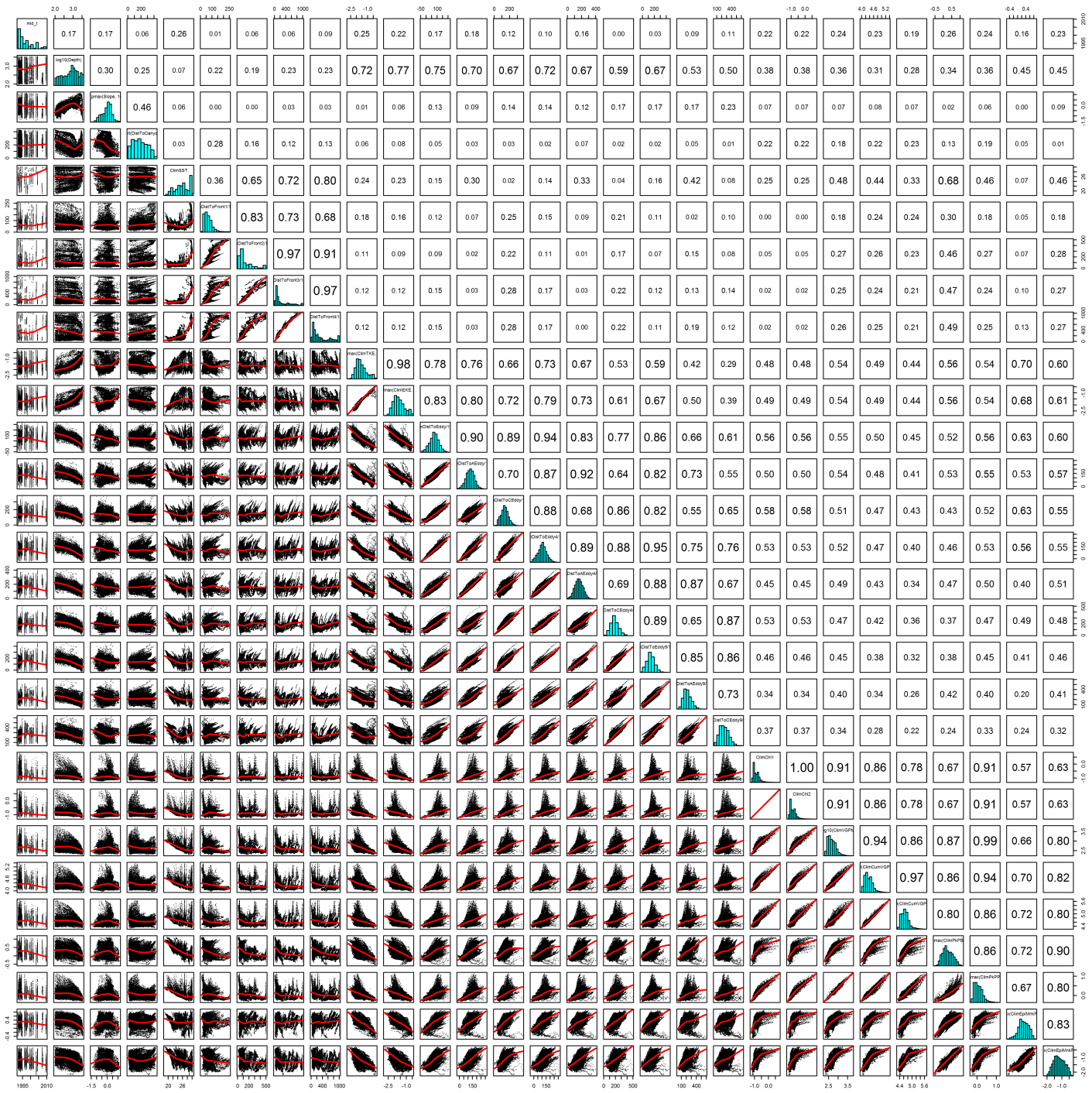

Figure 31: Scatterplot matrix for the Sperm whale Climatological model, Off Shelf. This plot is used to inspect the distribution of predictors (via histograms along the diagonal), simple correlation between predictors (via pairwise Pearson coefficients above the diagonal), and linearity of predictor correlations (via scatterplots below the diagonal). This plot is best viewed at high magnification.

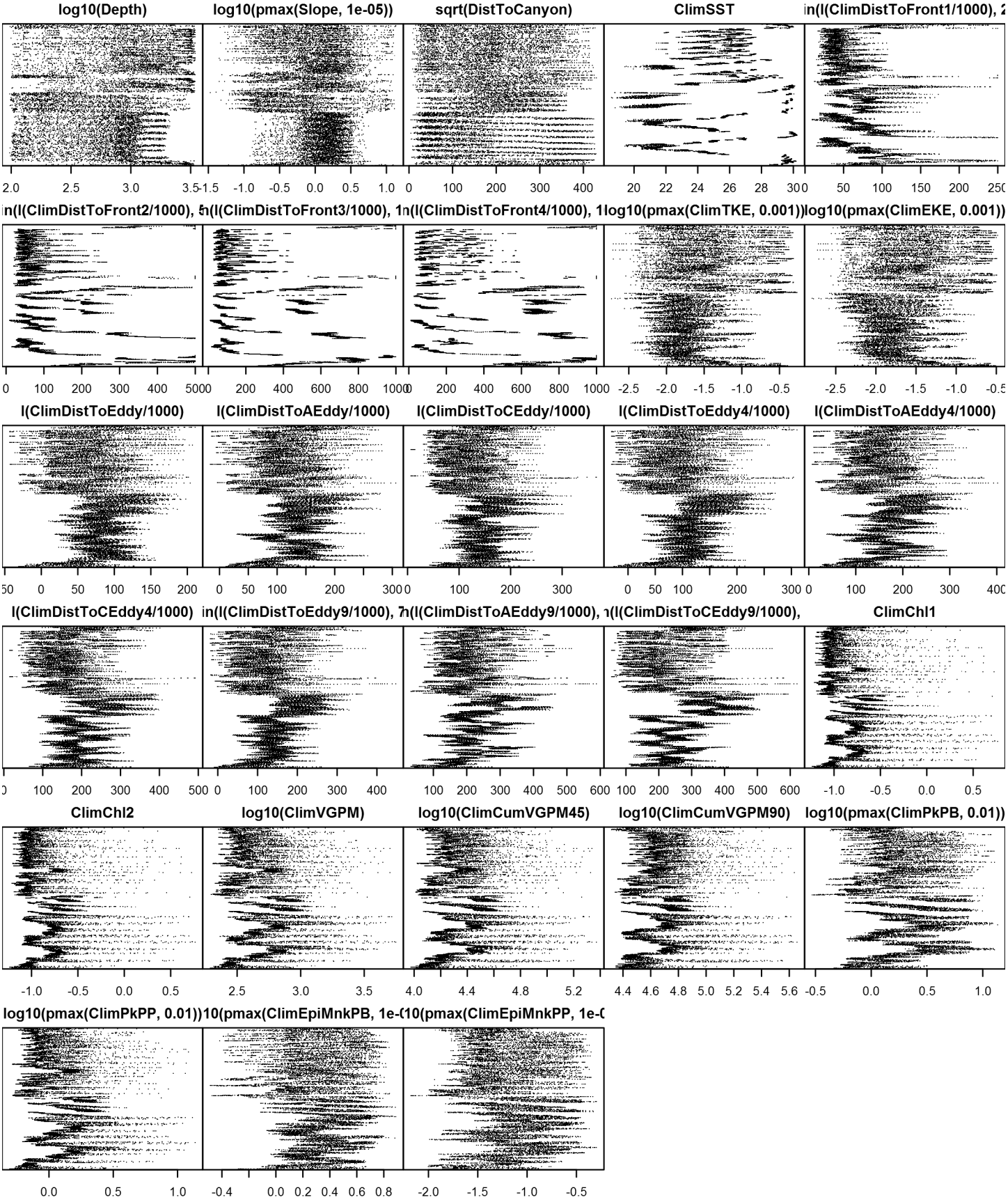

Figure 32: Dotplot for the Sperm whale Climatological model, Off Shelf. This plot is used to check for suspicious patterns and outliers in the data. Points are ordered vertically by transect ID, sequentially in time.

On Shelf

Density assumed to be 0 in this region.

Contemporaneous Model

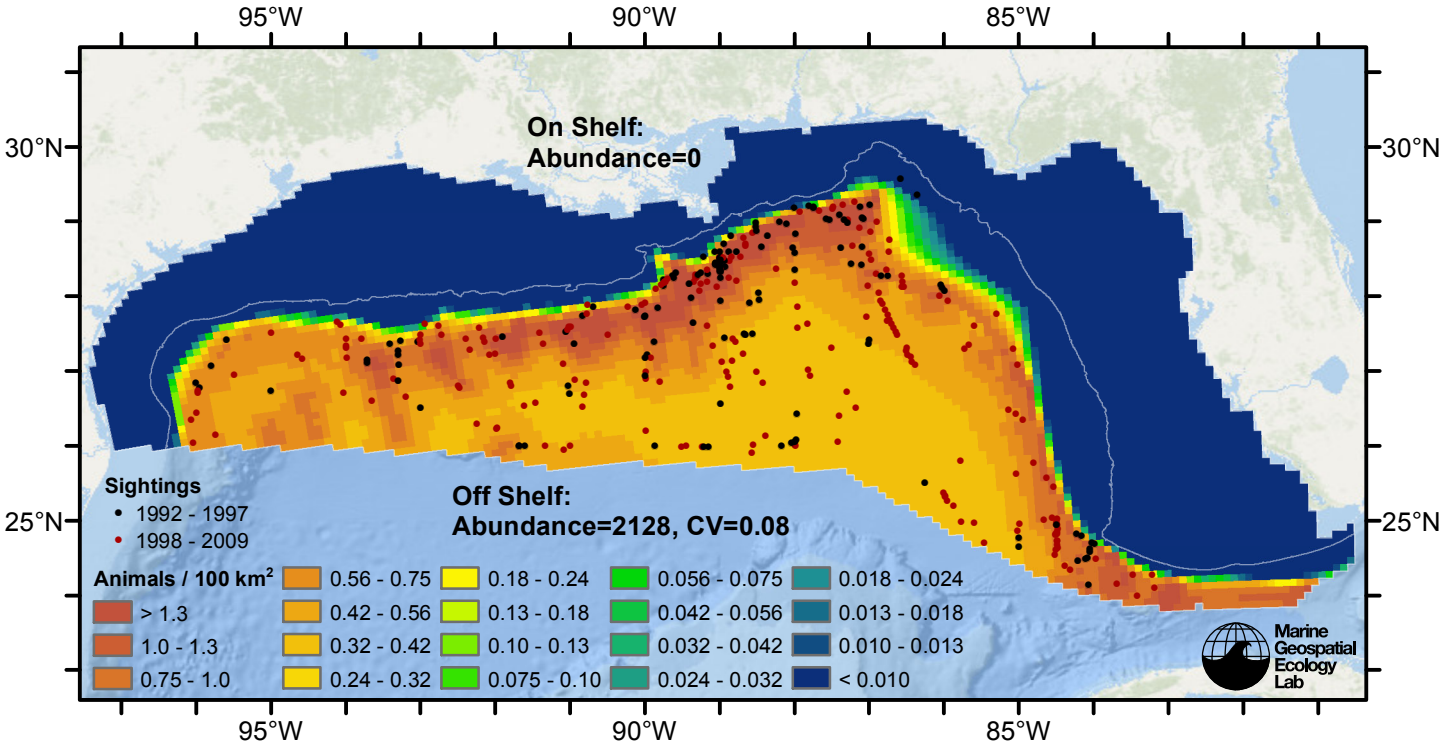

Figure 33: Sperm whale density predicted by the contemporaneous model that explained the most deviance. Pixels are 10x10 km. The legend gives the estimated individuals per pixel; breaks are logarithmic. Abundance for each region was computed by summing the density cells occuring in that region.

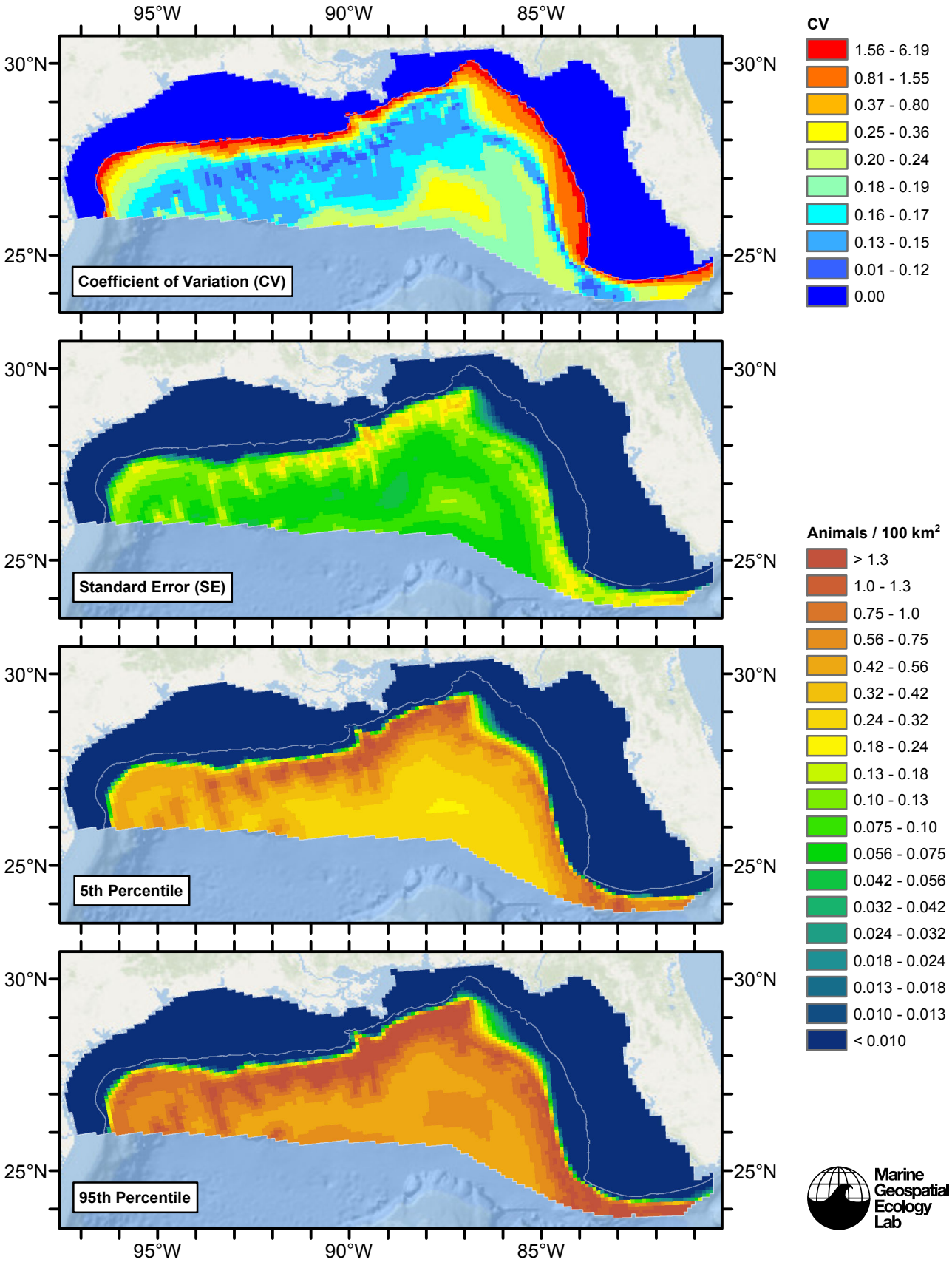

Figure 34: Estimated uncertainty for the contemporaneous model that explained the most deviance. These estimates only incorporate the statistical uncertainty estimated for the spatial model (by the R mgcv package). They do not incorporate uncertainty in the detection functions, g(0) estimates, predictor variables, and so on.

Off Shelf

Statistical output

```
Rscript.exe: This is mgcv 1.8-3. For overview type 'help("mgcv-package")'.


Family: Tweedie(p=1.326)
Link function: log

Formula:
abundance ~ offset(log(area_km2)) + s(log10(Depth), bs = "ts",
    k = 5) + s(sqrt(DistToCanyon), bs = "ts", k = 5) + s(I(DistToAEddy/1000),
    bs = "ts", k = 5)

Parametric coefficients:
            Estimate Std. Error t value Pr(>|t|)
(Intercept)  -6.6760     0.2894  -23.07   <2e-16 ***
---
Signif. codes:  0 '***' 0.001 '**' 0.01 '*' 0.05 '.' 0.1 ' ' 1

Approximate significance of smooth terms:
                          edf Ref.df      F  p-value
s(log10(Depth))         3.346      4 14.651 2.76e-13 ***
s(sqrt(DistToCanyon))   1.758      4  4.127 6.09e-05 ***
s(I(DistToAEddy/1000)) 1.011      4  4.958 5.09e-06 ***
---
Signif. codes:  0 '***' 0.001 '**' 0.01 '*' 0.05 '.' 0.1 ' ' 1

R-sq.(adj) =  0.00243   Deviance explained =   15%
-REML = 2308.1  Scale est. = 30.701    n = 12621

All predictors were significant. This is the final model.
Creating term plots.
Diagnostic output from gam.check():

Method: REML   Optimizer: outer newton
full convergence after 9 iterations.
Gradient range [-0.0001130601,2.404532e-05]
(score 2308.062 & scale 30.70055).
Hessian positive definite, eigenvalue range [0.2941849,1045.85].
Model rank =  13 / 13

Basis dimension (k) checking results. Low p-value (k-index<1) may
indicate that k is too low, especially if edf is close to k'.

                           k'   edf k-index p-value
s(log10(Depth))         4.000 3.346   0.761    0.00
s(sqrt(DistToCanyon))   4.000 1.758   0.794    0.18
s(I(DistToAEddy/1000)) 4.000 1.011   0.796    0.20

Predictors retained during the model selection procedure: Depth, DistToCanyon, DistToAEddy

Predictors dropped during the model selection procedure: Slope, SST, DistToFront1, TKE, DistToCEddy
```

Model term plots

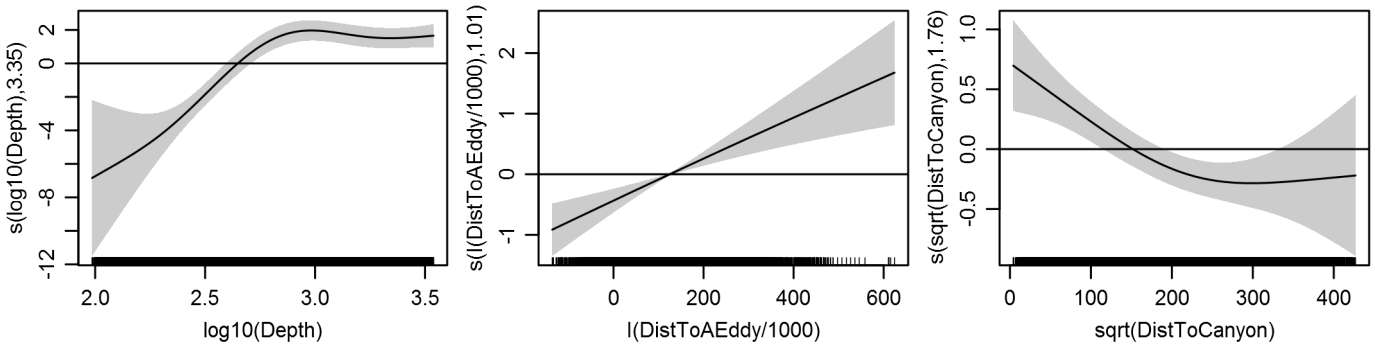

Diagnostic plots

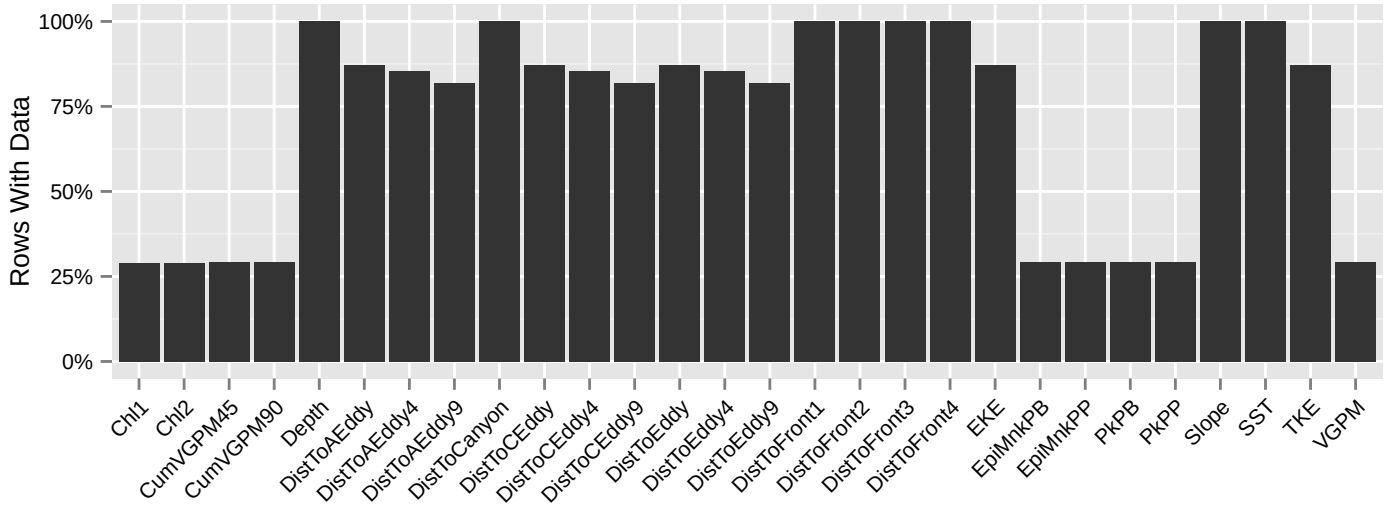

Figure 35: Segments with predictor values for the Sperm whale Contemporaneous model, Off Shelf. This plot is used to assess how many segments would be lost by including a given predictor in a model.

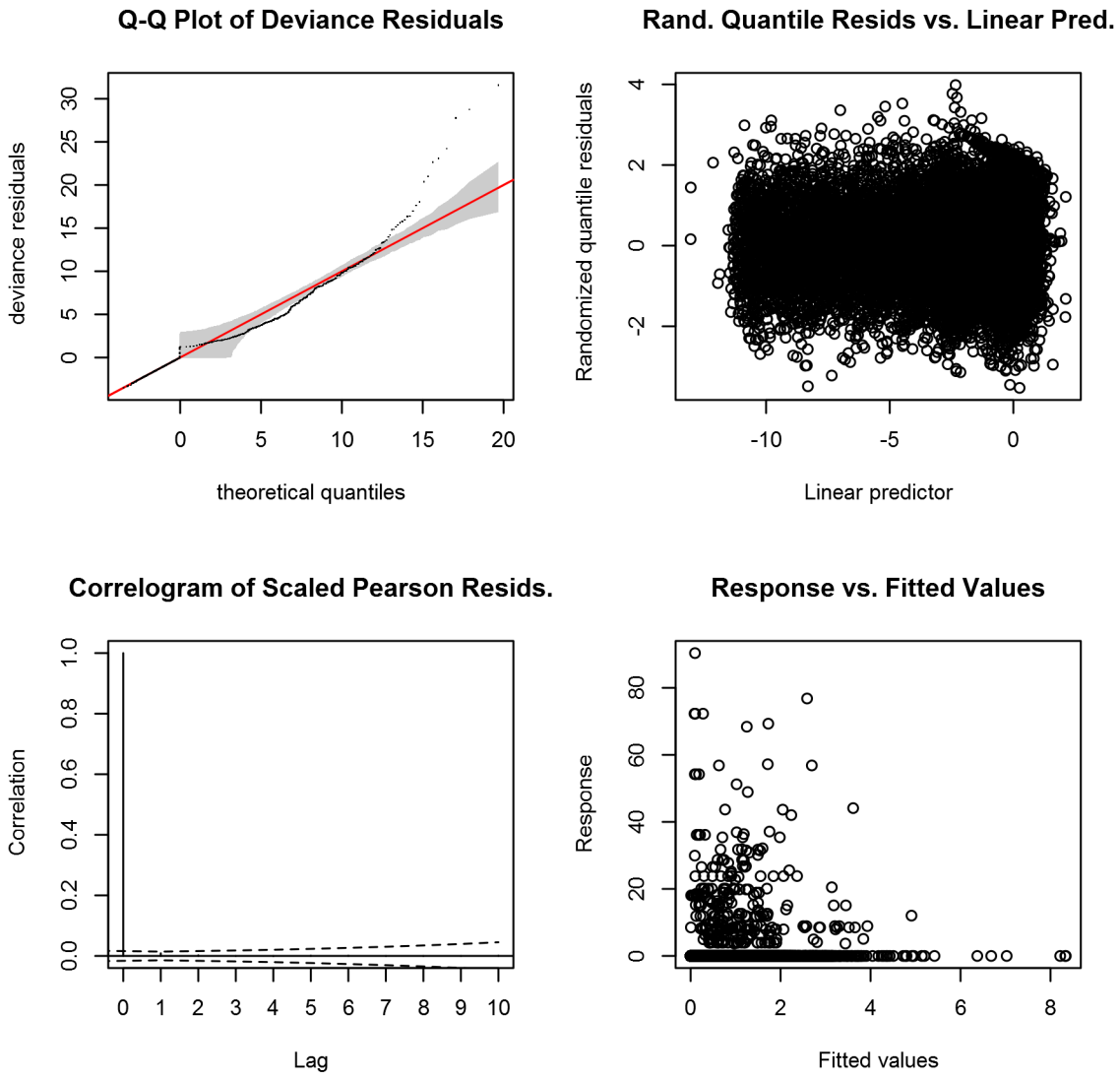

Figure 36: Statistical diagnostic plots for the Sperm whale Contemporaneous model, Off Shelf.

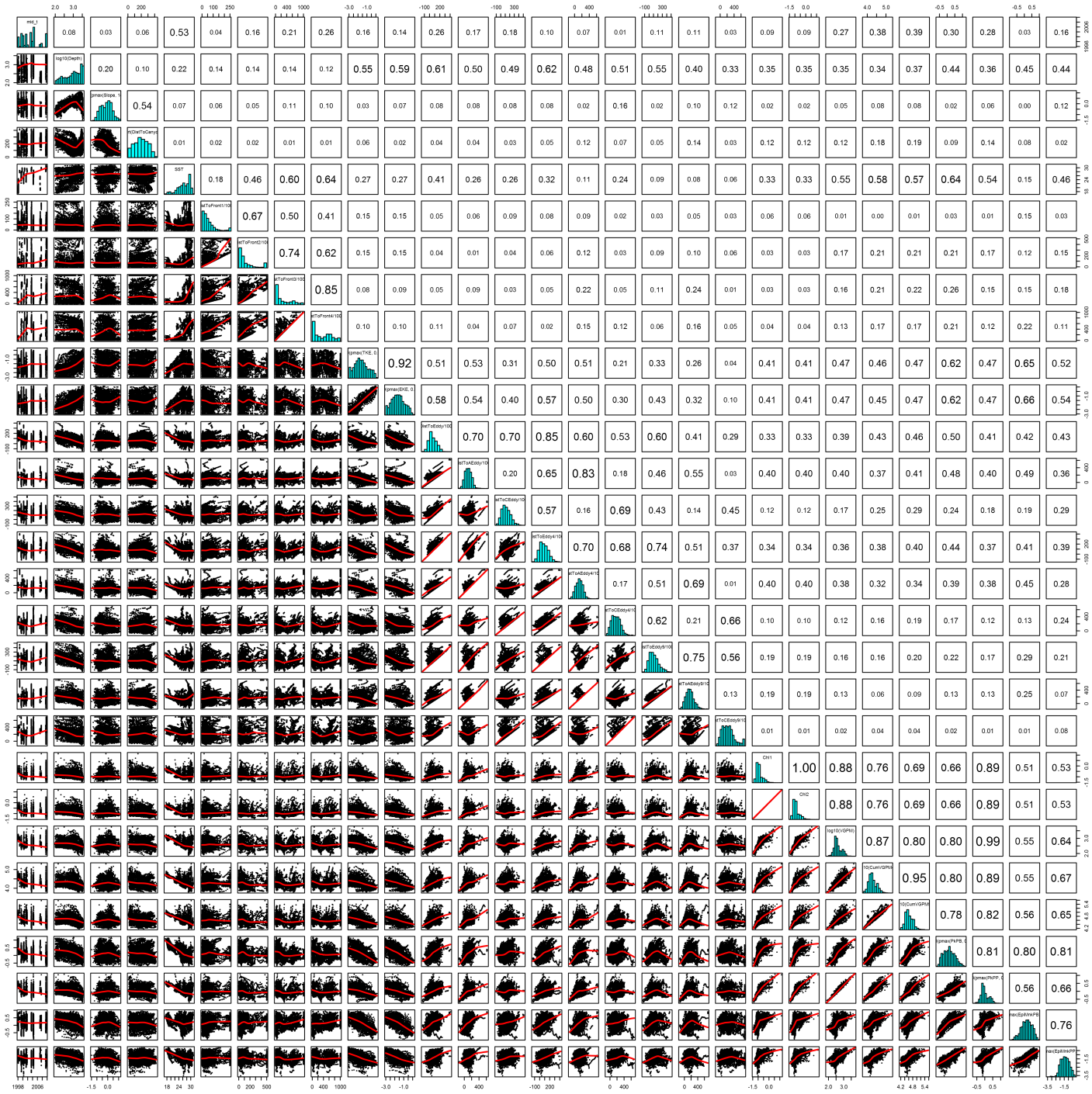

Figure 37: Scatterplot matrix for the Sperm whale Contemporaneous model, Off Shelf. This plot is used to inspect the distribution of predictors (via histograms along the diagonal), simple correlation between predictors (via pairwise Pearson coefficients above the diagonal), and linearity of predictor correlations (via scatterplots below the diagonal). This plot is best viewed at high magnification.

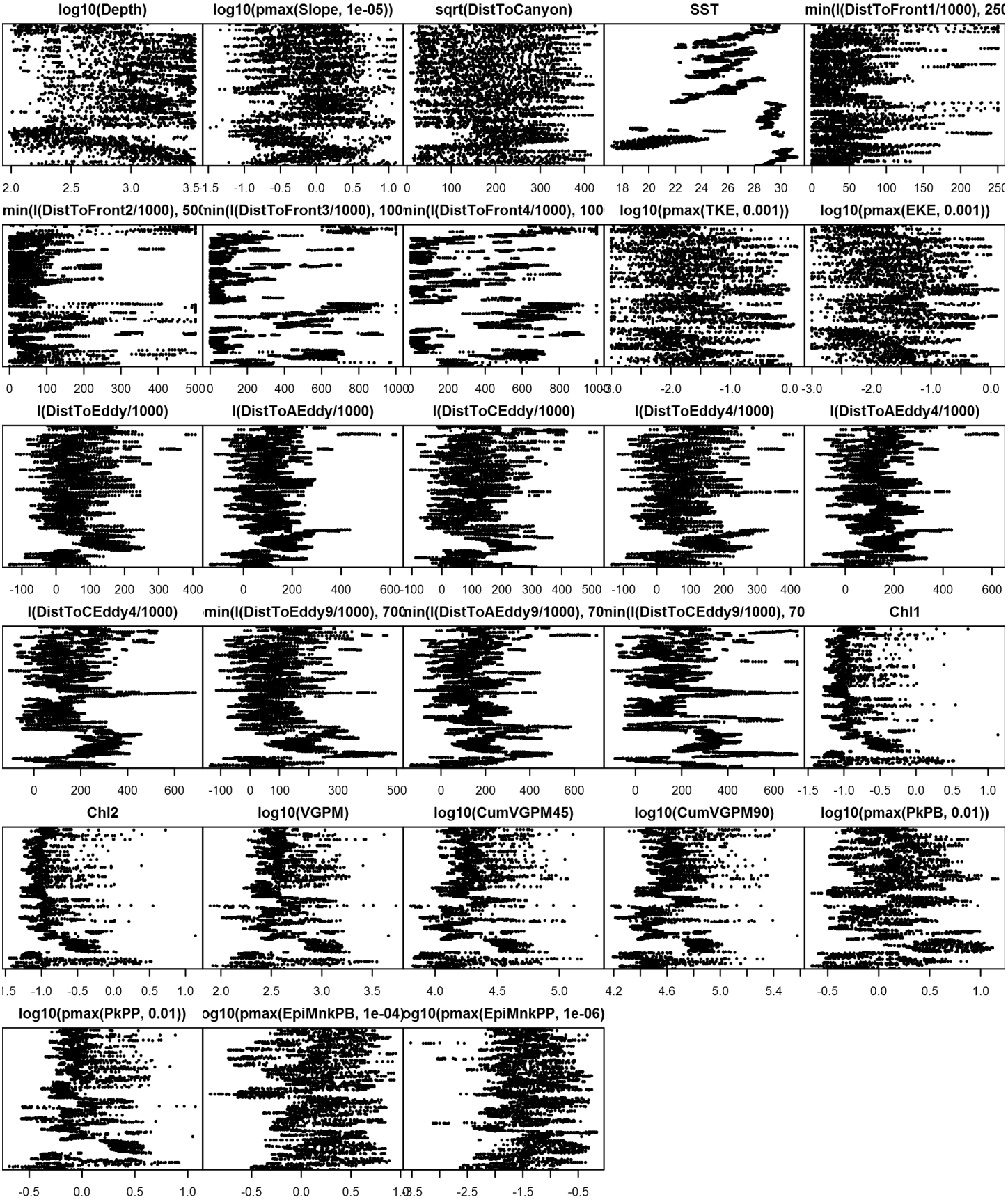

Figure 38: Dotplot for the Sperm whale Contemporaneous model, Off Shelf. This plot is used to check for suspicious patterns and outliers in the data. Points are ordered vertically by transect ID, sequentially in time.

On Shelf

Density assumed to be 0 in this region.

Climatological Same Segments Model

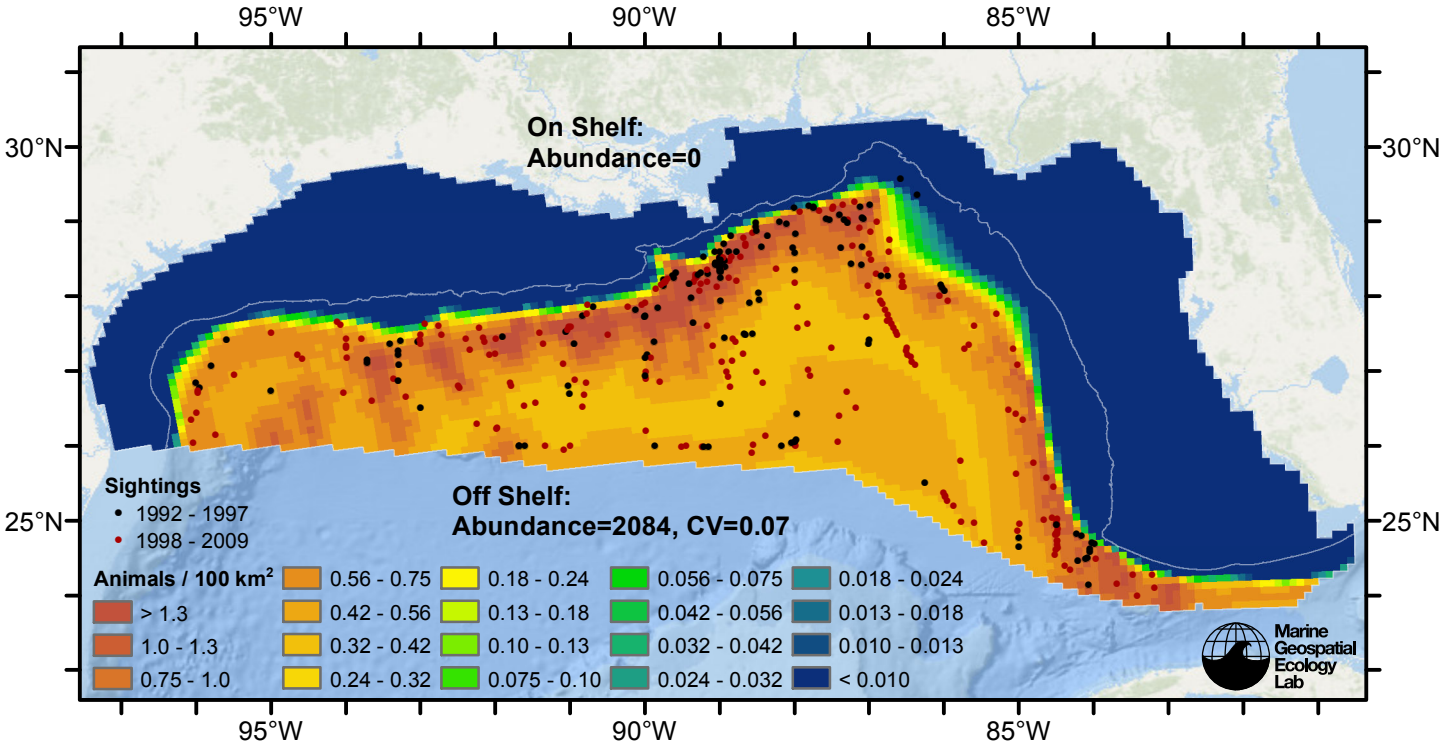

Figure 39: Sperm whale density predicted by the climatological same segments model that explained the most deviance. Pixels are 10x10 km. The legend gives the estimated individuals per pixel; breaks are logarithmic. Abundance for each region was computed by summing the density cells occuring in that region.

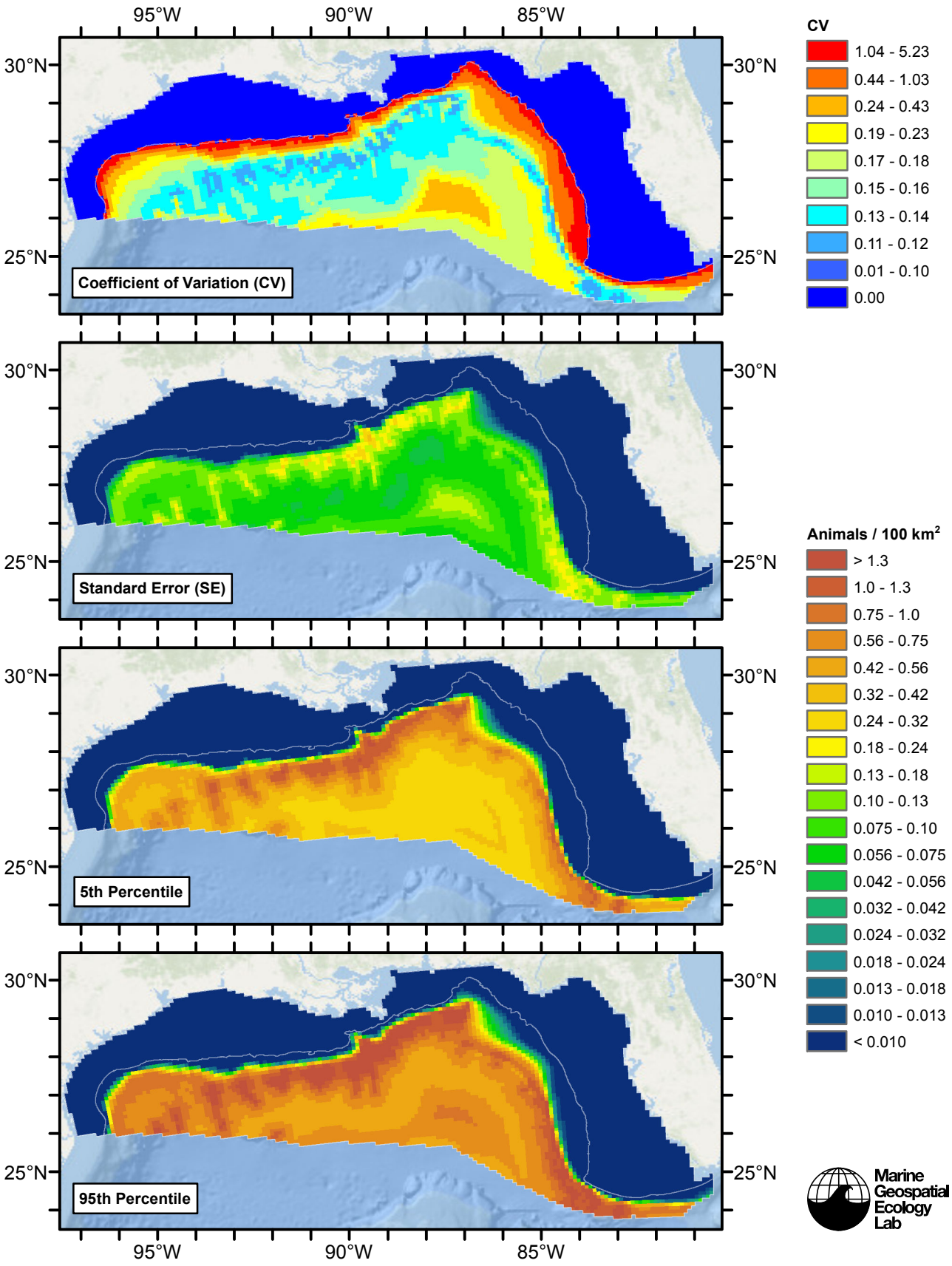

Figure 40: Estimated uncertainty for the climatological same segments model that explained the most deviance. These estimates only incorporate the statistical uncertainty estimated for the spatial model (by the R mgcv package). They do not incorporate uncertainty in the detection functions, g(0) estimates, predictor variables, and so on.

Off Shelf

Statistical output

```
Rscript.exe: This is mgcv 1.8-3. For overview type 'help("mgcv-package")'.


Family: Tweedie(p=1.32)
Link function: log

Formula:
abundance ~ offset(log(area_km2)) + s(log10(Depth), bs = "ts",
    k = 5) + s(sqrt(DistToCanyon), bs = "ts", k = 5)

Parametric coefficients:
            Estimate Std. Error t value Pr(>|t|)
(Intercept)  -6.5068     0.2445  -26.61   <2e-16 ***
---
Signif. codes:  0 '***' 0.001 '**' 0.01 '*' 0.05 '.' 0.1 ' ' 1

Approximate significance of smooth terms:
                        edf Ref.df      F  p-value
s(log10(Depth))       3.410      4 14.907 1.84e-13 ***
s(sqrt(DistToCanyon)) 1.965      4  5.175 7.76e-06 ***
---
Signif. codes:  0 '***' 0.001 '**' 0.01 '*' 0.05 '.' 0.1 ' ' 1

R-sq.(adj) =  0.00609   Deviance explained = 14.6%
-REML = 2479.8  Scale est. = 31.377    n = 14455

All predictors were significant. This is the final model.
Creating term plots.
Diagnostic output from gam.check():

Method: REML   Optimizer: outer newton
full convergence after 9 iterations.
Gradient range [-6.2267e-06,1.522162e-06]
(score 2479.765 & scale 31.37743).
Hessian positive definite, eigenvalue range [0.4355243,1141.909].
Model rank =  9 / 9

Basis dimension (k) checking results. Low p-value (k-index<1) may
indicate that k is too low, especially if edf is close to k'.

                        k'   edf k-index p-value
s(log10(Depth))       4.000 3.410   0.674    0.00
s(sqrt(DistToCanyon)) 4.000 1.965   0.724    0.05

Predictors retained during the model selection procedure: Depth, DistToCanyon

Predictors dropped during the model selection procedure: Slope, ClimSST, ClimDistToFront1
```

Model term plots

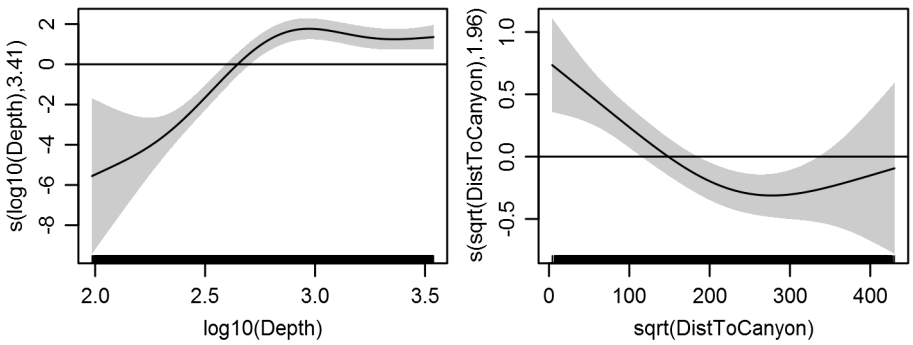

Diagnostic plots

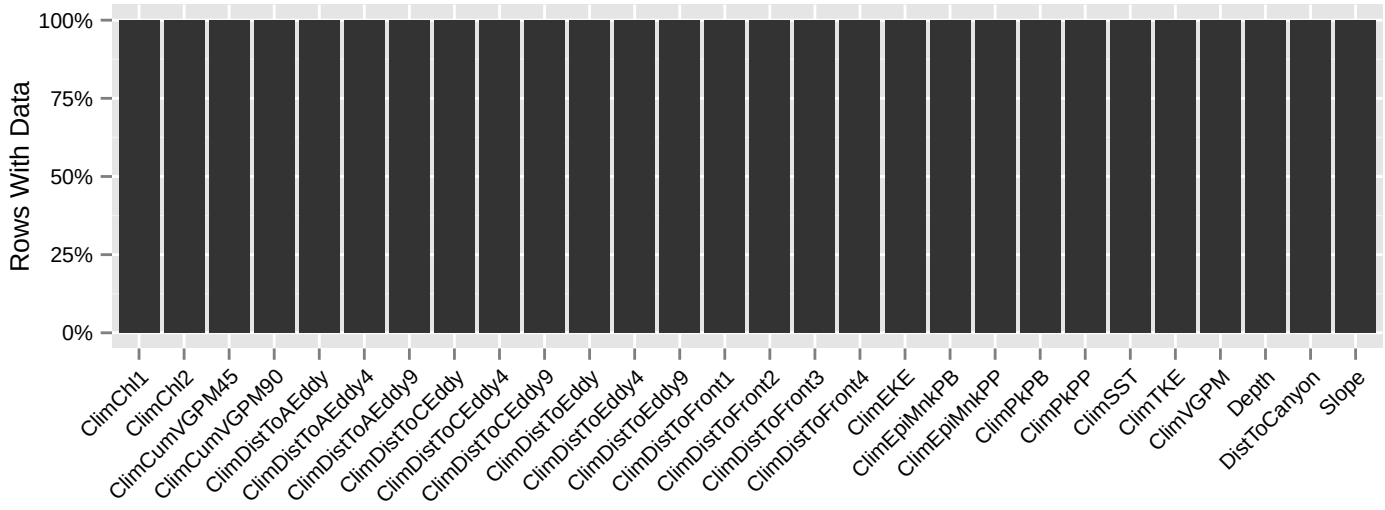

Figure 41: Segments with predictor values for the Sperm whale Climatological model, Off Shelf. This plot is used to assess how many segments would be lost by including a given predictor in a model.

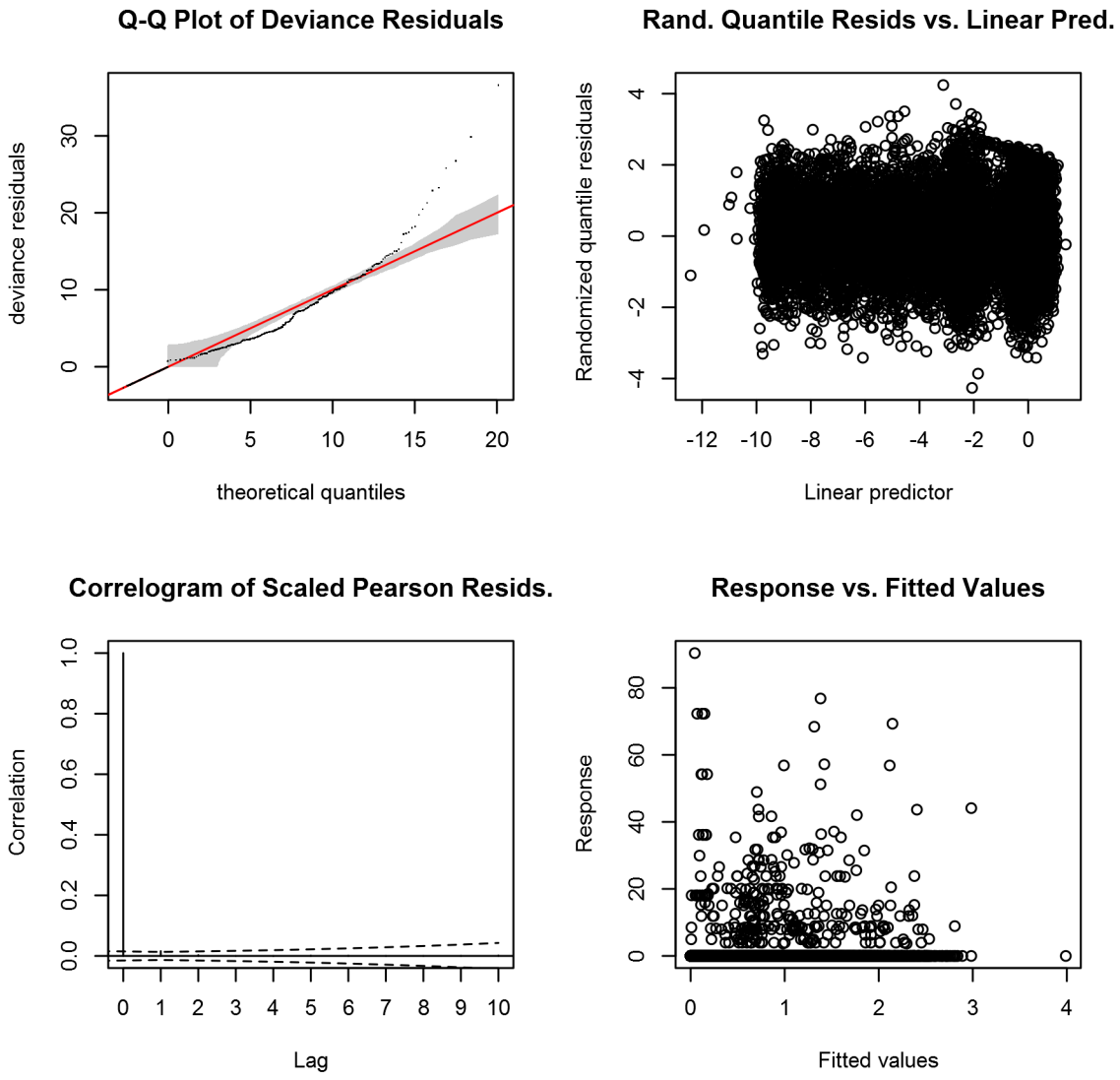

Figure 42: Statistical diagnostic plots for the Sperm whale Climatological model, Off Shelf.

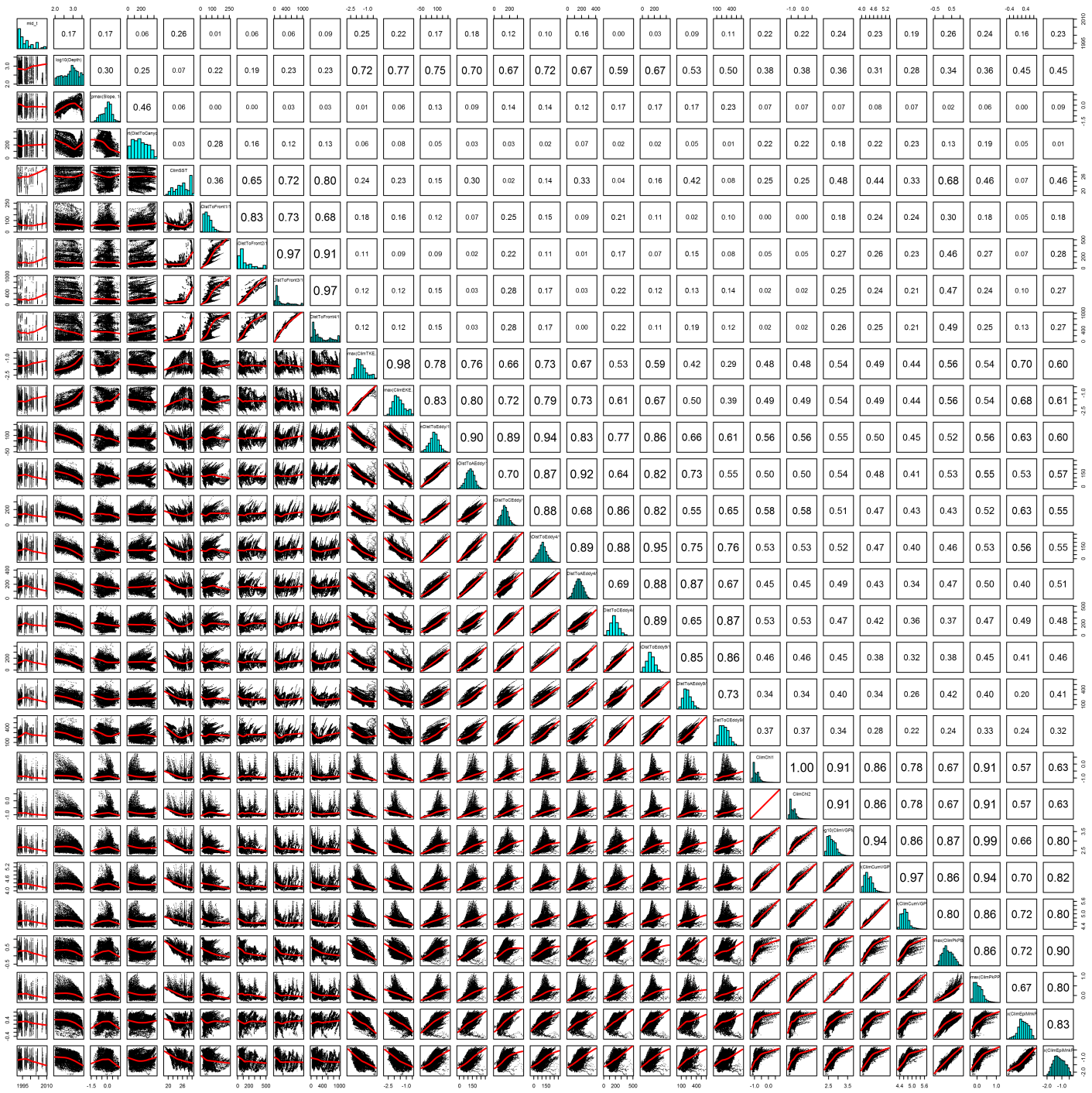

Figure 43: Scatterplot matrix for the Sperm whale Climatological model, Off Shelf. This plot is used to inspect the distribution of predictors (via histograms along the diagonal), simple correlation between predictors (via pairwise Pearson coefficients above the diagonal), and linearity of predictor correlations (via scatterplots below the diagonal). This plot is best viewed at high magnification.

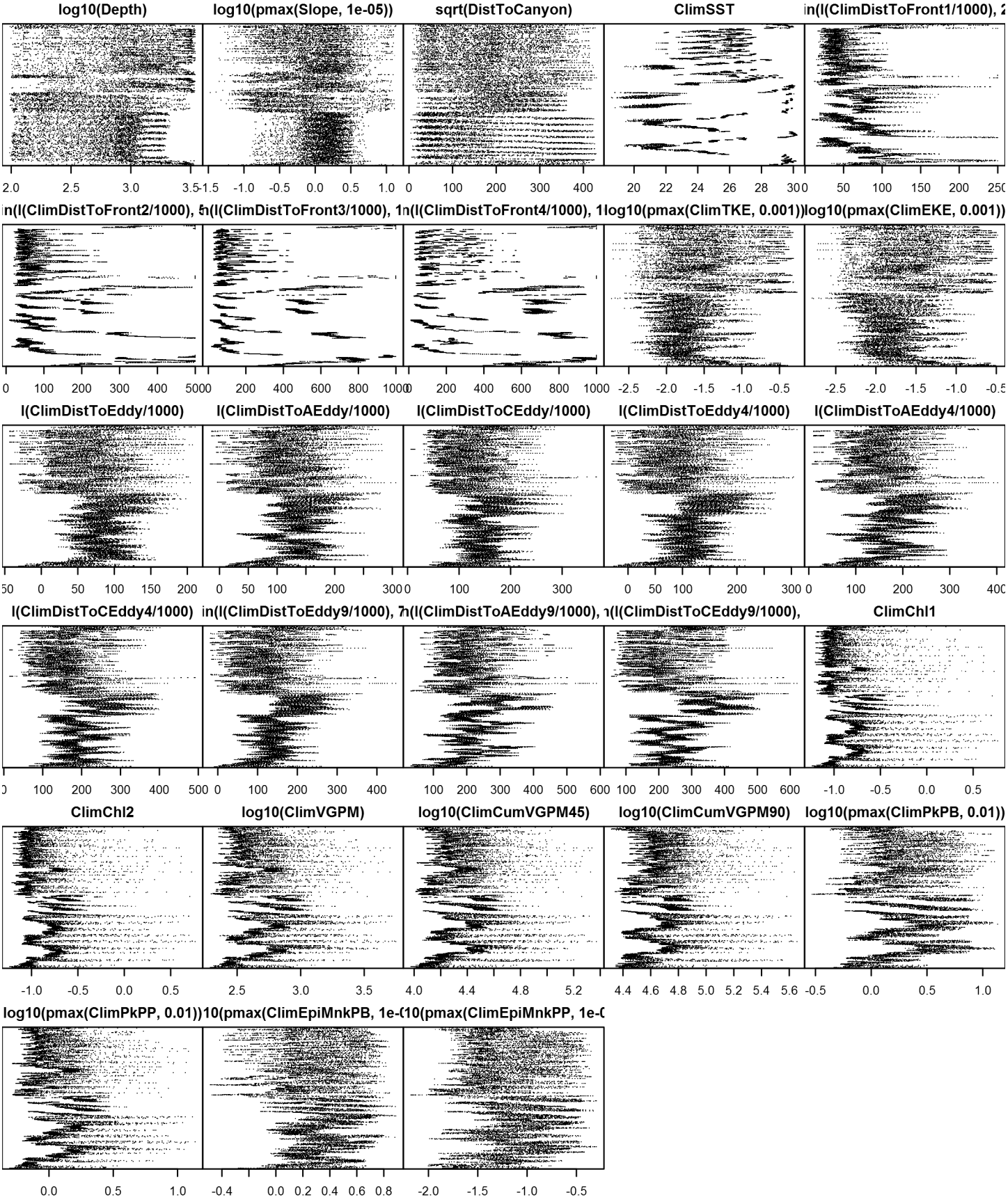

Figure 44: Dotplot for the Sperm whale Climatological model, Off Shelf. This plot is used to check for suspicious patterns and outliers in the data. Points are ordered vertically by transect ID, sequentially in time.

On Shelf

Density assumed to be 0 in this region.

Model Comparison

Spatial Model Performance

The table below summarizes the performance of the candidate spatial models that were tested. The first model contained only physiographic predictors. Subsequent models added additional suites of predictors of based on when they became available via remote sensing.

For each model, three versions were fitted; the % Dev Expl columns give the % deviance explained by each one. The "climatological" models were fitted to 8-day climatologies of the environmental predictors. Because the environmental predictors were always available, no segments were lost, allowing these models to consider the maximal amount of survey data. The "contemporaneous" models were fitted to day-of-sighting images of the environmental predictors; these were smoothed to reduce data loss due to clouds, but some segments still failed to retrieve environmental values and were lost. Finally, the "climatological same segments" models fitted climatological predictors to the segments retained by the contemporaneous model, so that the explantory power of the two types of predictors could be directly compared. For each of the three models, predictors were selected independently via shrinkage smoothers; thus the three models did not necessarily utilize the same predictors.

Predictors derived from ocean currents first became available in January 1993 after the launch of the TOPEX/Poseidon satellite; productivity predictors first became available in September 1997 after the launch of the SeaWiFS sensor. Contemporaneous and climatological same segments models considering these predictors usually suffered data loss. Date Range shows the years spanned by the retained segments. The Segments column gives the number of segments retained; % Lost gives the percentage lost.

Predictors	Climatol % Dev Expl	Contemp % Dev Expl	Climatol Same Segs % Dev Expl	Segments	% Lost	Date Range
Phys	14.6			14455		1992-2009
Phys+SST	14.6	14.6	14.6	14455	0.0	1992-2009
Phys+SST+Curr	16.3	15.0	13.9	12621	12.7	1993-2009
Phys+SST+Curr+Prod	16.7	14.9	12.1	4219	70.8	1998-2009

Table 16: Deviance explained by the candidate density models.

Abundance Estimates

The table below shows the estimated mean abundance (number of animals) within the study area, for the models that explained the most deviance for each model type. Mean abundance was calculated by first predicting density maps for a series of time steps, then computing the abundance for each map, and then averaging the abundances. For the climatological models, we used 8-day climatologies, resulting in 46 abundance maps. For the contemporaneous models, we used daily images, resulting in 365 predicted abundance maps per year that the prediction spanned. The Dates column gives the dates to which the estimates apply. For our models, these are the years for which both survey data and remote sensing data were available.

The Assumed g(0)=1 column specifies whether the abundance estimate assumed that detection was certain along the survey trackline. Studies that assumed this did not correct for availability or perception bias, and therefore underestimated abundance. The In our models column specifies whether the survey data from the study was also used in our models. If not, the study provides a completely independent estimate of abundance.

Dates	Model or study	Estimated abundance	CV	Assumed g(0)=1	In our models

1992-2009	Climatological model	2617	0.10	No	
1993-2009	Contemporaneous model*	2128	0.08	No	
1992-2009	Climatological same segments model	2084	0.07	No	
2009	Oceanic waters, Jun-Aug (Waring et al. 2013)	763	0.38	Yes	Yes
2003-2004	Oceanic waters, Jun-Aug (Mullin 2007)	1665	0.20	Yes	Yes
1996-2001	Oceanic waters, Apr-Jun (Mullin and Fulling 2004)	1349	0.23	Yes	Yes
1991-1994	Oceanic waters, Apr-Jun (Hansen et al. 1995)	530	0.31	Yes	Yes

Table 17: Estimated mean abundance within the study area. We selected the model marked with * as our best estimate of the abundance and distribution of this taxon. For comparison, independent abundance estimates from NOAA technical reports and/or the scientific literature are shown. Please see the Discussion section below for our evaluation of our models compared to the other estimates. Note that our abundance estimates are averaged over the whole year, while the other studies may have estimated abundance for specific months or seasons. Our coefficients of variation (CVs) underestimate the true uncertainty in our estimates, as they only incorporated the uncertainty of the GAM stage of our models. Other sources of uncertainty include the detection functions and g(0) estimates. It was not possible to incorporate these into our CVs without undertaking a computationally-prohibitive bootstrap; we hope to attempt that in a future version of our models.

Density Maps

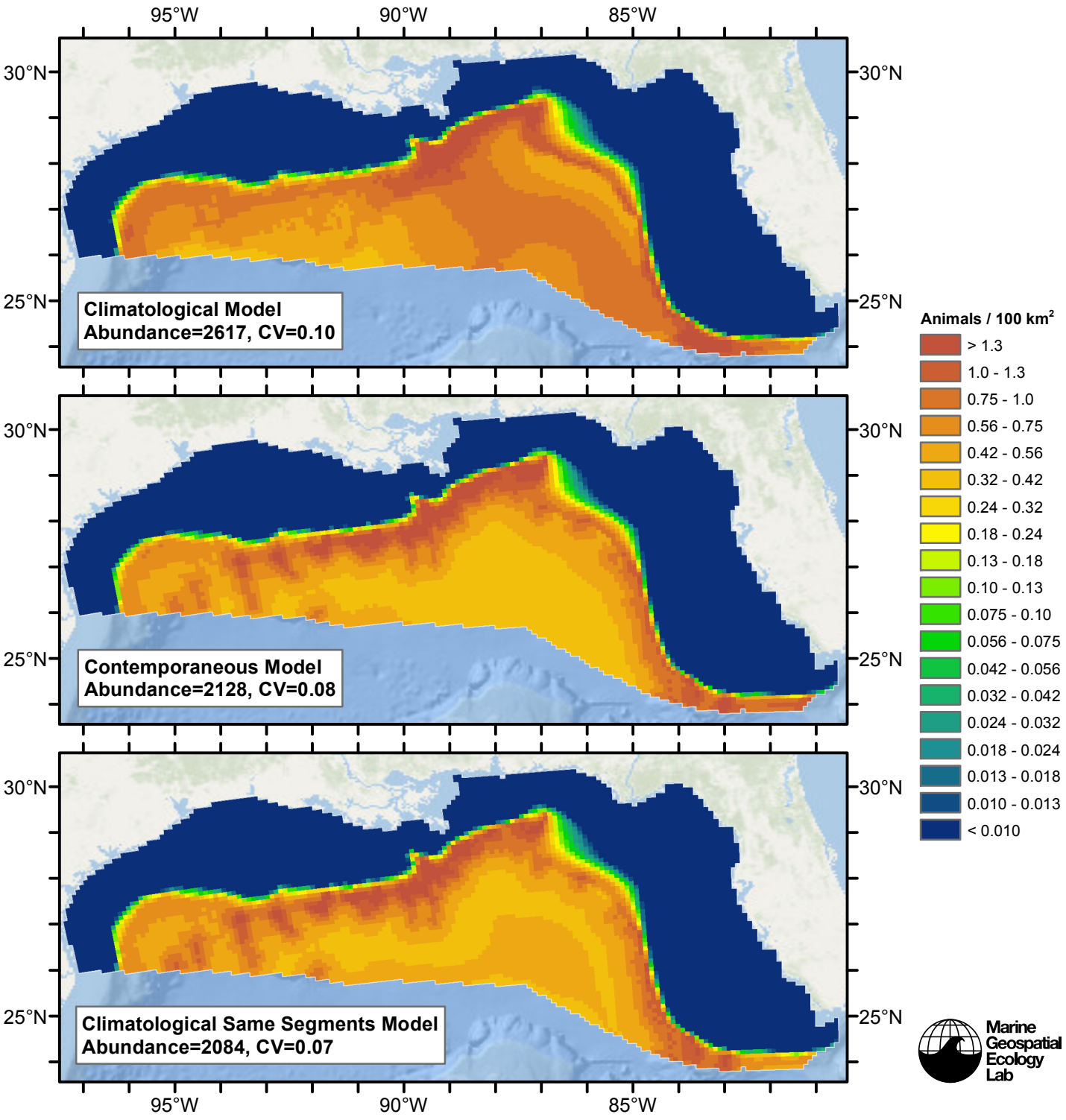

Figure 45: Sperm whale density and abundance predicted by the models that explained the most deviance. Regions inside the study area (white line) where the background map is visible are areas we did not model (see text).

Temporal Variability

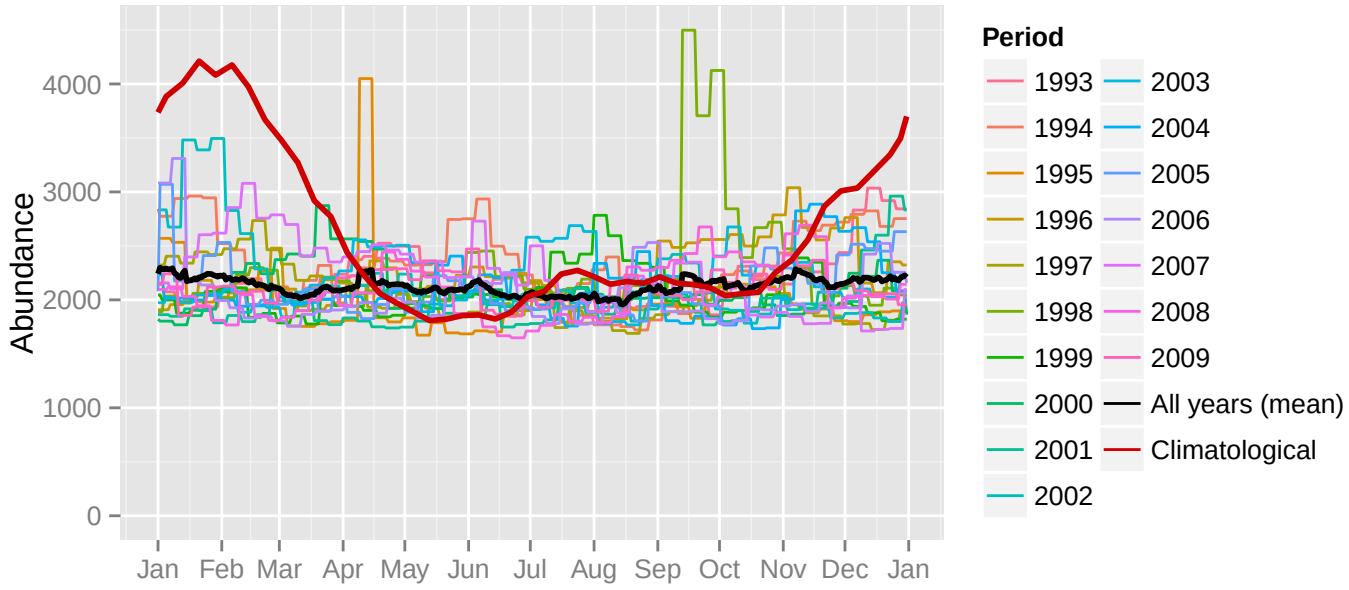

Figure 46: Comparison of Sperm whale abundance predicted at a daily time step for different time periods. Individual years were predicted using contemporaneous models. "All years (mean)" averages the individual years, giving the mean annual abundance of the contemporaneous model. "Climatological" was predicted using the climatological model. The results for the climatological same segments model are not shown.

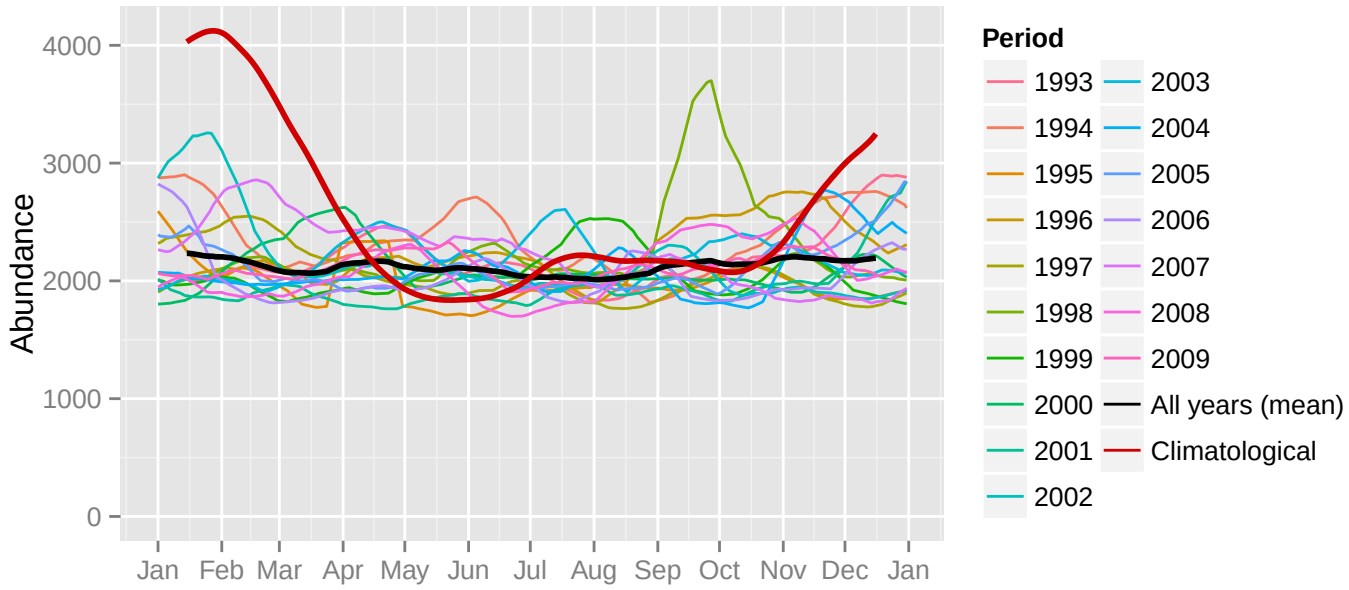

Figure 47: The same data as the preceding figure, but with a 30-day moving average applied.

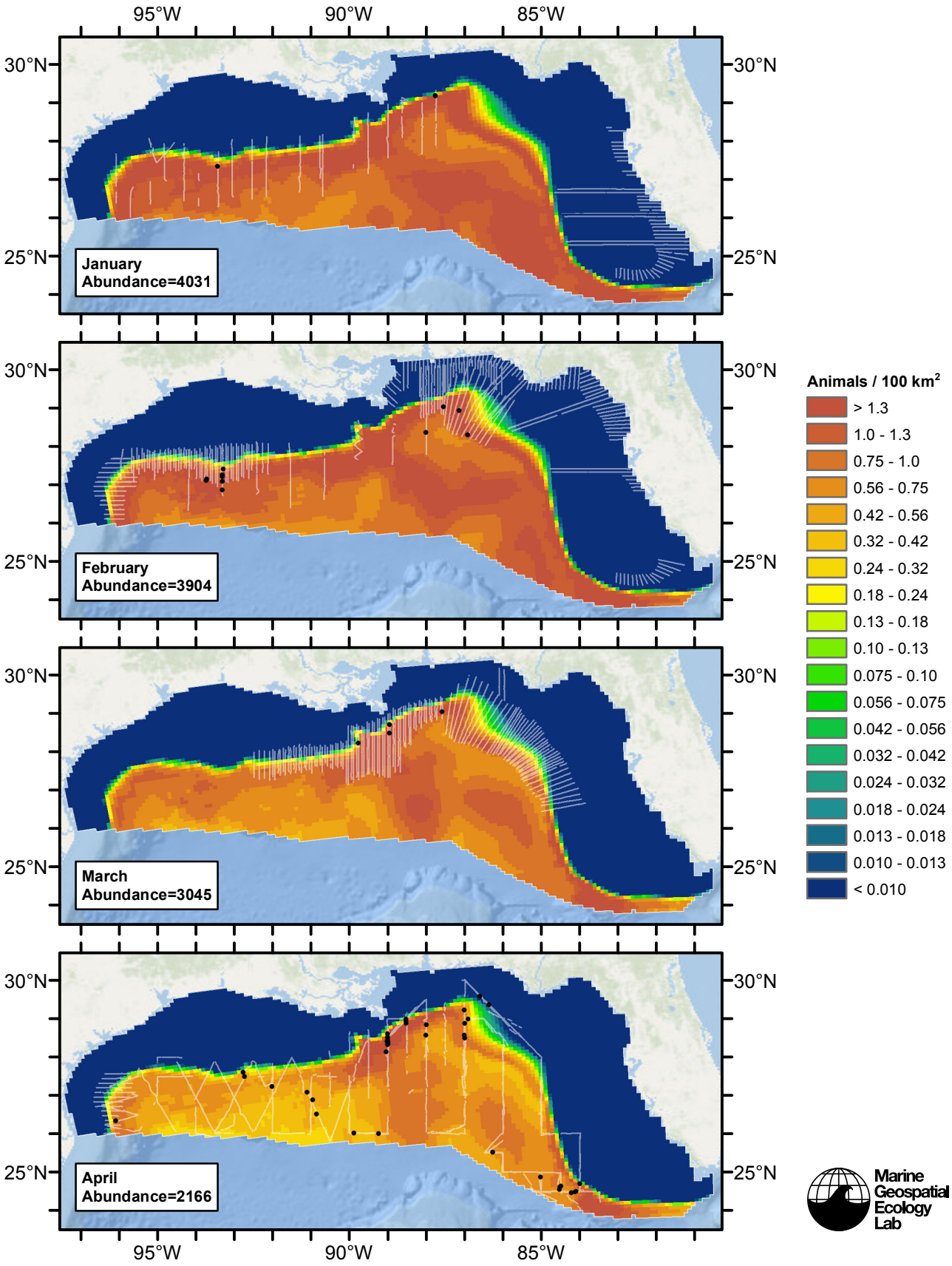
95°W
90°W
85°W
30°N
25°N
January
Abundance=4031
February
Abundance=3904
March
Abundance=3045
April
Abundance=2166
Animals / 100 km²
> 1.3
1.0 - 1.3
0.75 - 1.0
0.56 - 0.75
0.42 - 0.56
0.32 - 0.42
0.24 - 0.32
0.18 - 0.24
0.13 - 0.18
0.10 - 0.13
0.075 - 0.10
0.056 - 0.075
0.042 - 0.056
0.032 - 0.042
0.024 - 0.032
0.018 - 0.024
0.013 - 0.018
0.010 - 0.013
< 0.010
Marine
Geospatial
Ecology
Lab

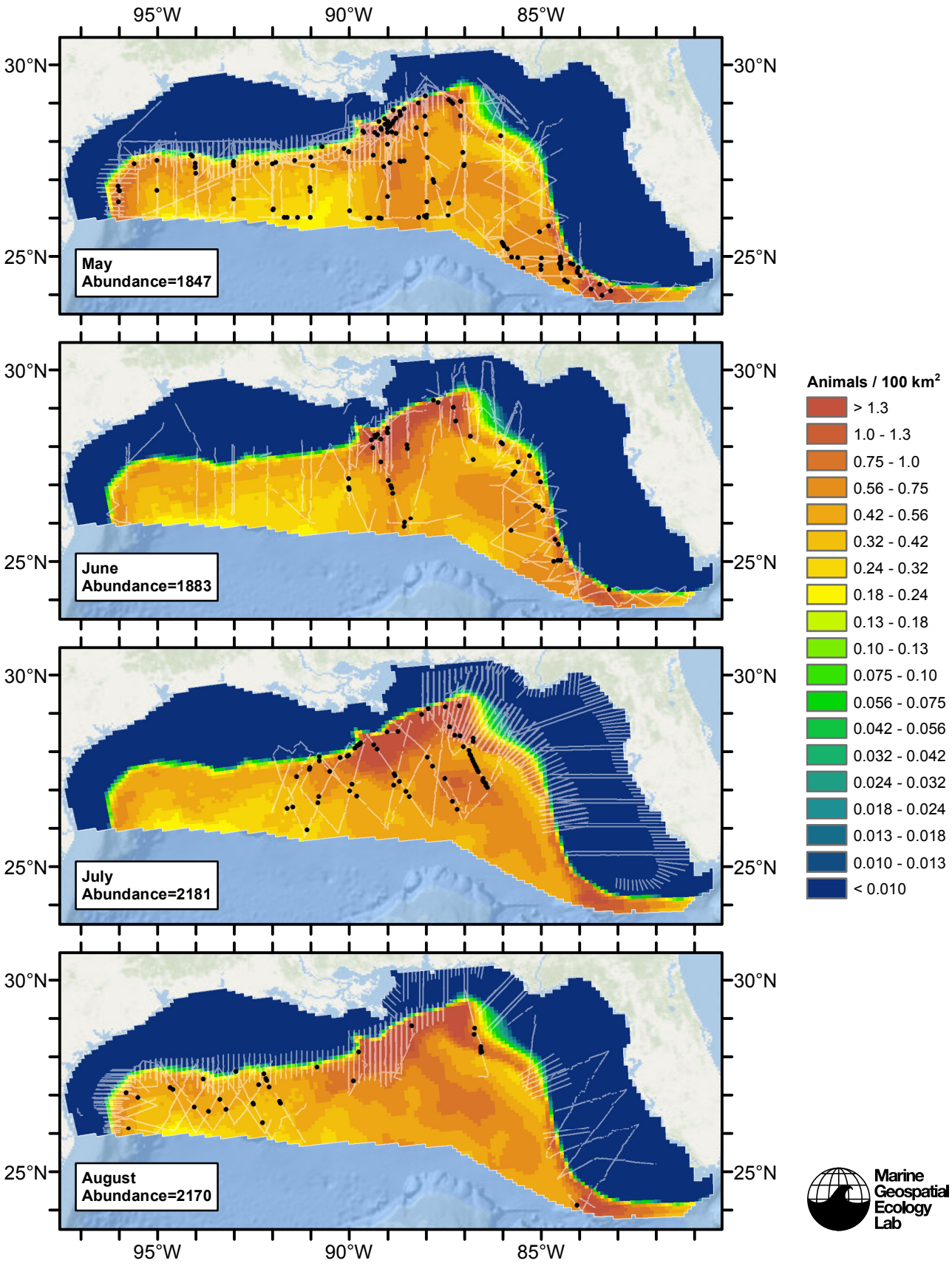
95°W
90°W
85°W
30°N
25°N
May
Abundance=1847
June
Abundance=1883
July
Abundance=2181
August
Abundance=2170
Animals / 100 km²
> 1.3
1.0 - 1.3
0.75 - 1.0
0.56 - 0.75
0.42 - 0.56
0.32 - 0.42
0.24 - 0.32
0.18 - 0.24
0.13 - 0.18
0.10 - 0.13
0.075 - 0.10
0.056 - 0.075
0.042 - 0.056
0.032 - 0.042
0.024 - 0.032
0.018 - 0.024
0.013 - 0.018
0.010 - 0.013
< 0.010
Marine
Geospatial
Ecology
Lab

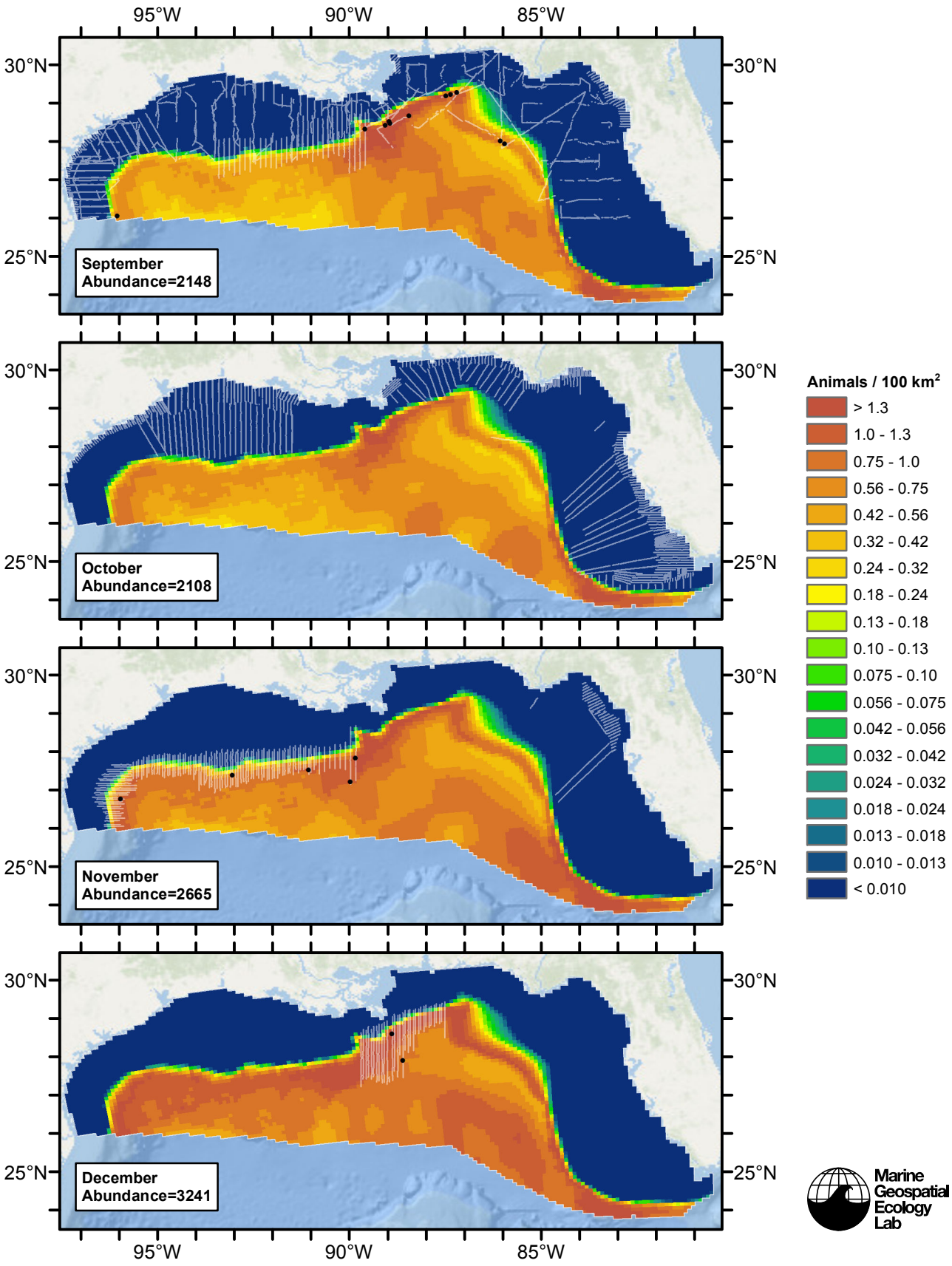
95°W
90°W
85°W
30°N
25°N
September
Abundance=2148
October
Abundance=2108
November
Abundance=2665
December
Abundance=3241
Animals / 100 km²
> 1.3
1.0 - 1.3
0.75 - 1.0
0.56 - 0.75
0.42 - 0.56
0.32 - 0.42
0.24 - 0.32
0.18 - 0.24
0.13 - 0.18
0.10 - 0.13
0.075 - 0.10
0.056 - 0.075
0.042 - 0.056
0.032 - 0.042
0.024 - 0.032
0.018 - 0.024
0.013 - 0.018
0.010 - 0.013
< 0.010
Marine
Geospatial
Ecology
Lab

Contemporaneous Model

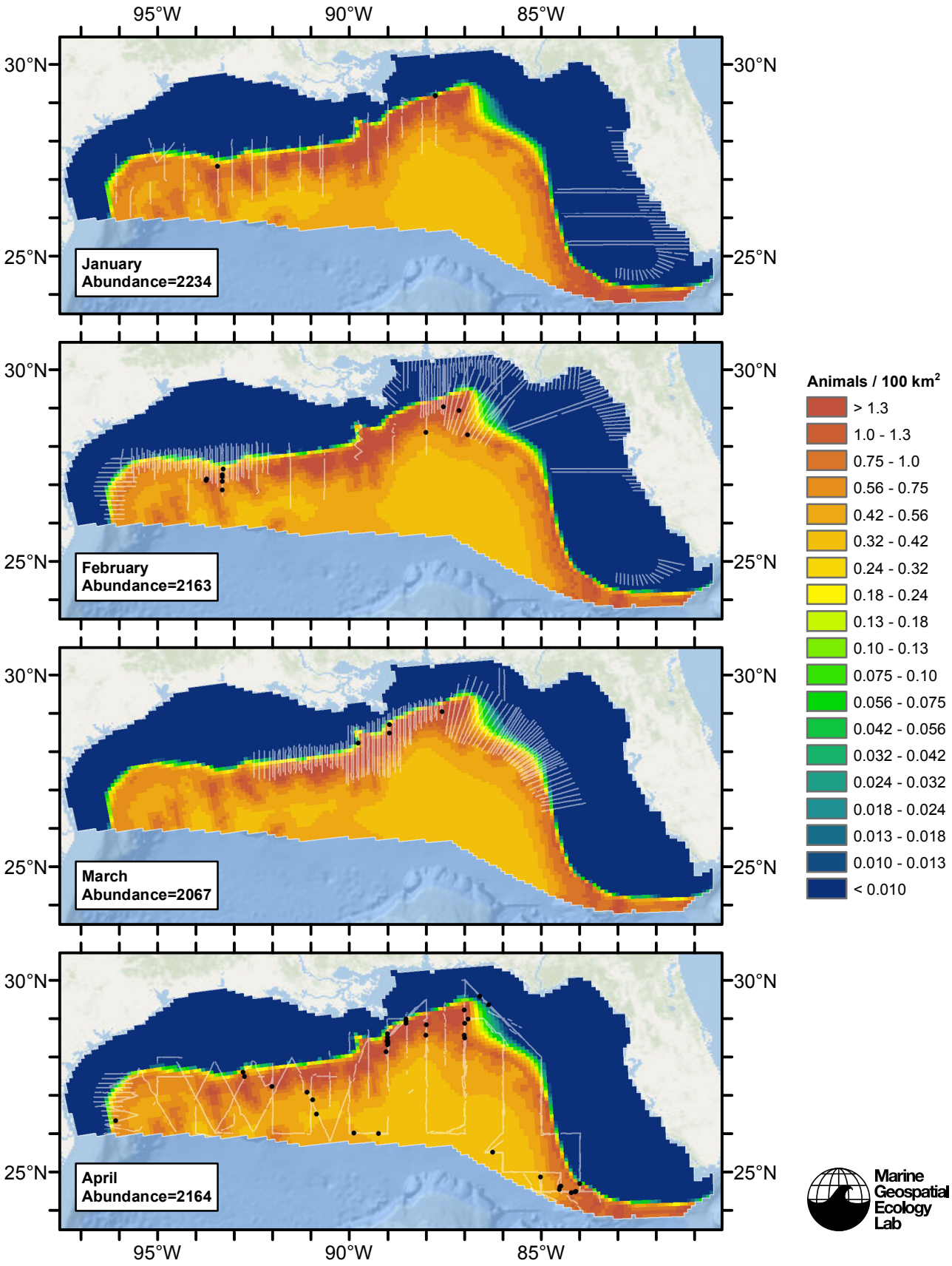

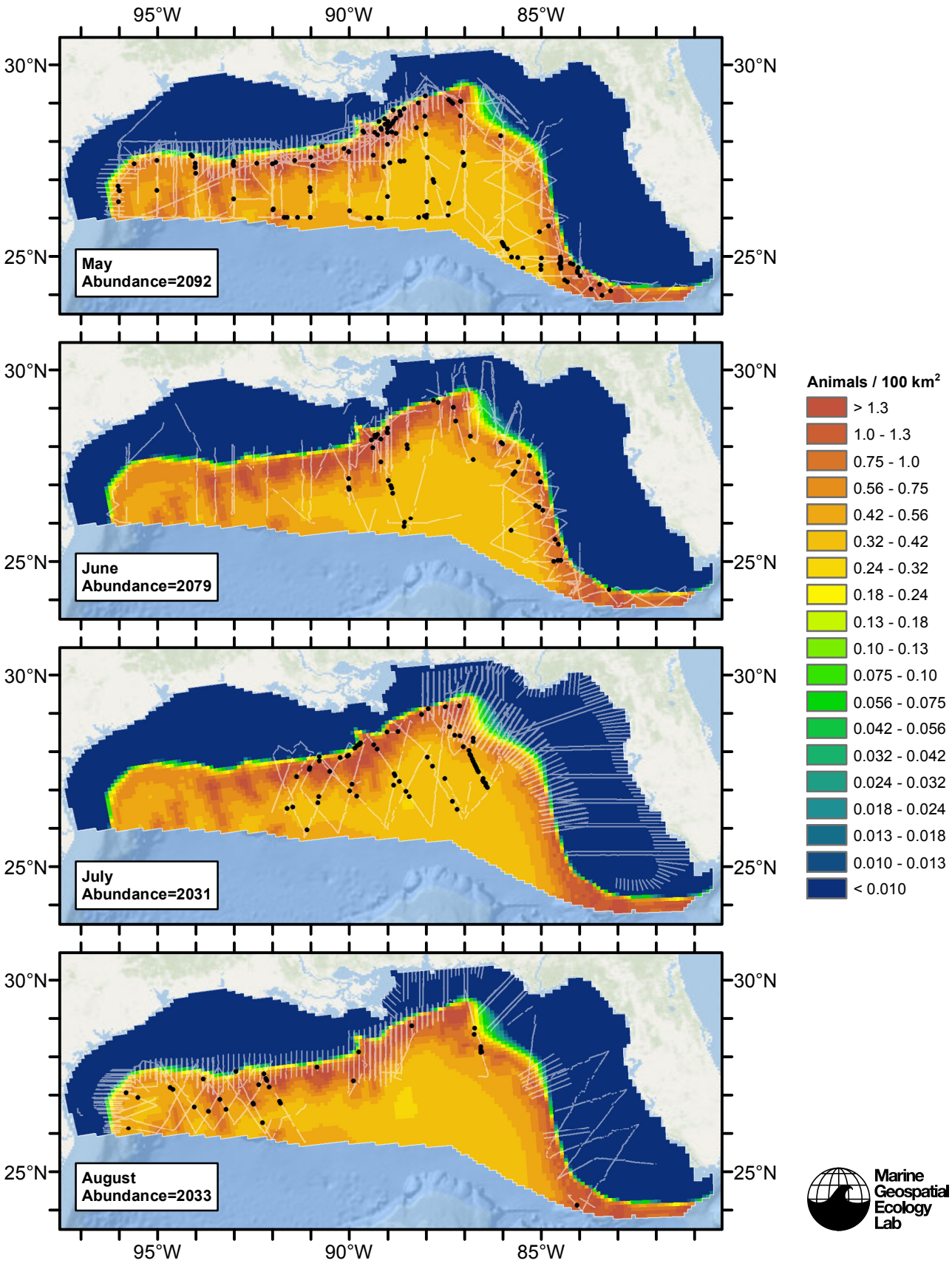
95°W
90°W
85°W
30°N
25°N
May
Abundance=2092
June
Abundance=2079
July
Abundance=2031
August
Abundance=2033
Animals / 100 km²
> 1.3
1.0 - 1.3
0.75 - 1.0
0.56 - 0.75
0.42 - 0.56
0.32 - 0.42
0.24 - 0.32
0.18 - 0.24
0.13 - 0.18
0.10 - 0.13
0.075 - 0.10
0.056 - 0.075
0.042 - 0.056
0.032 - 0.042
0.024 - 0.032
0.018 - 0.024
0.013 - 0.018
0.010 - 0.013
< 0.010
Marine
Geospatial
Ecology
Lab

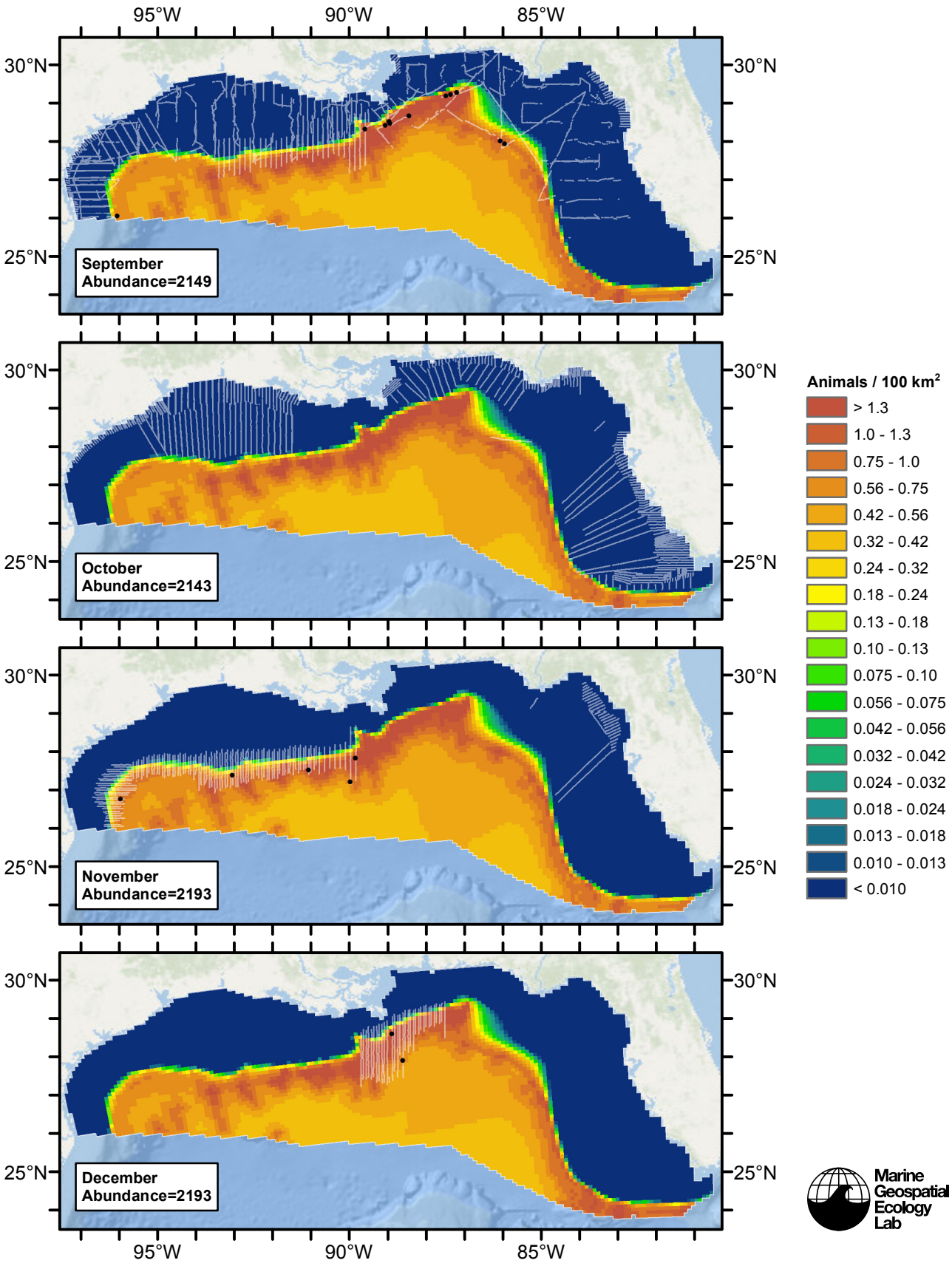
95°W
90°W
85°W
30°N
25°N
September
Abundance=2149
October
Abundance=2143
November
Abundance=2193
December
Abundance=2193
Animals / 100 km²
> 1.3
1.0 - 1.3
0.75 - 1.0
0.56 - 0.75
0.42 - 0.56
0.32 - 0.42
0.24 - 0.32
0.18 - 0.24
0.13 - 0.18
0.10 - 0.13
0.075 - 0.10
0.056 - 0.075
0.042 - 0.056
0.032 - 0.042
0.024 - 0.032
0.018 - 0.024
0.013 - 0.018
0.010 - 0.013
< 0.010
Marine
Geospatial
Ecology
Lab

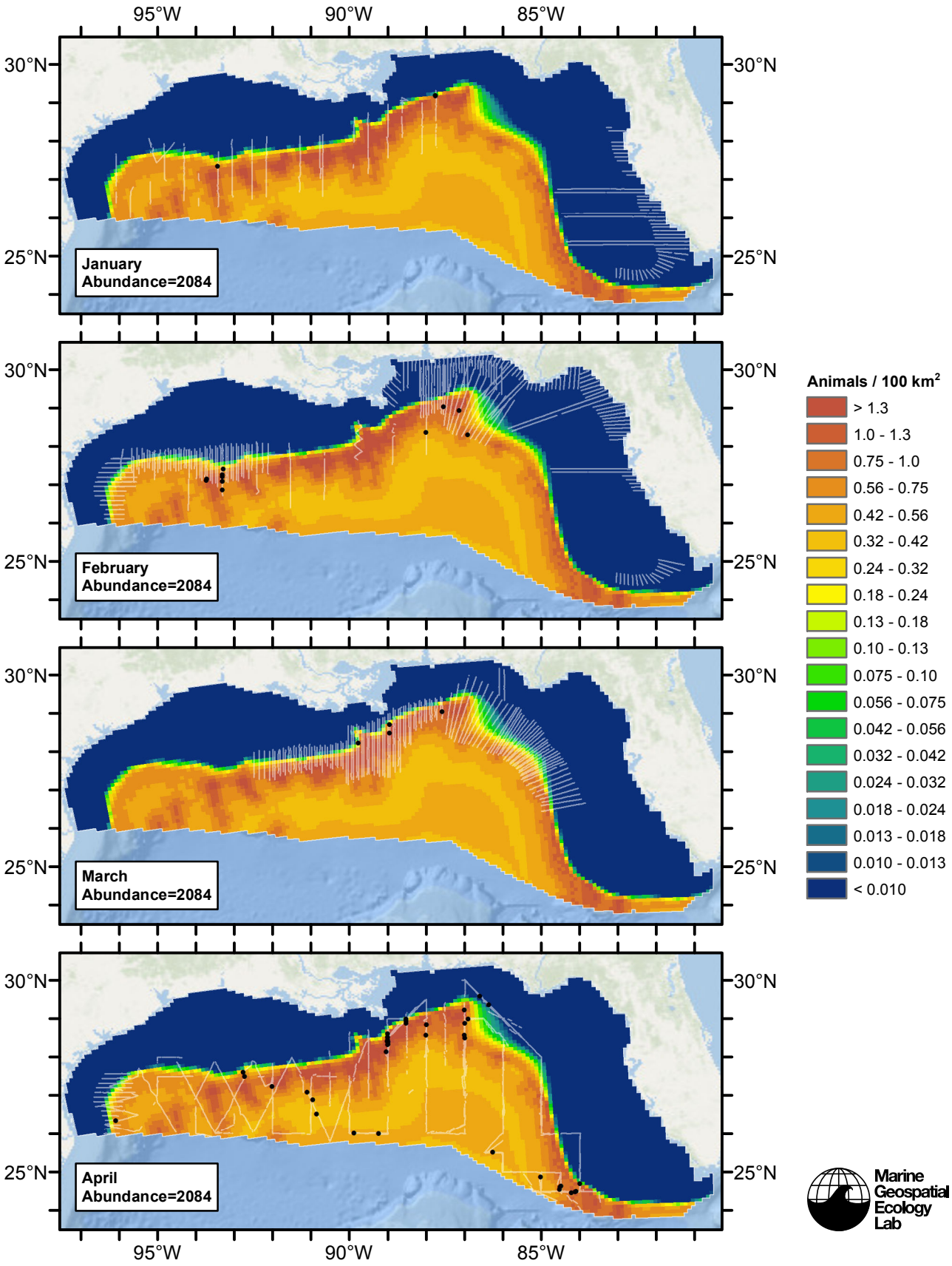
95°W
90°W
85°W
30°N
25°N
January
Abundance=2084
February
Abundance=2084
March
Abundance=2084
April
Abundance=2084
Animals / 100 km²
> 1.3
1.0 - 1.3
0.75 - 1.0
0.56 - 0.75
0.42 - 0.56
0.32 - 0.42
0.24 - 0.32
0.18 - 0.24
0.13 - 0.18
0.10 - 0.13
0.075 - 0.10
0.056 - 0.075
0.042 - 0.056
0.032 - 0.042
0.024 - 0.032
0.018 - 0.024
0.013 - 0.018
0.010 - 0.013
< 0.010
Marine
Geospatial
Ecology
Lab

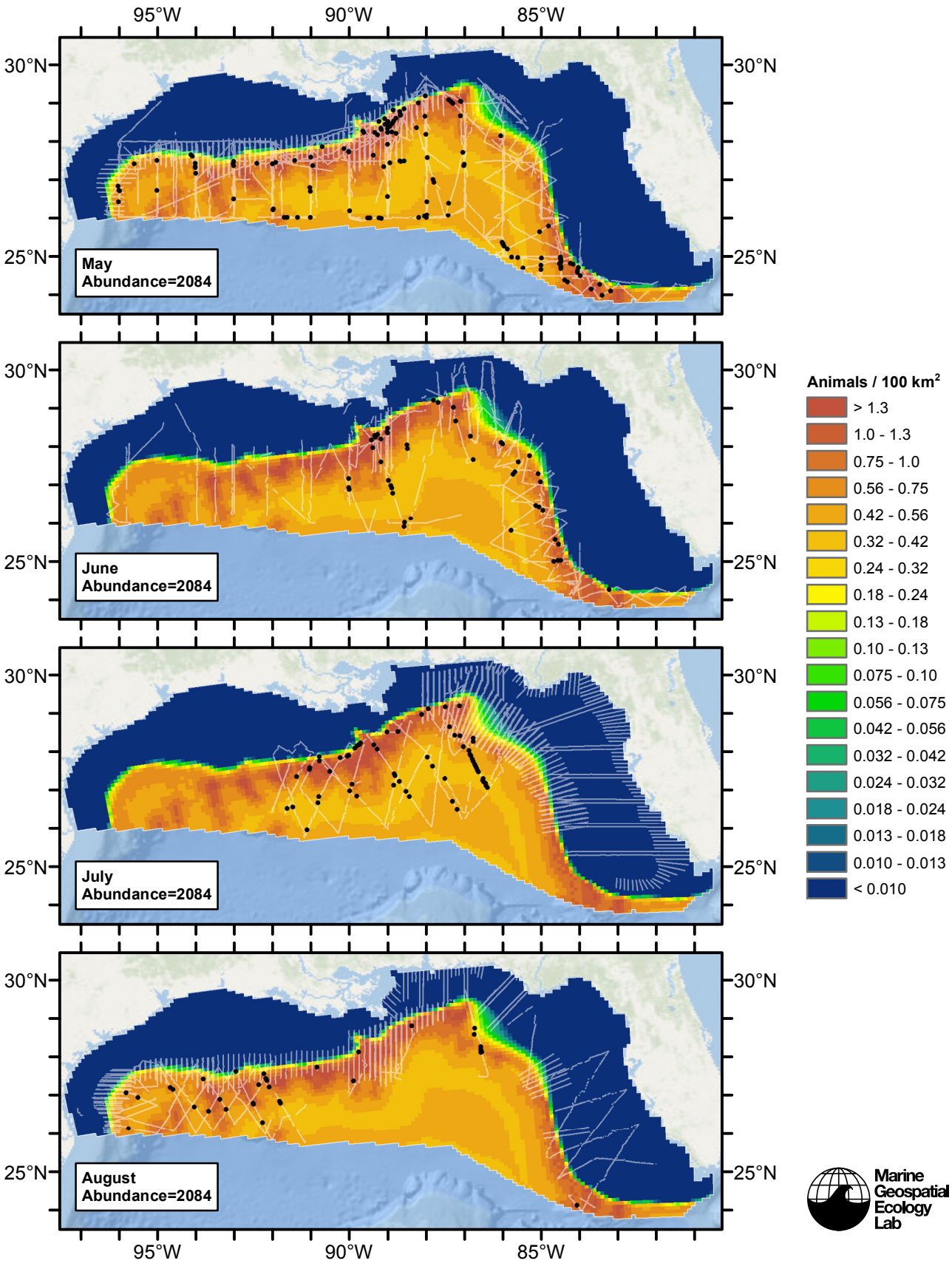
95°W
90°W
85°W
30°N
25°N
May
Abundance=2084
June
Abundance=2084
July
Abundance=2084
August
Abundance=2084
Animals / 100 km²
> 1.3
1.0 - 1.3
0.75 - 1.0
0.56 - 0.75
0.42 - 0.56
0.32 - 0.42
0.24 - 0.32
0.18 - 0.24
0.13 - 0.18
0.10 - 0.13
0.075 - 0.10
0.056 - 0.075
0.042 - 0.056
0.032 - 0.042
0.024 - 0.032
0.018 - 0.024
0.013 - 0.018
0.010 - 0.013
< 0.010
Marine
Geospatial
Ecology
Lab

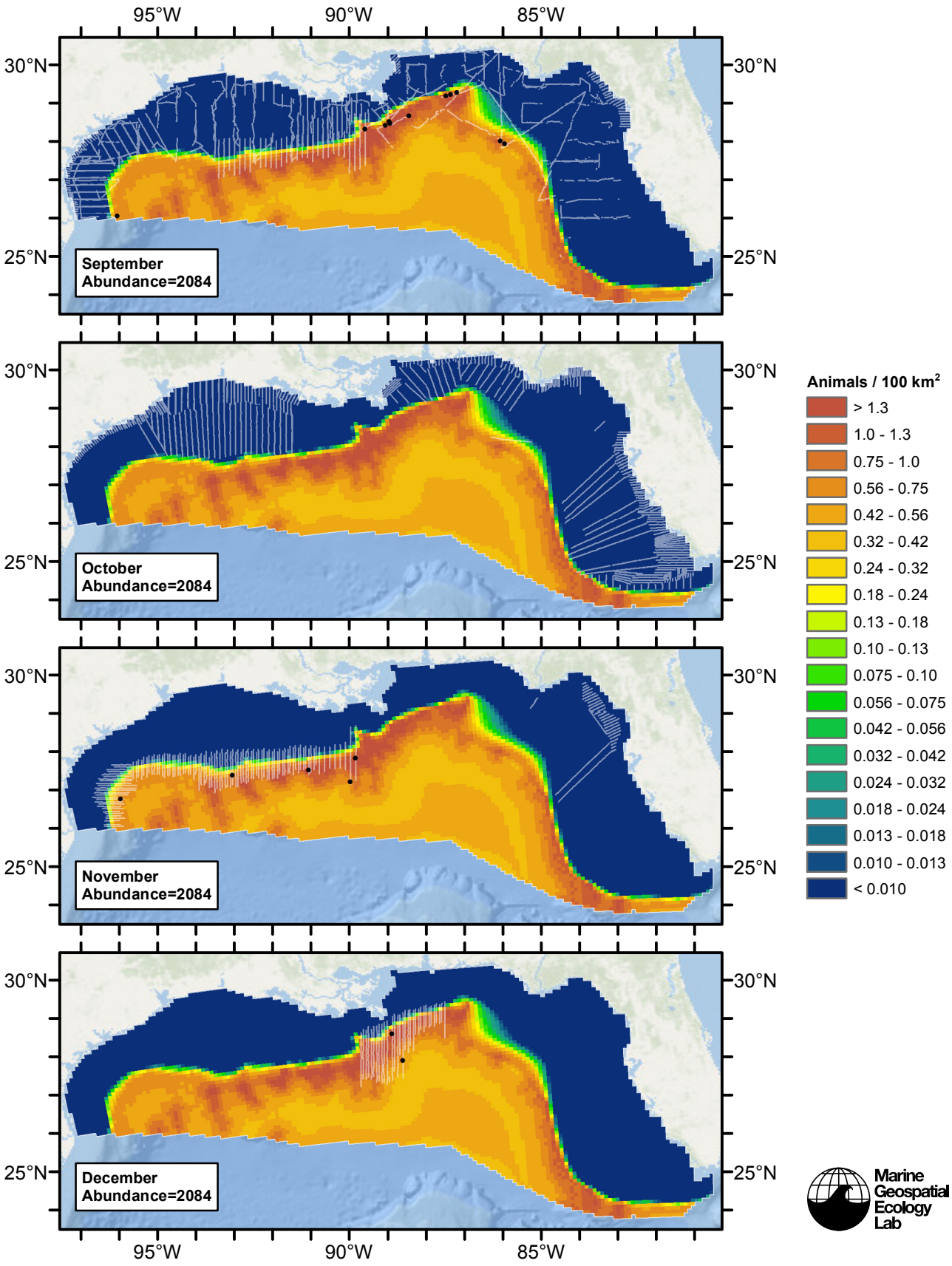
95°W
90°W
85°W
30°N
25°N
September
Abundance=2084
October
Abundance=2084
November
Abundance=2084
December
Abundance=2084
Animals / 100 km²
> 1.3
1.0 - 1.3
0.75 - 1.0
0.56 - 0.75
0.42 - 0.56
0.32 - 0.42
0.24 - 0.32
0.18 - 0.24
0.13 - 0.18
0.10 - 0.13
0.075 - 0.10
0.056 - 0.075
0.042 - 0.056
0.032 - 0.042
0.024 - 0.032
0.018 - 0.024
0.013 - 0.018
0.010 - 0.013
< 0.010
Marine
Geospatial
Ecology
Lab

Discussion

When only physiographic, SST, and SST front distance predictors were included in the models, all three models dropped the SST-related predictors and selected only depth and distance to canyon, explaining 14.6% of the deviance in the data. When predictors related to ocean currents and productivity were added, the climatological model that considered all of the segments explained the most deviance, but the contemporaneous models explained 1.1-2.8% more deviance than the climatological models that considered the same segments. Collectively, these results suggest that contemporaneous predictors are more suitable for modeling sperm whale distribution in this region, and the results are consistent with prior studies that asserted the importance of eddies, productivity, and the continental slope to sperm whale habitat (Biggs et al. 2005, Jochens et al. 2008).

We selected the contemporaneous model's predictions as our best estimate of sperm whale distribution and abundance. This model consistently outperformed the climatological model that considered the same segments, and the version of it that explained the most deviance (Phys+SST+Curr) only suffered a loss of 12.7% of the segments, allowing it to consider all of the them except those from 1992. While the climatological model that considered all segments explained the most deviance of all models, we believe this is because the segments from 1992 are simply easier to model, and that if contemporaneous currents and productivity predictors were available for that year, the contemporaneous model would have performed just as well or better.

The climatological model that considered all segments also predicted an unrealistic rise in sperm whale abundance between November and April (see Temporal Variability section). This pattern is not consistent with prior evidence that sperm whales are resident in the Gulf of Mexico year-round, with no discernible migration (Jochens et al. 2008). In contrast, the contemporaneous model predicts a relatively static abundance throughout the year.

Because the survey effort used as input to this model was biased toward spring and summer and was spatiotemporally patchy (see maps in the Temporal Variability section above), we were not confident that our models could produce realistic predictions at a monthly temporal resolution. This problem affected all species that we modeled in the Gulf of Mexico, and despite the relatively static abundance predicted for sperm whales, we recommend that year-round average predictions be used for all Gulf of Mexico species. In the case of sperm whales, this year-round average prediction is shown in the Contemporaneous Model panel of Figure 45 above.

The mean abundance predicted by our contemporaneous model is higher than earlier estimates, which ranged from 763 in 2009 (Waring et al. 2013) to 1665 in 2004 (Mullin 2007). But all of the earlier estimates assumed that g(0)=1. If these estimates were rescaled according to our shipboard g(0) of 0.53, they would range from 1440-3142. Thus, once g(0) is accounted for, our estimate is well within the range of these prior estimates.

References

Barlow J, Oliver CW, Jackson TD, Taylor BL (1988) Harbor Porpoise, Phocoena phocoena, Abundance Estimation for California, Oregon, and Washington: II. Aerial Surveys. Fishery Bulletin 86: 433-444.

Barlow J, Sexton S (1996) The effect of diving and searching behavior on the probability of detecting track-line groups, g(0), of long-diving whales during line transect surveys. NOAA National Marine Fisheries Service, Southwest Fisheries Center Administrative Report LJ-96-14. 21 pp.

Biggs DC, Jochens AE, Howard MK, DiMarco SF, Mullin KD, Leben RR, Muller-Karger FE, Hu C (2005) Eddy forced variations in on- and off-margin summertime circulation along the 1000-m isobath of the northern Gulf of Mexico, 2000-2003, and links with sperm whale distributions along the middle slope. In: Circulation in the Gulf of Mexico: Observations and Models (Sturges W, Lugo-Fernandez A, eds.), Geophysical Monograph Series, Volume 161, American Geophysical Union. pp. 71-85.

Carretta JV, Lowry MS, Stinchcomb CE, Lynn MS, Cosgrove RE (2000) Distribution and abundance of marine mammals at San Clemente Island and surrounding offshore waters: results from aerial and ground surveys in 1998 and 1999. Administrative Report LJ-00-02, available from Southwest Fisheries Science Center, P.O. Box 271, La Jolla, CA USA 92038. 44 p.

Hansen LJ, Mullin KD, Roden CL (1995) Estimates of cetacean abundance in the northern Gulf of Mexico from vessel surveys. Southeast Fisheries Science Center, Miami Laboratory, Contribution No. MIA-94/95-25, 9 pp.

Jochens A, Biggs D, Benoit-Bird K, Engelhaupt D, Gordon J, Hu C, Jaquet N, Johnson M, Leben R, Mate B, Miller P, Ortega-Ortiz J, Thode A, Tyack P, Wursig B (2008) Sperm whale seismic study in the Gulf of Mexico: Synthesis report. U.S. Dept. of the Interior, Minerals Management Service, Gulf of Mexico OCS Region, New Orleans, LA. OCS Study MMS 2008-006. 341 pp.

Mullin KD (2007) Abundance of cetaceans in the oceanic Gulf of Mexico based on 2003-2004 ship surveys. 26 pp.

Mullin KD, Fulling GL (2004) Abundance of cetaceans in the oceanic northern Gulf of Mexico. Mar. Mamm. Sci. 20(4): 787-807.

Waring GT, Josephson E, Maze-Foley K, Rosel PE, eds. (2013) U.S. Atlantic and Gulf of Mexico Marine Mammal Stock Assessments – 2012. NOAA Tech Memo NMFS NE 223; 419 p.

Watwood SL, Miller PJO, Johnson M, Madsen PT, Tyack PL (2006) Deep-diving foraging behaviour of sperm whales (Physeter macrocephalus). Journal of Animal Ecology 75:814-825.

Whitehead H (2002) Estimates of the current global population size and historical trajectory for sperm whales. Mar Ecol Prog Ser. 242: 295-304.